Discussion Paper Series
No. 2301
February, 2023

Understanding Trend Inflation Through the Lens of the Goods and Services Sectors

By Yunjong Eo, Luis Uzeda, Benjamin Wong

The Institute of Economic Research – Korea University
Anam-dong, Sungbuk-ku, Seoul, 136-701, South Korea, Tel: (82-2) 3290-1632, Fax: (82-2) 928-4948

Understanding Trend Inflation Through the Lens of the Goods and Services Sectors

Yunjong Eo* Korea University

Luis Uzeda† Bank of Canada

Benjamin Wong‡ Monash University

February 24, 2023

Abstract

We distinguish between the goods and services sectors in an unobserved components model of U.S. inflation. We find that prior to the early 1990s, both sectors contributed to volatility of aggregate trend inflation, while since then, this has been predominantly driven by the services sector, with the trend in goods inflation being essentially flat. We document that the large reduction in the volatility of the trend for goods inflation has been the most important driver of the decline in the volatility in aggregate trend inflation reported by Stock and Watson (2007). Our results appear robust to COVID-19 inflation developments.

Keywords: sectoral trend inflation; unobserved components model; disaggregated inflation;

JEL classification: C11; C32; E31; E52;

*Yunjong Eo: Department of Economics, Korea University, Seoul 02841, South Korea; Tel: +82 2 3290 2212; Email: yunjongeo@korea.ac.kr

†Luis Uzeda: Bank of Canada, 234 Wellington Ave W, Ottawa, ON, K1A 0H9, Canada; Email: luzedagarcia@bank-banque-canada.ca

‡Benjamin Wong (Corresponding Author): Department of Econometrics and Business Statistics, Monash University, Caulfield East, VIC 3145, Australia; Email: benjamin.wong@monash.edu

1 Introduction

A key objective of monetary policy is managing trend (or the long-run path of) inflation (see, e.g., Mishkin, 2007; Draghi, 2015). For example, in addition to headline inflation, the Federal Reserve monitors measures of inflation that exclude food and energy prices. This strategy is based on the belief that food and energy inflation is largely transitory and, consequently, of less immediate concern for monetary policy. In a prominent contribution, Stock and Watson (2007) show that the main change in U.S. inflation dynamics from the Great Inflation period compared to the post-1990s period is a considerable drop in the volatility of trend inflation. More specifically, while trend inflation was volatile during the 1970s, it has become markedly stable since the mid-1980s (and especially since the 1990s). While Stock and Watson's finding is a widely accepted description of *aggregate* trend inflation dynamics, it remains an open question of how much sectoral forces contribute to their narrative on the decline in trend inflation volatility.

Our main contribution is to shed light on the role of the goods and services sectors as sources of aggregate trend inflation volatility for the U.S. economy. At the same time, the COVID-19 pandemic has sparked interest in understanding sector-specific repercussions on inflation, especially in light of a large increase in goods inflation. Our key finding is the following: we find that variation in aggregate trend inflation has been entirely dominated by trend services inflation since the 1990s.[1] Our key result is a direct manifestation of the change in the goods sector, where its variation used to be partly permanent, but is now almost entirely dominated by transitory components. We note that these results are robust in the context of a sample that accounts for observations up to 2021Q4; hence, they include inflation developments related to the COVID-19 pandemic.[2] That said, it should be noted that the results for the pandemic period are interpreted with a larger degree of estimation uncertainty.

Methodologically, we develop a two-sector unobserved components model with stochastic volatility (Two-Sector UC-SV, hereafter) that features time-varying correlation between

[1] Throughout this paper we use the terms volatility and variation interchangeably.

[2] At the time of writing, it is not clear whether, and if so when, the COVID-19 pandemic ended. Therefore, when we mention the pandemic period, we refer to the period from 2020 until the end of our sample in 2021.

goods and services. Our approach is built directly from Stock and Watson's (2007) univariate unobserved components model with stochastic volatility, or univariate UC-SV. We also consider a multi-sector UC-SV factor model like Stock and Watson (2016) as an alternative to our baseline Two-Sector UC-SV. While we largely leave details of the multi-sector UC-SV factor model to the Online Appendix, we highlight a key difference between the two approaches is with regards to the modeling of comovement across sectors. Our approach relies on time-varying correlations while the multi-sector UC-SV factor model relies on time-varying loadings on a common trend. In the two-sector case we consider, our approach is a more parsimonious choice. Nevertheless, we show that the general conclusions of the paper are insensitive even when employing the multi-sector UC-SV factor model.

We relate our work to two specific strands of the literature on modeling inflation dynamics. First, like several contributions in the trend inflation literature (see, e.g., Chan et al., 2013; Mertens, 2016; Stock and Watson, 2016; Chan et al., 2018; Hwu and Kim, 2019), Stock and Watson (2007) represents a basic building block for our work. At a high level, these studies all mainly aim to sharpen trend inflation estimates in terms of in-sample and out-of-sample (i.e., forecasting) fits relative to the original univariate UC-SV framework. However, our objective is somewhat different. While building on the same modeling framework, our goal is not so much to improve the model fit, but instead to provide a better understanding of the sources of variation in trend inflation through the lens of the goods and services sectors. In addition, like Stock and Watson (2007), we similarly decompose inflation into a permanent and a transitory component in our Two-Sector UC-SV model. The permanent component is then labeled "trend inflation." Consequently, our approach is conceptually a removal-of-noise exercise used to obtain a signal about underlying and, ultimately, future inflation.[3]

[3]Anecdotally, this is the interpretation of trend inflation within policy circles. For example, in the minutes of the Federal Open Market Committee held on June 17-18, 2014, James Bullard asks, *"If inflation comes in at 1.9 percent and we've got underlying inflation at 1.75 percent, then should I say that we've got above-normal or above-trend inflation, or am I supposed to compare it with 2 percent, which is the Committee's official target?"* To which Jeremy Rudd replied, *"In our judgment, you should be comparing it with 1.75 percent. We think* $1\frac{3}{4}$ *percent is the underlying rate of inflation."* We also acknowledge work that interprets trend inflation as a time-varying inflation target (e.g., Kozicki and Tinsley, 2001; Ireland, 2007; Cogley et al., 2010; Coibion and Gorodnichenko, 2011; Ascari and Sbordone, 2014) or optimal inflation rate (Adam and Weber, 2019). While our work is explicitly set up as a removal-of-noise exercise, it is conceptually related to the aforementioned broad area of work since the persistent component of inflation is ultimately linked to inflation expectations and the effectiveness of monetary policy.

Second, the goods and services dichotomy has been used to frame inflation in terms of imported and domestic components (see Baldwin, 2022). In particular, services inflation is often hypothesized as having a much tighter link to domestic economic slack, and possibly cyclically sensitive (see, e.g., Tallman and Zaman, 2017; Stock and Watson, 2020; Borio et al., 2021). In contrast, goods inflation is typically discussed in terms of imported inflation (see, e.g., Clark, 2004; Linder et al., 2013) with China's growing role in the consumer goods market over the last 30 years, spurring a strand of work exploring how and whether inflation has become increasingly globalized (see, e.g., Kamin et al., 2006; Borio and Filardo, 2007; Bianchi and Civelli, 2015; Kamber and Wong, 2020). From this perspective, our approach of adopting the goods and services dichotomy also serves as a natural broad split to understand domestic and imported inflation.[4] At the same time, the shift in consumer spending patterns that followed government policies to contain the spread of COVID-19 has placed the goods and services split at the forefront of the current debate on inflation dynamics.[5]

The remainder of this paper proceeds as follows: Section 2 describes the Two-Sector UC-SV model. Section 3 presents the results from our model. Section 4 extends our analysis to considering other approaches. Section 5 concludes.

2 A Two-Sector UC-SV Model

We begin by describing our Two-Sector UC-SV model. We decompose goods inflation (π_t^G) and services inflation (π_t^S) into their corresponding sector-specific permanent ($\tau_t^G,\ \tau_t^S$) and transitory noise ($\zeta_t^G,\ \zeta_t^S$) components.[6] Formally, we have:

$$\pi_t^G = \tau_t^G + \zeta_t^G, \tag{1}$$

$$\pi_t^S = \tau_t^S + \zeta_t^S, \tag{2}$$

[4] We also relate to work which attempts to understand how important relative price changes are to understanding aggregate inflation (see Reis and Watson, 2010; Ahn and Luciani, 2021).

[5] For example, see the April 18, 2020 edition of The Economist, *"COVID-19 could lead to the return of inflation - eventually"*.

[6] We specify the transitory components as noise to keep our model specification as close as possible to that of Stock and Watson (2007), which helps with comparing relative to existing approaches. In Section A2.2 of the Online Appendix, we explore different specifications for the transitory component, such as allowing for some persistence, and discuss why our choice specification is still the preferred one.

where trends are modeled as driftless random walk processes:

$$\tau_t^G = \tau_{t-1}^G + u_t^{\tau^G}, \tag{3}$$

$$\tau_t^S = \tau_{t-1}^S + u_t^{\tau^S}. \tag{4}$$

The driftless random walk is a common modeling strategy in the trend inflation literature.[7] The driftless random walk assumption implies that the long-horizon forecasts of π_t^G and π_t^S are, respectively, τ_t^G and τ_t^S, which is consistent with the Beveridge and Nelson (1981) (BN) decomposition. The BN decomposition defines the trend component of time series as its long-horizon forecast based on information at time t, for each sector i, or, $\tau_t^i = \lim_{h\to\infty} \mathbb{E}_t \left[\pi_{t+h}^i\right]$. The BN decomposition is a convenient link to trend inflation work that constructs trend inflation by appealing to the BN decomposition under different modeling frameworks (e.g., Cogley et al., 2010; Kamber and Wong, 2020), but does not necessarily involve UC models.

Next, to allow for changes in the (conditional) volatility and correlation of the innovations $u_t^{\tau^i}$ and ζ_t^i for $i = G,\ S$, we specify the following covariance structure:

$$\begin{bmatrix} (u_t^{\tau^G},\ u_t^{\tau^S})' \\ (\zeta_t^G,\ \zeta_t^S)' \end{bmatrix} \sim \mathcal{N}\left(\begin{bmatrix} 0_{2\times 1} \\ 0_{2\times 1} \end{bmatrix} \begin{bmatrix} \Omega_{\tau,t} & 0_{2\times 2} \\ 0_{2\times 2} & \Omega_{\zeta,t} \end{bmatrix} \right), \tag{5}$$

where a triangular (or LDL) factorization of $\Omega_{\tau,t}$ and $\Omega_{\zeta,t}$ yields:

$$\Omega_{j,t} = \begin{bmatrix} \sigma^2_{j^G,t} & \sigma_{j,t} \\ \sigma_{j,t} & \sigma^2_{j^S,t} \end{bmatrix} = \begin{bmatrix} 1 & 0 \\ \gamma_t^j & 1 \end{bmatrix} \begin{bmatrix} \exp\left(h_t^{j^G}\right) & 0 \\ 0 & \exp\left(h_t^{j^S}\right) \end{bmatrix} \begin{bmatrix} 1 & \gamma_t^j \\ 0 & 1 \end{bmatrix} \quad \text{for } j \in \{\tau, \zeta\}. \tag{6}$$

Therefore, in addition to sector-specific trends, we introduce six new state variables, $(\gamma_t^\tau, \gamma_t^\zeta,\ h_t^{\tau^G}, h_t^{\tau^S}, h_t^{\zeta^G}, h_t^{\zeta^S})$, to accommodate changes in the correlation between, and volatility of goods and services inflation.[8]

[7] See Stock and Watson (2007) and works that build directly on theirs (e.g., Mertens, 2016; Chan et al., 2018, etc.). Shephard (2015) generalizes the random-walk assumption to martingale UC models.

[8] It is straightforward to see that time-varying correlation estimates, ρ_t^j, can be backed out from

Equations (5) and (6) embed much of the mechanism that drives our key results. Our goal is to examine the role of the goods and services sectors as sources of aggregate trend inflation volatility. Time-varying volatility in $u_t^{\tau^G}$ and $u_t^{\tau^S}$ accommodates the possibility that these sectors may become more (or less) relevant to understand overall trend volatility over time. Next, note from Equation (6), we define $\Omega_{\tau,t}$ as a full, rather than a diagonal, matrix. Such a parameterization allows for the possibility that variation in aggregate trend inflation reflects common dynamics between the goods and services sectors instead of relying exclusively on sector-specific volatilities. Moreover, time-varying correlation between $u_t^{\tau^G}$ and $u_t^{\tau^S}$ accommodates the possibility that these common dynamics might be more (or less) salient during different episodes. Finally, to avoid over-attributing changes in inflation second moments to its trend component, we parameterize the covariance matrix for the noise term ($\Omega_{\zeta,t}$) in a similar fashion as we do for $\Omega_{\tau,t}$.[9]

For completeness, we present the law of motion for the remaining state variables:

$$h_t^{j^i} = h_{t-1}^{j^i} + u_t^{h^{j^i}}, \quad j \in \{\tau, \zeta\}, i \in \{G, S\}, \tag{7}$$

$$\gamma_t^j = \gamma_{t-1}^j + u_t^{\gamma^j}, \quad j \in \{\tau, \zeta\}, \tag{8}$$

$$\begin{bmatrix} (u_t^{h^{\tau^G}}, \ u_t^{h^{\tau^S}}, \ u_t^{h^{\zeta^G}}, \ u_t^{h^{\zeta^S}})' \\ (u_t^{\gamma^\tau}, \ u_t^{\gamma^\zeta})' \end{bmatrix} \sim \mathcal{N}\left(\begin{bmatrix} 0_{4\times 1} \\ 0_{2\times 1} \end{bmatrix} \begin{bmatrix} \Omega_h & 0_{4\times 2} \\ 0_{2\times 4} & \Omega_\gamma \end{bmatrix} \right), \tag{9}$$

where

$$\Omega_h = \texttt{diag}\left(\sigma^2_{h^{\zeta^G}}, \ \sigma^2_{h^{\zeta^S}}, \ \sigma^2_{h^{\tau^G}}, \ \sigma^2_{h^{\tau^S}}\right) \text{ and } \Omega_\gamma = \texttt{diag}\left(\sigma^2_{\gamma^\zeta}, \ \sigma^2_{\gamma^\tau}\right). \tag{10}$$

Equation (6) by computing $\rho_t^j = \frac{\gamma_t^j \exp\left(h_t^{j^G}\right)}{\left\{\exp\left(h_t^{j^G}\right)\left[\gamma_t^{j^2}\exp\left(h_t^{j^G}\right)+\exp\left(h_t^{j^S}\right)\right]\right\}^{0.5}}$ for $j \in \{\tau, \zeta\}$.

[9] Following Stock and Watson (2007), we assume that inflation's permanent and transitory components are orthogonal, which is reflected in the block exogeneity assumption in Equation (5). Another possibility is to allow for correlations between the innovations driving the trends and the noise (within and across sectors). We leave this for future research, but note that Uzeda (2022) examines a related issue in the context of a univariate UC-SV model, and finds that a trend-noise correlation leads to measures of trend inflation that are similar to (survey-based) short-run inflation expectations. In contrast, the usual orthogonal trend-noise assumption leads to measures of trend inflation that are more in line with (survey-based) long-run inflation expectations; hence, it is closer to our interpretation of trend inflation in this study.

Equations (1)-(10) describe a bivariate state space model, with the measurement and state equations given by Equations (1)-(2) and (3)-(10), respectively. Aggregate trend inflation, τ_t, can be approximately calculated as a weighted average of sector-specific trends:

$$\tau_t \approx \omega_{G,t}\tau_t^G + \omega_{S,t}\tau_t^S, \tag{11}$$

where $\omega_{G,t}$ and $\omega_{S,t}$ are the expenditure weights of goods and services, respectively, and $\omega_t^G + \omega_t^S = 1$. These weights are not estimated; they denote nominal expenditure shares out of the total (nominal) personal consumption expenditures (PCE).[10]

2.1 Data and Estimation

Both goods and services inflation are constructed from seasonally adjusted deflators, as they are subcomponents of the U.S. PCE. Our data are from the FRED databank.[11] We annualize the first difference of the logarithms of the deflators to obtain the goods and services inflation rates. Our sample is for the period 1959Q1 to 2021Q4, i.e., $T = 258$ observations. The last 2 years at the end of the sample coincide with the COVID-19 pandemic and associated events such as global supply-chain disruptions as well as large unprecedented fiscal and monetary stimuli.

As our Two-Sector UC-SV model is a nonlinear state space model, we conduct the estimations using a Bayesian approach, as is common.[12] The states are estimated using precision sampling techniques as described in Chan and Jeliazkov (2009). In particular, the (log) volatility states (i.e., $h_t^{\tau^G}$, $h_t^{\tau^S}$, $h_t^{\zeta^G}$, and $h_t^{\zeta^S}$) are estimated by combining a precision sampler with the auxiliary mixture sampling method of Omori et al. (2007).

[10] Our aggregation approach follows Stock and Watson (2016). Moreover, Whelan (2002) shows that the Fisher index approach can be approximated by the Tornqvist formula, for which the weights at time t are given by the average of the nominal shares in periods t and $t-1$. The changes in nominal PCE shares quarter-on-quarter are very small (the average change in the weight for services has a mean of less than 0.001 with a standard deviation of 0.003), implying there is very little to no cost in ignoring these changes in weights.

[11] The FRED mnemonics for the goods and services deflators are DGDSRD3Q086SBEA and DSERRD3Q086SBEA, respectively. If we require the PCE deflator, for example, when we estimate the univariate UC-SV model, we use DPCERD3Q086SBEA. The FRED mnemonics for nominal expenditures for goods and services are DGDSRC1 and PCESV, respectively. We construct the weights as the nominal expenditure for goods or services divided by the total nominal expenditure for goods and services.

[12] A detailed description of the posterior sampling algorithm can be found in Section A1 of the Online Appendix.

Priors

There are three blocks of model parameters in our baseline Two-Sector UC-SV model to which priors are assigned. These blocks are the covariance matrices in Equation (10), i.e., $\Omega_h = \texttt{diag}\left(\sigma^2_{h^{\zeta^G}},\ \sigma^2_{h^{\zeta^S}},\ \sigma^2_{h^{\tau^G}},\ \sigma^2_{h^{\tau^S}}\right)$ and $\Omega_\gamma = \texttt{diag}\left(\sigma^2_{\gamma^\zeta},\ \sigma^2_{\gamma^\tau}\right)$, and the state initialization conditions collected as $\mathrm{z}_0 = \left(\tau_0^G\ \tau_0^S\ h_0^{\zeta^G}\ h_0^{\zeta^S}\ h_0^{\tau^G}\ h_0^{\tau^S}\ \gamma_0^\zeta\ \gamma_0^\tau\right)'$. We assume mutually independent priors for each parameter in these three blocks.

More precisely, we adopt an inverse-gamma prior for each (conditional) variance term in Ω_h and Ω_γ, i.e., $\sigma^2_{h^{\ell^i}} \sim \mathcal{IG}\left(\nu_{h^{\ell^i}},\ S_{h^{\ell^i}}\right)$ and $\sigma^2_{\gamma^\ell} \sim \mathcal{IG}\left(\nu_{\gamma^\ell},\ S_{\gamma^\ell}\right)$, for $\ell \in \{\zeta, \tau\}$ and $i \in \{G, S\}$, where we set $\nu_{h^{\ell^i}} = \nu_{\gamma^\ell} = \frac{T}{10}$ and $S_{h^{\ell^i}} = S_{\gamma^\ell} = 0.2^2(\nu_{h^{\ell^i}} - 1)$. The last expression implies $\mathbb{E}\sigma^2_{h^{\ell^i}} = \mathbb{E}\sigma^2_{\gamma^\ell} = 0.2^2$. In other words, we assume that the conditional variance for the states that govern second moments in our model are, on average, equivalent *a priori*. However, our priors are diffuse, as reflected in the calibration of the shape hyperparameters $\nu_{h^{\ell^i}} = \nu_{\gamma^\ell} = \frac{T}{10}$.[13] Lastly, we assume a diffuse Gaussian prior for the initial conditions, i.e., $\mathrm{z}_0 \sim \mathcal{N}\left(\widehat{\mathrm{z}_0}, \mathbf{\Sigma}_{z_0}\right)$, where $\widehat{\mathrm{z}_0} = \left(\pi_1^G,\ \pi_1^S,\ 0, \cdots, 0\right)'$ and $\mathbf{\Sigma}_{z_0} = 100 \times I_8$.

We note that our priors are comparable to those used in the extant trend inflation literature. The choice of hyperparameter calibration described above is guided by empirical research on U.S. inflation that relies on a similar modeling framework (e.g., Stock and Watson, 2007; Mertens, 2016; Stock and Watson, 2016; Chan et al., 2018). We also conduct a number of prior sensitivity checks to assess the robustness of our results. In particular, we allow for alternative prior calibrations and also change the class of prior distribution, which we report in Section A2.1 of the Online Appendix. We stress, however, that our key findings carry over to all prior sensitivity checks we conduct.

3 Results

We first present and discuss the estimates of both aggregate and sector-specific trend inflation before moving on to our key finding about the sources of variation in aggregate trend inflation.

[13] See, e.g., Kroese and Chan (2014), chapter 11 for details on the parametrization of the inverse gamma distribution which we adopt.

3.1 Sectoral and Aggregate Trend Inflation Estimates from a Two-Sector UC-SV

Figure 1: Estimated Aggregate Trend Inflation with a 67% Credible Interval

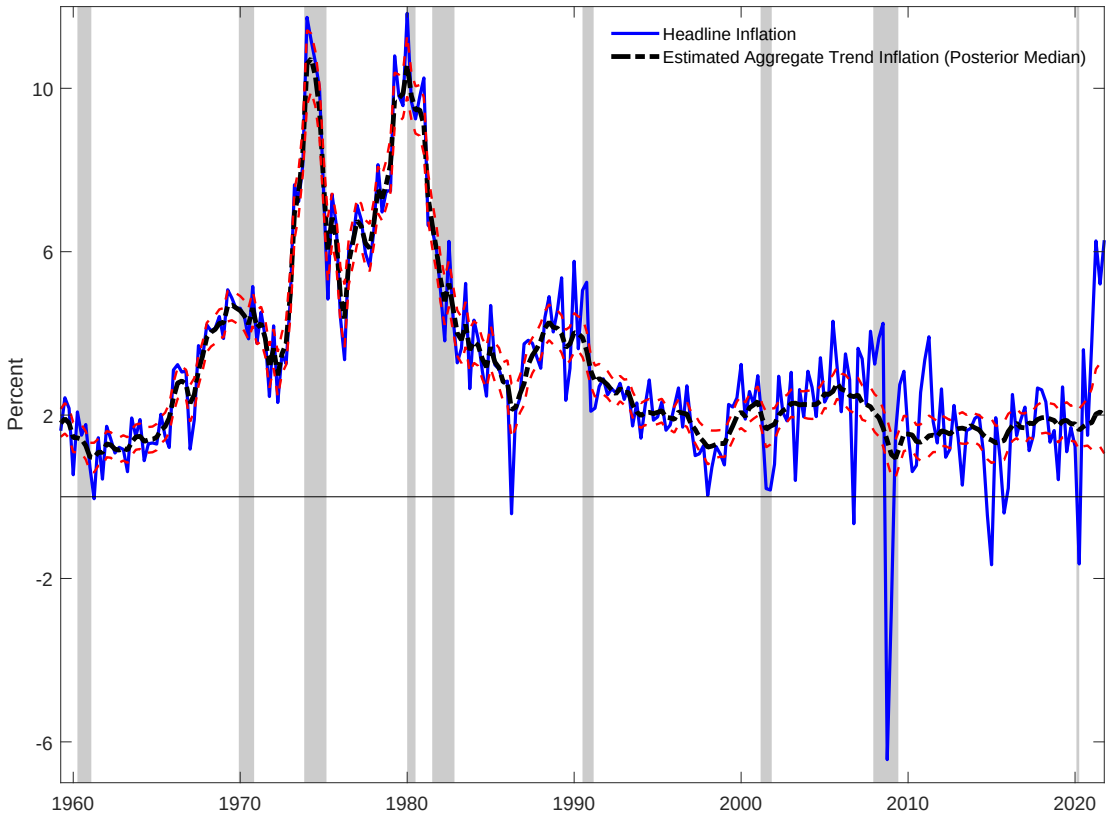

Notes: Headline inflation is the annualized quarter-on-quarter PCE inflation. The shaded areas denote NBER recession dates.

Figure 1 plots the (smoothed) estimates of aggregate trend inflation from the Two-Sector UC-SV model, together with PCE inflation. We report the posterior median as well as the 67% credible interval of our trend estimate. Overall, our trend inflation estimate broadly mimics the history of postwar U.S. inflation. In particular, trend inflation peaked during the Great Inflation in the 1970s, and began to disinflate in the early to mid-1980s. While there have been episodes of large swings in quarter-on-quarter headline inflation since the 1990s, trend inflation has remained low and stable.

Towards the end of our sample, our point estimates suggest that trend inflation has been

rising, albeit modestly, since the beginning of the COVID-19 pandemic and sits slightly above two percent. We do, however, document a widening of the posterior credible interval towards the end of the sample. Since the sudden shift in inflation dynamics occurs at the end of the sample, it is less certain whether such a shift implies the early stages of a permanent change in inflation or a more transitory phenomenon, and is accordingly reflected in a greater degree of estimation uncertainty towards the end of the sample. Correspondingly, the credible interval of the estimated level of trend inflation at the end of the sample is between 1-4%, which is reasonably large. It is known that smoothed estimates have less estimation uncertainty relative to filtered estimates and that the smoothed and filtered estimate are equivalent for the final sample point. Nonetheless, the large degree of estimation uncertainty associated with the pandemic at the end of the sample is not just due to the presentation of smoothed estimates. Even if one only focused on filtered estimates, the width of the credible interval in 2021Q4 (the final sample point) is the largest it has been throughout the sample and is more than twice the average width of the filtered credible interval for the entire sample. Therefore, the wide credible interval at the end of the sample is not an issue of presenting smoothed, rather than filtered, estimates, but reflects estimation uncertainty that inherently stems from the inflation data associated with the pandemic.

Turning to our sector-specific results, Figure 2 presents the posterior median estimates and 67% credible interval of our sector-specific trends, together with the annualized quarter-on-quarter inflation in the goods and service sectors. Notably, estimates of sector-specific trend inflation are quite different when comparing their dynamics during the 1970s and early 1980s against the period from the mid-1980s onwards. In particular, during the 1970s both trend services and trend goods inflation are roughly equivalent to actual goods and services inflation, respectively. In contrast, the second half of our sample shows marked differences in the dynamics of sector-specific trend inflation. More precisely, while there has been a large degree of high frequency fluctuation in goods inflation since the 1990s, the sector-specific trend is essentially flat and features almost no variation. In contrast, trend services inflation has continued to closely track services inflation. We also observe that, akin to the aggregate case, sector-specific trends have been rising modestly since the onset of the COVID-19 pandemic. The relative lack of variation in trend goods inflation since the

Figure 2: Estimated Sectoral-Specific Trend Inflation

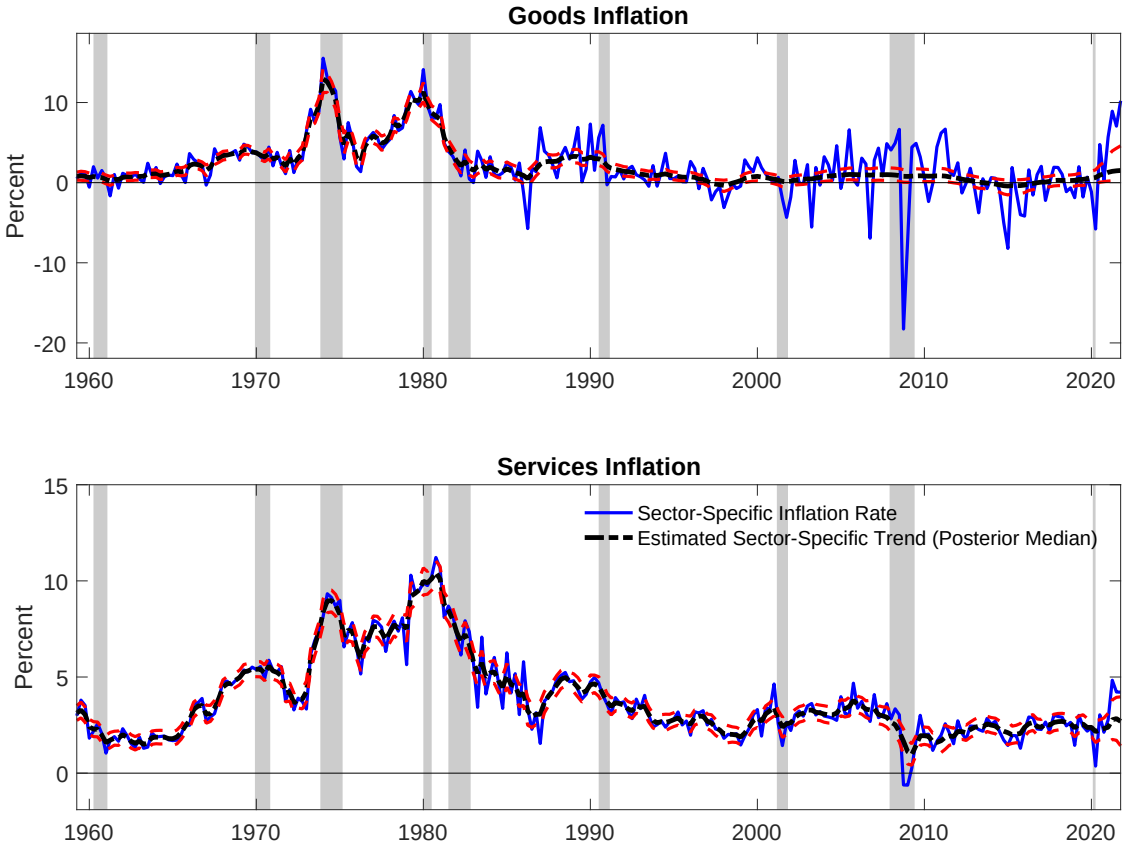

Notes: The solid lines are sector-specific annualized quarter-on-quarter inflation rates and the dotted lines represent our posterior median estimate of the sector-specific trend with its associated 67% credible interval. The shaded areas denote NBER recession dates.

1990s, despite goods inflation remaining extremely volatile, manifests in various guises and is a recurring theme as we report the results from our model.

The associated 67% credible interval suggests that our sector-specific trends are fairly precisely estimated throughout most of the sample, although we note (again) that the posterior bands become relatively wider towards the end of the sample. On a related note, due to the noisier nature of goods inflation, especially since the 1990s, trend detection may be intrinsically more challenging, which may manifest in wider posterior credible bands for trend goods inflation relative to its services counterpart. We find that the average width of the associated 95%, 67%, and 50% posterior credible intervals is approximately 20% wider for trend goods inflation (relative to services) over the whole sample. Therefore, we conclude

that while trend detection may be more challenging for goods relative to services inflation, it is not by a substantially large margin.

3.2 Sources of Variation in Aggregate Trend Inflation

We now turn to understanding the sources of variation in aggregate trend inflation. By expanding on Equation (11), the variance of aggregate trend inflation, *conditional* on information up to t-1 from the Two-Sector UC-SV model can be written as:[14]

$$var(\tau_{t|t-1}) \approx \omega_{G,t}^2 var(u_t^{\tau^G}) + \omega_{S,t}^2 var(u_t^{\tau^S}) + 2\omega_{G,t}\omega_{S,t} Cov(u_t^{\tau^G}, u_t^{\tau^S}). \tag{12}$$

Equation (12) shows that the Two-Sector UC-SV model naturally implies a simple decomposition where the conditional variance of aggregate trend inflation can be approximately decomposed into three components: the variances of the innovations to the goods and services sectors, and a covariance term that accounts for the comovement between the two sectors.

Figure 3 presents the decomposition of the estimated variance of aggregate trend inflation into the three components implied by Equation (12), which we denote as *Goods*, *Services*, and *Covariance*. The overall volatility has a hump-shaped pattern, as per the narrative by Stock and Watson (2007) (see also Cecchetti et al., 2007; Eo, 2016). All three components contributed to the total variance of aggregate trend inflation before the 1990s and especially so during the Great Inflation in the 1970s. However, since the 1990s, the goods and covariance components no longer contribute significantly to the variation in aggregate trend inflation. In other words, over the past three decades, the volatility of aggregate trend inflation has been driven (almost) exclusively by the services sector. Figure 3 also provides a context for why our estimates of trend inflation have only risen modestly during the COVID-19 pandemic presented in Figure 1. Because a large proportion of the increase in inflation during the COVID-19 pandemic has been associated with the disruption of global supply-chains, manifesting primarily as a surge in the prices of goods, our model interprets this rise in inflation as mostly characterized by transitory variation.

[14]Note that because trend inflation is a random walk, the (asymptotic) unconditional variance is not defined. Thus, when we mention the variance of trend inflation throughout the paper, we are, in fact, referring to its conditional variance.

Figure 3: Decomposition of Volatility of Aggregate Trend Inflation

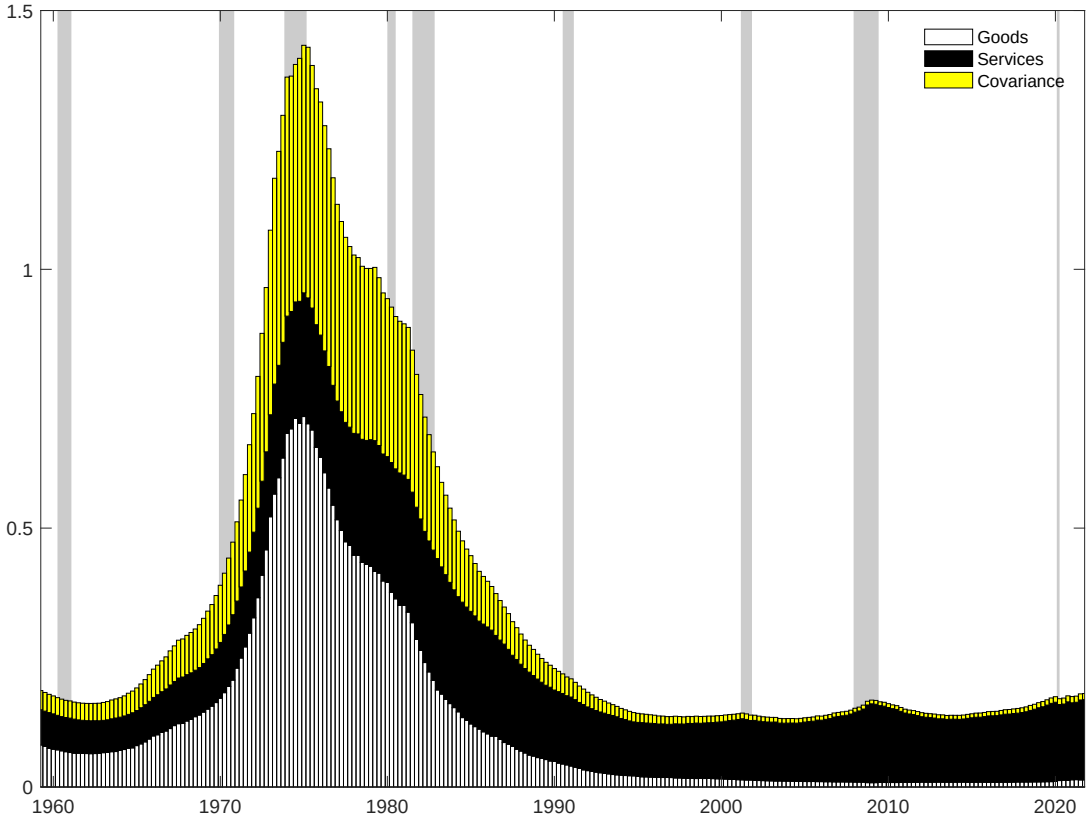

Notes: Trend inflation is in units of annualized quarter-on-quarter inflation. Goods, services, and covariance refer to the decomposition components of aggregate trend inflation, as presented in Equation (12). The shaded areas denote NBER recession dates.

Table 1 focuses on the overall volatility of trend inflation and sectoral contributions associated with Figure 3 for three selected periods, namely, 1975Q1, 2019Q4, and 2021Q4. We choose 1975Q1 as it coincides with the estimated peak in aggregate trend inflation volatility and 2019Q4 because it is the last pre-pandemic data point. Given the impact of the pandemic-related inflation surge towards the end of the sample, we also report results for 2021Q4 to provide some perspective on the effect the inflation surge has on estimates near the end of the sample. Panel (a) reports the relative contributions using the posterior median and 67% credible interval based on the estimates for each term in Equation (12). We note that the estimation uncertainty did increase with the COVID-19 period where the credible interval for the sectoral contributions in 2021Q4 relative to 2019Q4 are about 15% wider for services and the covariance term, and almost 40% larger for goods. Nevertheless,

Table 1: Decomposition of aggregate trend inflation volatility for selected periods

	(a) Sectoral contributions (%)		
	Goods	Services	Covariance
1975Q1	49.3	16.9	33.8
	[35.7, 70.2]	[11.9, 26.2]	[13.7, 42.3]
2019Q4	4.0	92.7	3.5
	[1.5, 13.4]	[71.3, 106.3]	[-13.2, 20.0]
2021Q4	5.0	90.1	4.9
	[1.7, 18.2]	[65.8 106.3]	[-16.0, 22.9]

	(b) Role of trend goods volatility in reducing aggregate volatility		
	Aggregate volatility	Counterfactual volatility	Share accounted for
1975Q1	1.450		
2019Q4	0.154	0.331	86%
2021Q4	0.158	0.332	86%

Notes: Panel (a): We report aggregate volatility and sectoral contributions based on Equation (12). All estimates denote the posterior median and their associated 67% credible interval (squared brackets) for the three selected periods (1975Q1 for the highest volatility period; 2019Q4 for the pre-COVID-19 period; 2021Q4 for the COVID-19 pandemic period). Sectoral contributions are measured as a percentage of aggregate volatility in the three selected periods. Note that while the sum of the contributions must equal 100%, the contribution of the covariance can be negative given the possibility of a negative covariance (i.e., a negative correlation), and subsequently, the sum of the goods and services contribution to sum over 100% to offset the negative contribution. Panel (b): Counterfactual volatility is the volatility of aggregate trend inflation if trend goods volatility is at its 2019Q4 or 2021Q4 levels, but keeping everything else constant. The final column represents the the percentage reduction in aggregate volatility that can be accounted for by just the fall in trend goods volatility.

even allowing for estimation uncertainty, our general conclusion about the dominance of trend services inflation still holds.

In panel (b) of Table 1, we calculate the counterfactual aggregate trend inflation volatility where only the volatility of trend goods inflation fell to 2019Q4 or 2021Q4 levels, but everything else stayed at 1975Q1 levels. We find that from 1975Q1 to 2019Q4, aggregate volatility, which fell from 1.450 to 0.154, would still have fallen to 0.331, implying that the decline in the volatility of trend goods inflation can account for 86% of the total reduction in the volatility of aggregate trend inflation. We note that this conclusion holds when considering 2021Q4 and allowing for any rise of trend good volatility associated with COVID-19. Put differently, our results suggest that the decrease in overall trend inflation volatility documented by Stock and Watson (2007) is largely driven by a sharp drop in the volatility of trend inflation for goods. Such a decline, in turn, underlies the flat dynamics for trend

goods inflation since the 1990s as shown in Figure 2.

Figure 4: Estimates of Time-Varying Second Moments for Trend Innovations

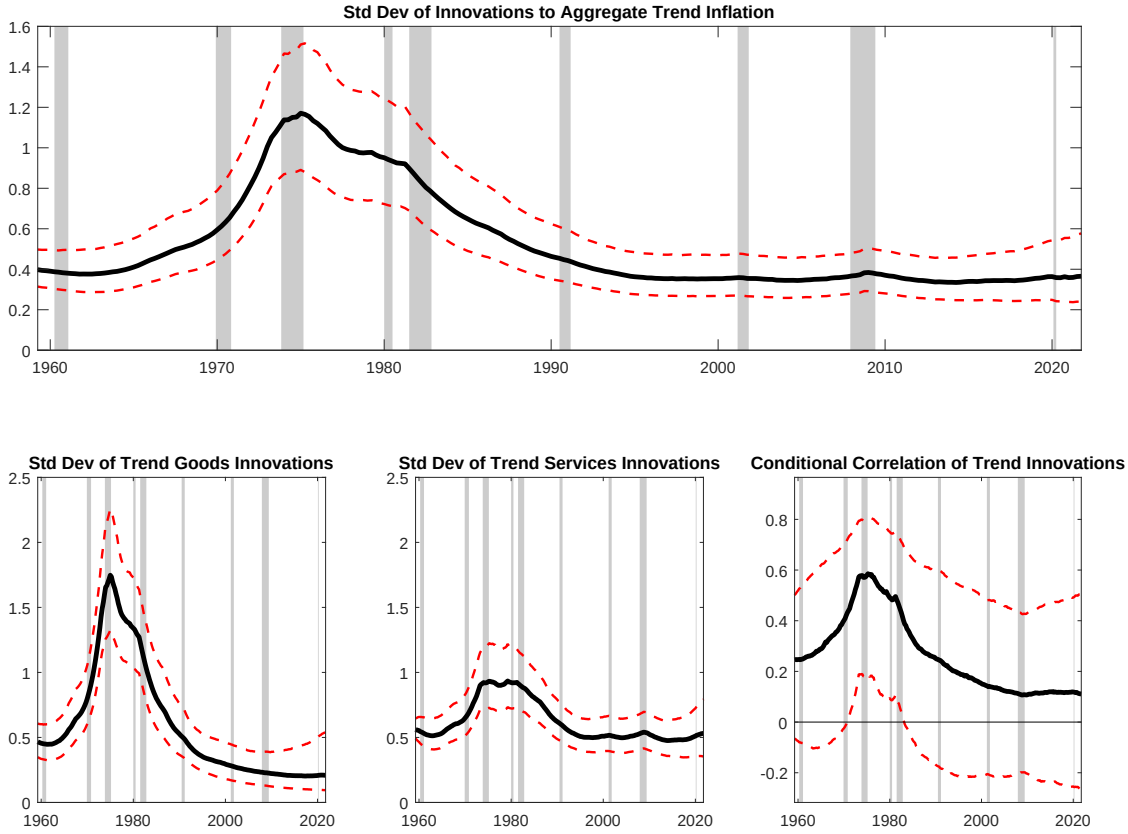

Notes: All (posterior median) estimates are plotted with their associated 67% posterior credible intervals. The shaded areas denote NBER recession dates.

For completeness, Figure 4 presents the estimated time-varying second-moments associated with trend inflation in each sector and the time-varying standard deviation of aggregate trend inflation.[15] Because the decomposition in Equation (12) is mechanically driven by the volatility of sector-specific trends and the correlation of trend innovations between both sectors, it is not surprising that the bottom panels in Figure 4 reiterate our findings in Figure 3. In other words, the standard deviation of the innovations to trend goods and services inflation (i.e., $std(u_t^{\tau^G})$ and $std(u_t^{\tau^S})$ in Equations (3) and (4)) exhibit the same hump-shaped pattern in Figure 3, although this pattern is much sharper and pronounced in

[15]Section A3 of the Online Appendix reproduces corresponding analysis for the transitory components.

the goods sector. Similarly, correlation between the innovations to the trends in both sectors was modest before the 1970s, but steadily rose during the Great Inflation. Thereafter, with the 1980s disinflation, the correlation in both sectors fell steadily and is essentially close to zero in the last two decades or so. We also show in Section A3 of the Online Appendix that our results are robust to considering core inflation measures. At the same time, our main result may also be more general than just the U.S. economy. In Section A6 of the Online Appendix, the same patterns in Figure 3 emerge for Australia and Canada, both of which are small open economies.

4 Comparison with Other Methods

There may be alternative approaches to conduct our analysis, including employing different models, considering further data disaggregation, or making use of simpler data smoothing methods. In the following sections, we compare our approach with these alternatives.

4.1 Univariate and Multi-Sector UC-SV Models

We begin by comparing our estimates of aggregate trend inflation relative to two approaches in the broader literature, namely the univariate UC-SV model by Stock and Watson (2007) (SW07 hereafter) and the multi-sector UC-SV factor model by Stock and Watson (2016) (SW16 hereafter). For ease of comparison, we present the specifications of aggregate trend inflation under these two alternative approaches compared to our approach:

$$\texttt{SW07:}\begin{cases} \tau_t = \tau_{t-1} + u_t^{\tau} \quad u_t^{\tau} \sim \mathcal{N}\left(0,\ \sigma_t^2\right), \end{cases} \tag{13}$$

$$\texttt{SW16:}\begin{cases} \tau_t = \sum_{i=1}^{17} w_{i,t}\tau_t^i \ s.t.\ \tau_t^i = \alpha_t^i \tau_t^c + \tau_t^{i,*}, \\ \tau_t^{i,*} = \tau_{t-1}^{i,*} + u_t^{i,*},\ \tau_t^c = \tau_{t-1} + u_t^c,\ \alpha_t^i = \alpha_{t-1}^i + u_t^{\alpha^i}, \\ u_t^{i,*} \sim \mathcal{N}\left(0,\ \sigma^2_{t,\tau^{i,*}}\right),\ u_t^c \sim \mathcal{N}\left(0,\ \sigma^2_{t,\tau^c}\right),\ u_t^{\alpha^i} \overset{i.i.d.}{\sim} \mathcal{N}\left(0,\ \sigma^2_{\alpha^i}\right), \\ u_t^{i,*},\ u_t^c,\ u_t^{\alpha^i} \text{ are mutually uncorrelated,} \end{cases} \tag{14}$$

$$\texttt{Two-Sector UC-SV:}\begin{cases} \tau_t = \sum_{i \in \{G,\ S\}} w_{i,t}\tau_t^i \ s.t.\ \tau_t^i = \tau_{t-1}^i + u_t^{\tau^i}, \\ \left(u_t^{\tau^G}\ u_t^{\tau^S}\right)' \sim \mathcal{N}\left(0,\ \Omega_{\tau,t}\right), \\ u_t^{\tau^G},\ u_t^{\tau^S} \text{ are correlated.} \end{cases} \tag{15}$$

From the expressions above, one can see that each model (or econometric strategy) implies a different parametrization for aggregate trend inflation (τ_t). As shown in Equation (13), SW07 defines τ_t as a latent univariate random walk process driven by an innovation, u_t^{τ}, that exhibits time-varying volatility. In their setting, τ_t is extracted directly from headline inflation. In contrast, SW16 and our framework model inflation subcomponents to recover τ_t. In particular, τ_t is obtained as the weighted average of sector-specific trends, τ_t^i, with the weights being the nominal expenditure shares, $w_{i,t}$, as discussed in Section 2. SW16 defines τ_t as the aggregation of seventeen sub-components of PCE inflation, while we recover τ_t from a more parsimonious, two-sector split.

The number of sectors, however, is not the key difference between our setting and SW16. In principle, one could consider the 17 sectors using our approach or model two sectors using the SW16 approach. However, the key difference is how comovement is specified. Building on the dynamic factor approach by Del Negro and Otrok (2008), SW16 defines sector-specific trends (τ_t^i) as the composition of three latent variables: (i) a common trend (or factor), τ_t^c, that captures common (low-frequency) dynamics across all inflation subcomponents; (ii) a time-varying loading, α_t^i, that captures the importance of common dynamics to the determination of each sector-specific trend; and (iii) an additional idiosyncratic trend component,

$\tau_t^{i,*}$, that captures (low-frequency) dynamics at the subcomponent-specific level. The innovations driving $\tau_t^{i,*}$, τ_t^c and α_t^i are mutually uncorrelated, with stochastic volatility applied to model the conditional variance of $\tau_t^{i,*}$ and τ_t^c. More precisely, SW16 introduces a common trend (τ_t^c) to model sectoral comovement in terms of *first-moment* dynamics, while we specify the same metric in terms of *second-moment* dynamics, captured by the time-varying covariance matrix $\Omega_{\tau,t}$ described in Equation (6). Notably, the aforementioned state parametrization for τ_t in SW16 entails estimating *five* state variables ($\tau_t^{i,*}$, τ_t^c, α_t^i plus two stochastic volatility states) to recover each sector-specific trend. This contrasts with our two-sector model, where each sector-specific trend corresponds to *three* state variables (i.e., estimating τ_t^i plus the conditional variance and conditional covariance associated with $u_t^{\tau^i}$). Section A5 in the Online Appendix offers a more formal comparison between our approach and SW16, but it suffices to note that in the two-sector case, our modeling strategy represents a more parsimonious strategy than the factor-based approach by SW16. On the other hand, in the seventeen-sector case, the number of states required to model covariances proliferates to the point that the factor-based approach by SW16 then becomes the more parsimonious (and computationally tractable) choice.

Implications for the Estimated Level of Aggregate Trend Inflation

Figure 5 presents the smoothed estimates of aggregate trend inflation obtained via our Two-Sector UC-SV and the other two approaches. We include the 67% credible interval from the Two-Sector UC-SV to provide a sense of the differences relative to these alternative approaches once we account for estimation uncertainty in our approach. In general, our Two-Sector UC-SV model produces aggregate trend inflation measures that are similar to the other two approaches. In fact, the estimates of aggregate trend inflation from both the SW07 and SW16 models have historically been largely within the credible interval of the Two-Sector UC-SV. This similarity provides external validation for our approach since it allows us to reproduce a key narrative of Stock and Watson (2007), namely the large fall in both the level and variance of aggregate trend inflation in the 1970s.

That said, the end of the sample sees a key point of departure where the aggregate trend inflation estimates from the SW07 and SW16 models rise and are beyond the estimation

Figure 5: Estimated Aggregate Trend Inflation from Different UC-SV Models

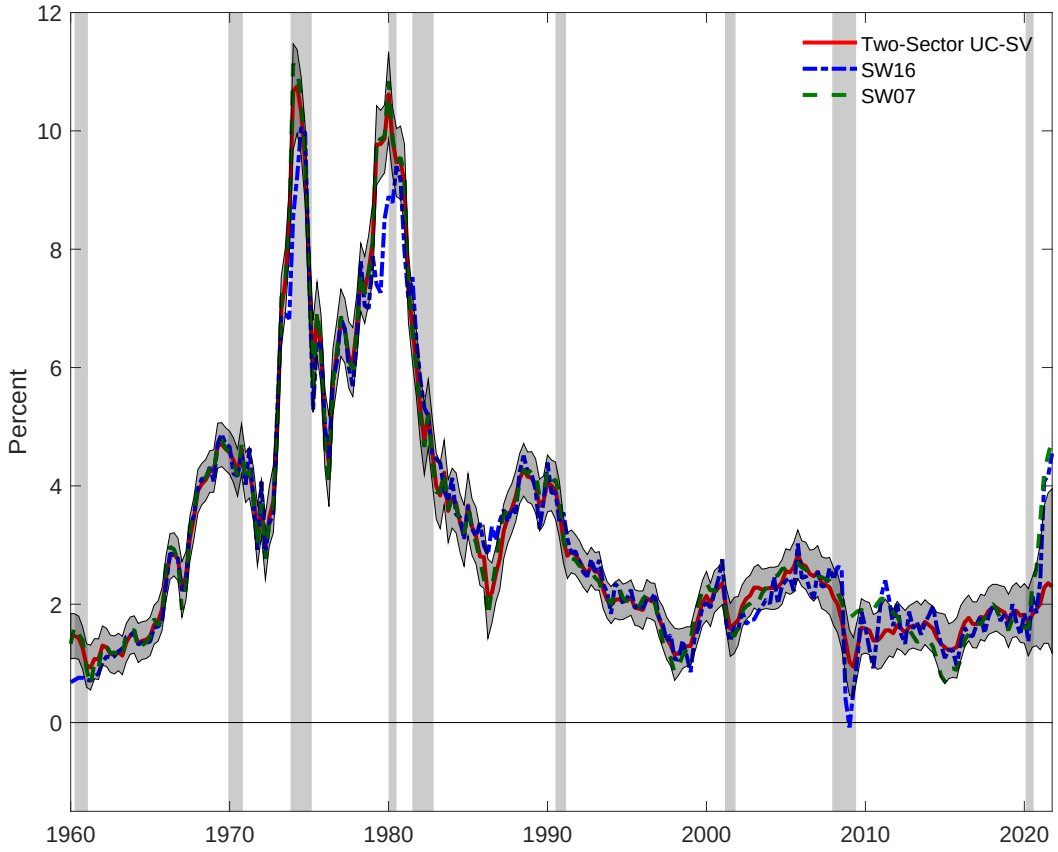

Notes: Headline inflation is the annualized quarter-on-quarter PCE inflation. SW07 and SW16 denote the estimated aggregate trend obtained from the univariate UC-SV and multivariate UC-SV models by Stock and Watson (2007) (Equation (13)) and Stock and Watson (2016) (Equation (14)), respectively. Two-Sector UC-SV denotes the estimate aggregate trend obtained from our baseline model discussed in Section 2. The shaded area around the red solid lines denotes the 67% posterior credible interval associated with the estimated trends from our model. The vertical shaded areas denote NBER recession dates.

uncertainty implied by the Two-Sector UC-SV. We make three observations on this front. First, the rising headline inflation at the end of the sample can partly be traced to supply-chain disruptions leading to elevated goods inflation. As a recurring theme throughout the paper, estimates of aggregate trend inflation do not rise as much, since the Two-Sector UC-SV is down-weighting the high goods inflation when determining aggregate trend inflation. This follows from the fact that the Two-Sector UC-SV still interprets goods inflation as largely transitory noise which contrasts to the other two approaches, where aggregate trend inflation has risen markedly. Second, while it is not clear how much trend inflation has risen

at the end of the sample, we show in section A4 of the Online Appendix, that the Two-Sector UC-SV produces trend inflation estimates that are more consistent with measured inflation expectations in 2021Q4, as also documented by Cascaldi-Garcia et al. (2022). Third, we previously documented an unprecedented increase in estimation uncertainty at the end of the sample. Once we consider the estimation uncertainty, there is substantial overlap between the 90% credible interval for aggregate trend inflation estimates for all three models at the end of the sample, and substantial overlap for even the 67% credible interval of the Two-Sector UC-SV and SW07 model.

For completeness, we also conduct an out-of-sample forecasting exercise using the three approaches. We present these results in Section A4 of the Online Appendix, but we note that our Two-Sector UC-SV produces very similar (and in some instances even slightly superior) forecasting performance relative to the other two models.[16]

In summary, perhaps the most important message from Figure 5 is that our Two-Sector UC-SV produces very similar aggregate trend inflation estimates throughout the sample compared to two alternative approaches. While the estimates diverge at the end of the sample, it is challenging at this point to make any definitive statement given the unprecedented estimation uncertainty of the level of trend inflation across all three models, coupled with the unique economic circumstances at the end of the sample.

Implications for the Estimated Level of Sector-Specific Trend Inflation

We also compare the estimated trends for goods and services inflation obtained from each of the three approaches. When using the univariate approach by SW07, we apply the specification of τ_t in Equation (13) to the observable measure of inflation in the goods and services sectors. To recover sector-specific trends at the two-sector level in the case of SW16, we sum (using the expenditure shares) the eight and nine subcomponent-specific trends (i.e., $\tau_t^{i,*}$ in Equation (14)) associated with the goods and services sectors, respectively. As shown in Figure 6, all three approaches generate reasonably similar measures of sector-specific trends. Analogous to the aggregate trend inflation results in Figure 5, the SW07 and SW16

[16]Section A3 of the Online Appendix also reports out-of-sample forecasting results where we fit the SW16 model to two sectors (i.e. goods and services) as in our baseline model.

Figure 6: Sector-Specific Trends from Different UC-SV Models

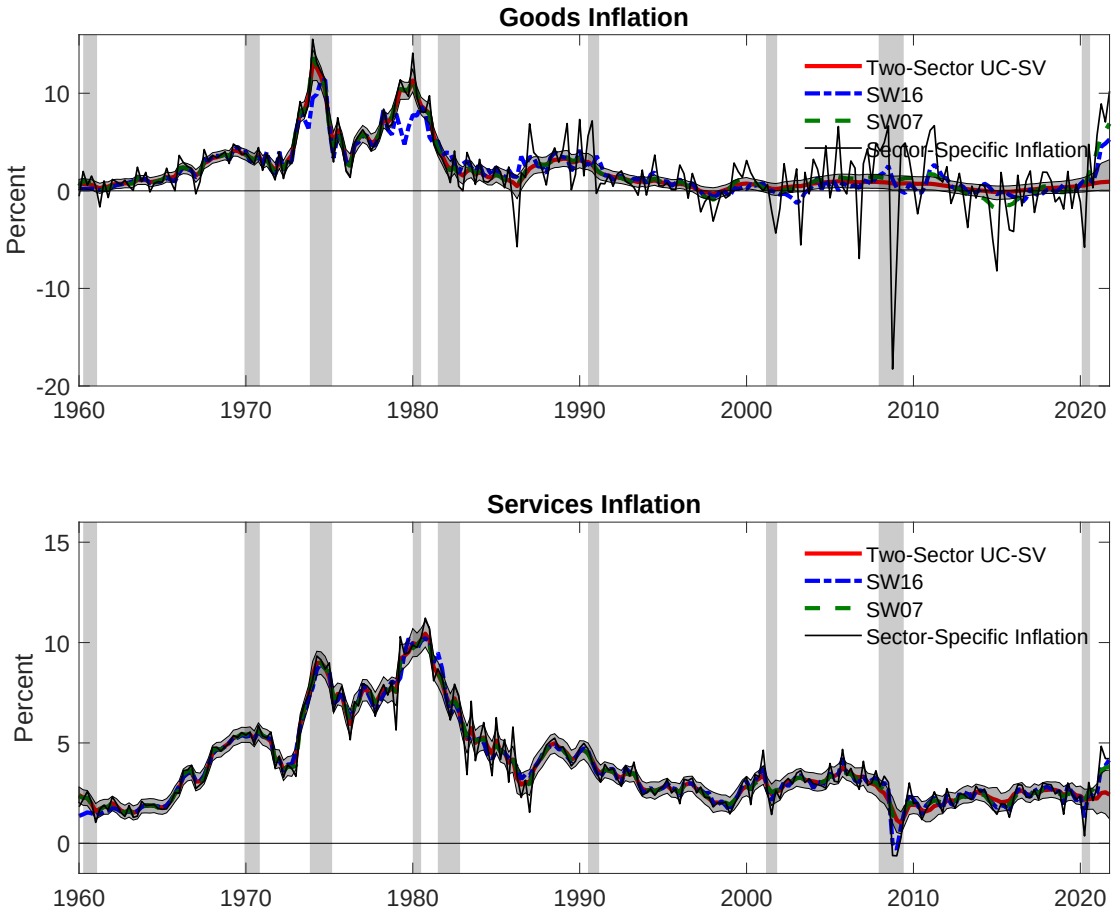

Notes: SW07 and SW16 denote the sector-specific trends obtained from the univariate UC-SV and multivariate UC-SV models by Stock and Watson (2007) and Stock and Watson (2016), respectively. Two-Sector UC-SV denotes the sector-specific trends obtained from our baseline model discussed in Section 2. When using the univariate approach in SW07, we apply the specification of τ_t in Equation (13) to the observable measure of inflation in the goods and services sectors. For SW16, sector-specific trends at the two-sector level are recovered by summing (using the expenditure shares) the eight and nine subcomponent-specific trends (i.e., $\tau_t^{i,*}$ in Equation (14)) associated with the goods and services sectors, respectively. The shaded area around the red solid lines denotes the 67% posterior credible intervals associated with the estimated trends from our model. The vertical shaded areas denote NBER recession dates.

approaches suggest a more noticeable rise in sector-specific trends towards the end of the sample, although the unprecedented estimation uncertainty associated with the COVID-19 pandemic once again makes it unclear about the precise level of the sector-specific trends towards the end of the sample.

Table 2: Decomposition of aggregate trend inflation volatility: results from different models for selected periods (percentage contribution)

	1975Q1		
Model	Goods	Services	Covariance
Two-Sector UC-SV	49.3	16.9	33.8
	[35.7, 70.2]	[11.9, 26.2]	[13.7, 42.3]
SW16	81.3	18.5	0.2
	[71.9, 97.8]	[14.1, 27.8]	[0.0, 0.5]
	2019Q4		
Model	Goods	Services	Covariance
Two-Sector UC-SV	3.9	91.3	4.8
	[1.5, 13.4]	[71.3, 106.3]	[-13.2, 20.0]
SW16	25.3	73.6	1.1
	[11.5, 43.2]	[55.7, 87.3]	[0.2, 3.2]
	2021Q4		
Model	Goods	Services	Covariance
Two-Sector UC-SV	5.0	90.1	4.9
	[1.7, 18.2]	[65.8, 106.3]	[-16.0, 22.9]
SW16	38.6	60.6	0.8
	[20.1, 59.3]	[37.8, 78.9]	[0.1, 2.6]

Notes: We report the contributions of goods, services, and covariance terms in Equation (12) to aggregate trend inflation volatility with the posterior median and the 67% credible interval (squared brackets) as a percentage of the volatility in the three selected periods (1975Q1 for the highest volatility period; 2019Q4 for the pre-COVID-19 period; 2021Q4 for the COVID-19 pandemic period). SW16 denotes the volatility decomposition results obtained from the factor-based approach in Stock and Watson (2016) when applied to a seventeen-sector split of inflation data. These results were computed using Equation A51 in Section A5.1.1 of the Online Appendix. Two-Sector UC-SV denotes the volatility decomposition results obtained from our baseline UC model discussed in Section 2. These results were computed using Equation (12).

Implications for Decomposing the Variance of Aggregate Trend Inflation

Table 2 reports the contribution from the goods and services sectors to the overall volatility of trend inflation from both the Two-Sector UC-SV and SW16 models. We report estimates for the same dates used in the exercises for Table 1: 1975Q1 (i.e., peak volatility), 2019Q4 (last pre-COVID-19 observation) and 2021Q4 (last observation in our sample). In short, using the SW16 model lends further support to the main finding that services inflation has been the main driver of trend inflation variation in recent years. In addition, like our model, Stock and Watson's (2016) framework reinforces the idea that the goods sector had a larger influence on trend inflation volatility in the 1970s.

We note some quantitative differences in the volatility decomposition between both

approaches. These differences, in part, reflect the different parametrization of trend inflation between both models, implying that the expression for the variance of aggregate trend inflation takes a different algebraic form in the SW16 setting relative to our expression in Equation (11) as discussed above. We present further details on how the different parametrizations of trend inflation imply different expressions for decomposing the variance of aggregate trend inflation in Section A5 of the Online Appendix. However, for now, intuitively, the states associated with common trend dynamics in SW16 (i.e., τ_t^c, α_t^i, and their corresponding conditional volatilities) play a similar role as the covariance term in our decomposition in Equation (11).

Regardless, we conclude that the key takeaway from Figure 6 and Table 2 is that our empirical finding on the importance of services inflation is neither specific to a particular class of model nor contingent on the level of data disaggregation.

4.2 Year-on-Year Measures of Sectoral Inflation

Finally, while we adopt a UC model to estimate the sector-specific trends, simpler smoothing approaches may lead to similar results. One approach commonly used by practitioners to address this issue is to look at the 1-year sectoral inflation rates (i.e., $100 \times \left[p_t^i - p_{t-4}^i\right]$, where p_t^i represents the log of the price index in sector i). Figure 7 reports these calculations against our sector-specific trends. While reasonably similar for services inflation, the 1-year measure for goods inflation is markedly different from our UC estimates in the latter part of the sample. In particular, 1-year goods inflation fluctuates significantly more than its UC (trend) counterpart, highlighting a potential drawback of using 1-year measures. Moreover, 1-year measures are (by construction) more likely to produce sharp and short-lived reversals, especially if the series is extremely volatile, which may seem counterintuitive when considering long-run (or trend) dynamics. A clear example is the large (but quickly reversed) drop in goods inflation during the 2008/09 financial crisis. To be clear, we are not advocating that 1-year measures are uninformative to understand inflation dynamics more broadly. Instead, we simply see the task of identifying the high- and low-frequency components of inflation as one that warrants formalizing a signal extraction approach, which a UC model does.

Figure 7: Comparison Relative to the 1-year (year-on-year) Sector-specific Inflation Rate

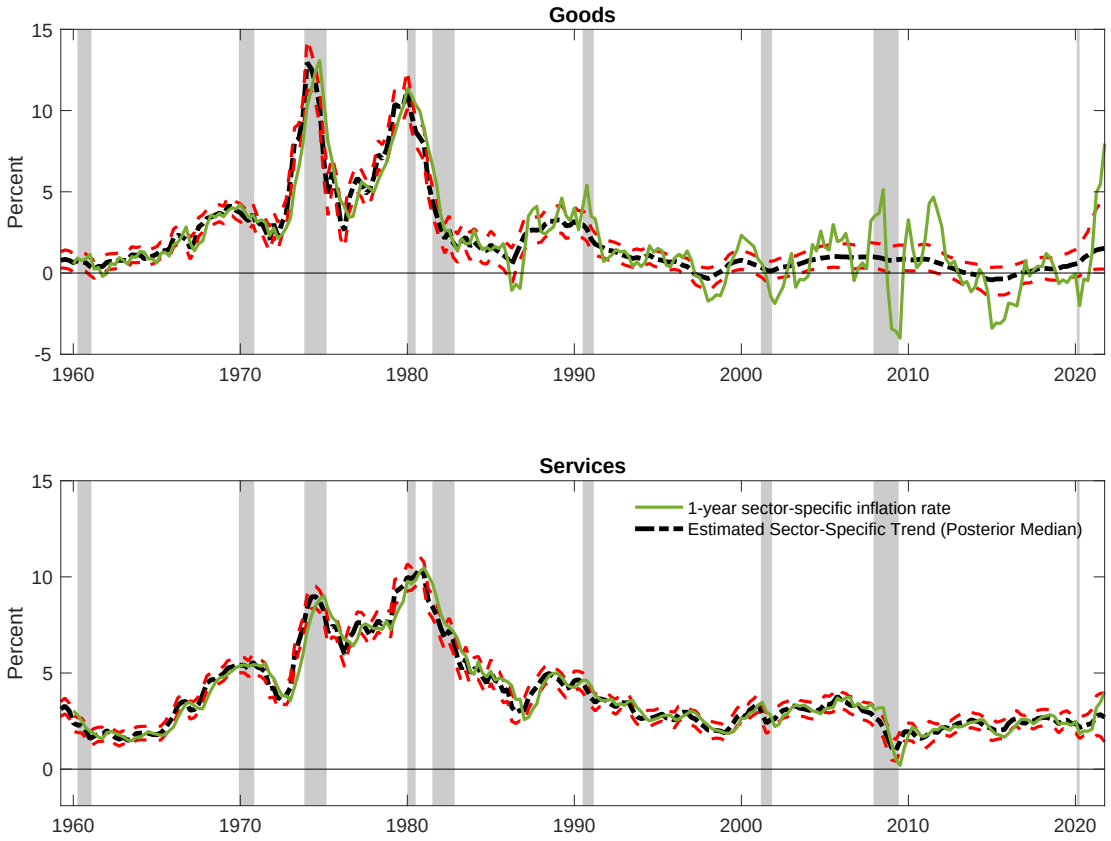

Notes: The dotted lines represent our posterior median estimate of the sector-specific trend with its associated 67% credible interval. 1-year sector-specific trend inflation is the year-on-year sector-specific inflation rate. The shaded areas denote NBER recession dates.

5 Conclusion

We develop an empirical two-sector model of trend inflation to understand the role of the goods and services sectors in explaining the dynamics of trend inflation. Our main finding is that variation in aggregate trend inflation is now predominantly driven by that in services inflation. This is a more recent occurrence, as before the 1990s, both the goods and services sectors contributed to the variation in aggregate trend inflation, with goods inflation being the main driver in the 1970s. A key change driving our main result is that, while overall goods inflation has remained volatile, the variance of trend goods inflation has fallen so sharply that we estimated trend goods inflation featuring little to no volatility since around

the 1990s. That is, the change in dynamics for the trend for goods inflation has been the most important driver of the decline in the volatility in overall inflation documented by Stock and Watson (2007). Notably, our results are also robust to the inclusion of the COVID-19 pandemic, albeit with a caveat of a larger degree of estimation uncertainty.

While the main focus of this paper is to document new stylized facts about changes in trend inflation volatility in the goods and services sectors and how these changes relate at an aggregate level, the interpretation and policy implications of our results remain more suggestive. First, because variation in goods inflation appears to be mostly transitory since the 1990s and potentially represents foreign inflation (see, e.g., Kamber and Wong, 2020; Luciani, 2020), it raises the issue of whether monetary policy should actively offset swings in goods, or more broadly foreign, inflation. This is especially true given that there are indications that goods and services inflation may respond very differently to monetary policy (see Cœuré, 2019; Borio et al., 2021) and to the general state of business cycles (Stock and Watson, 2020). Second, using more indirect evidence, Cecchetti et al. (2007) argue that the conduct of monetary policy can explain the large fall in the volatility in aggregate trend inflation. It is worth exploring whether one can reconcile the Cecchetti et al. (2007) narrative to potentially draw a more direct link to the conduct of monetary policy in understanding our key result. Third, our results may provide a starting point for considering cross-country and global determinants of inflation. As we report in the Online Appendix, similar patterns also hold for Australia and Canada, two small open economies, suggesting that our results may reflect a broader phenomenon beyond just the U.S. economy. We leave these avenues for future research.

Acknowledgement

The views expressed are those of the authors and do not necessarily reflect the position of the Bank of Canada. We thank the Editor, Marco Del Negro, five anonymous referees, Hie Joo Ahn, Todd Clark, Daniel de Munnik, José Dorich, Ippei Fujiwara, Stefano Gnocchi, Hanbaek Lee, Matteo Luciani, Eunseong Ma, James Morley, Rodrigo Sekkel, Etsuro Shioji, Shang-Jin Wei, Saeed Zaman as well as conference and seminar participants at the Bank of Canada,

the European Central Bank, the Bank of Korea, Korea University, Korea Development Institute, University of Melbourne, Reserve Bank of Australia, the 26^{th} Symposium of the Society for Nonlinear Dynamics and Econometrics, the 2018 Bayesian Analysis and Modeling Summer Workshop at the University of Melbourne, the 2019 Workshop of the Australasia Macroeconomic Society, the 2020 Monash Macro/Finance Workshop, the Virtual Australian Macroeconomic Seminar, the 2020 Hitotsubashi Summer Institute, and the 2021 St. Louis Fed Applied Time Series Econometrics Workshop for helpful comments and suggestions. This research is supported by the Australian Research Council (DP190100202 and DE200100693) and Korea University grant (K2109411). All remaining errors are our own.

References

Adam K, Weber H. 2019. Optimal trend inflation. *American Economic Review* **109**: 702–37.

Ahn HJ, Luciani M. 2021. Relative prices and pure inflation since the mid-1990s. Finance and Economics Discussion Series 2021-069, Board of Governors of the Federal Reserve System (U.S.).
URL https://ideas.repec.org/p/fip/fedgfe/2021-69.html

Ascari G, Sbordone AM. 2014. The macroeconomics of trend inflation. *Journal of Economic Literature* **52**: 679–739.

Baldwin R. 2022. Globotics and macroeconomics: Globalisation and automation of the service sector. In *ECB Forum on Central Banking*.

Beveridge S, Nelson CR. 1981. A new approach to decomposition of economic time series into permanent and transitory components with particular attention to measurement of the business cycle. *Journal of Monetary Economics* **7**: 151–174.

Bianchi F, Civelli A. 2015. Globalization and inflation: Evidence from a time varying VAR. *Review of Economic Dynamics* **18**: 406–433.

Borio C, Disyatat P, Xia D, Zakrajšek E. 2021. Monetary policy, relative prices and inflation control: Flexibility born out of success. *BIS Quarterly Review* .

Borio CEV, Filardo A. 2007. Globalisation and inflation: New cross-country evidence on the global determinants of domestic inflation. Technical report.

Cascaldi-Garcia D, López-Salido JD, Loria F. 2022. Is trend inflation at risk of becoming unanchored? The role of inflation expectations. FEDS Notes 2022-03-31, Board of Governors of the Federal Reserve System (U.S.).

Cecchetti SG, Hooper P, Kasman BC, Schoenholtz KL, Watson MW. 2007. Understanding the evolving inflation process. *US Monetary Policy Forum* .

Chan JC, Clark TE, Koop G. 2018. A new model of inflation, trend inflation, and long-run inflation expectations. *Journal of Money, Credit and Banking* **50**: 5–53.

Chan JC, Jeliazkov I. 2009. Efficient simulation and integrated likelihood estimation in state space models. *International Journal of Mathematical Modelling and Numerical Optimisation* **1**: 101–120.

Chan JCC, Koop G, Potter SM. 2013. A new model of trend inflation. *Journal of Business & Economic Statistics* **31**: 94–106.

Clark TE. 2004. An evaluation of the decline in goods inflation. *Economic Review-Federal Reserve Bank of Kansas City* **89**: 19–52.

Cœuré B. 2019. The rise of services and the transmission of monetary policy. *Speech at 21st Geneva Conference on the World Economy, 16 May 2019* .

Cogley T, Primiceri GE, Sargent TJ. 2010. Inflation-gap persistence in the US. *American Economic Journal: Macroeconomics* **2**.

Coibion O, Gorodnichenko Y. 2011. Monetary policy, trend inflation, and the Great Moderation: An alternative interpretation. *American Economic Review* **101**: 341–370.

Del Negro M, Otrok C. 2008. Dynamic factor models with time-varying parameters: Measuring changes in international business cycles. Technical report.

Draghi M. 2015. Global and domestic inflation. *Speech at Economic Club of New York, 4 December 2015* .

Eo Y. 2016. Structural changes in inflation dynamics: Multiple breaks at different dates for different parameters. *Studies in Nonlinear Dynamics & Econometrics* **20**: 211–231.

Hwu ST, Kim CJ. 2019. Estimating trend inflation based on unobserved components model: Is it correlated with the inflation gap? *Journal of Money, Credit and Banking* **51**: 2305–2319.

Ireland PN. 2007. Changes in the Federal Reserve's inflation target: Causes and consequences. *Journal of Money, credit and Banking* **39**: 1851–1882.

Kamber G, Wong B. 2020. Global factors and trend inflation. *Journal of International Economics* **122**: 103265.

Kamin SB, Marazzi M, Schindler JW. 2006. The impact of Chinese exports on global import prices. *Review of International Economics* **14**: 179–201.

Kozicki S, Tinsley PA. 2001. Shifting endpoints in the term structure of interest rates. *Journal of monetary Economics* **47**: 613–652.

Kroese DP, Chan JC. 2014. *Statistical modeling and computation*. Springer.

Linder MH, Peach R, Rich RW. 2013. The parts are more than the whole: Separating goods and services to predict core inflation. *Current Issues in Economics and Finance* **19**.

Luciani M. 2020. Common and idiosyncratic inflation. Finance and Economics Discussion Series 2020-024, Board of Governors of the Federal Reserve System (U.S.).

Mertens E. 2016. Measuring the level and uncertainty of trend inflation. *The Review of Economics and Statistics* **98**: 950–967.

Mishkin FS. 2007. Headline versus core inflation in the conduct of monetary policy. Business Cycles, International Transmission and Macroeconomic Policies Conference, HEC Montréal, Montréal, Canada, October 20, 2007.

Omori Y, Chib S, Shephard N, Nakajima J. 2007. Stochastic volatility with leverage: Fast and efficient likelihood inference. *Journal of Econometrics* **140**: 425–449.

Reis R, Watson MW. 2010. Relative goods' prices, pure inflation, and the Phillips correlation. *American Economic Journal: Macroeconomics* **2**: 128–157.

Shephard N. 2015. Martingale unobserved component models. In Koopman SJ, Shephard N (eds.) *Unobserved Components and Time Series Econometrics*. Oxford: Oxford University Press, 218–249.

Stock JH, Watson MW. 2007. Why has U.S. inflation become harder to forecast? *Journal of Money, Credit and Banking* **39**: 3–33.

Stock JH, Watson MW. 2016. Core inflation and trend inflation. *The Review of Economics and Statistics* **98**: 770–784.

Stock JH, Watson MW. 2020. Slack and cyclically sensitive inflation. *Journal of Money, Credit and Banking* **52**: 393–428.

Tallman EW, Zaman S. 2017. Forecasting inflation: Phillips curve effects on services price measures. *International Journal of Forecasting* **33**: 442–457.

Uzeda L. 2022. State correlation and forecasting: A Bayesian approach using unobserved components models. *Advances in Econometrics (Essays in Honor of Fabio Canova)* **46**: 22–53.

Whelan K. 2002. A guide to US chain aggregated NIPA data. *Review of Income and Wealth* **48**: 217–233.

Online Appendix to *Understanding Trend Inflation Through the Lens of the Goods and Services Sectors* *

Yunjong Eo[†] Korea University

Luis Uzeda[‡] Bank of Canada

Benjamin Wong[§] Monash University

Contents

*The views expressed are those of the authors and do not necessarily reflect the position of the Bank of Canada. All remaining errors are ours.

[†]Yunjong Eo: Department of Economics, Korea University, Seoul 02841, South Korea; Tel: +82 2 3290 2212; Email: yunjongeo@korea.ac.kr

[‡]Luis Uzeda: Bank of Canada, 234 Wellington Ave W, Ottawa, ON, K1A 0H9, Canada; Email: luzedagarcia@bank-banque-canada.ca

[§]Benjamin Wong: Department of Econometrics and Business Statistics, Monash University, Caulfield East, VIC 3145, Australia; Email: benjamin.wong@monash.edu

A1 Estimation Details

Estimation of the states in our model is carried out using precision sampling methods as in Chan and Jeliazkov (2009). Under this approach, the signal extraction exercise operates on a parametrization of the model in Section 2.1 where all observables and state variables are stacked over $t = 1, ..., T$. For convenience, below we reproduce the stacked representation of the two-sector UC model that we base our posterior sampler upon. Formally, we have

$$\mathbf{y} = \boldsymbol{\tau} + \boldsymbol{\zeta} \tag{A1}$$

$$\mathbf{L}_\tau \boldsymbol{\tau} = \boldsymbol{\tau}_0 + \mathbf{u}^\tau \tag{A2}$$

$$\mathbf{L}_h \mathbf{h} = \mathbf{h}_0 + \mathbf{u}^h \tag{A3}$$

$$\mathbf{L}_\gamma \boldsymbol{\gamma} = \boldsymbol{\gamma}_0 + \mathbf{u}^\gamma \tag{A4}$$

$$\begin{bmatrix} \boldsymbol{\zeta} \\ \mathbf{u}^\tau \\ \mathbf{u}^h \\ \mathbf{u}^\gamma \end{bmatrix} \sim \mathcal{N}\left(\begin{bmatrix} \mathbf{0} \\ \mathbf{0} \\ \mathbf{0} \\ \mathbf{0} \end{bmatrix}, \begin{bmatrix} \boldsymbol{\Sigma}_\zeta & \mathbf{0} & \mathbf{0} & \mathbf{0} \\ \mathbf{0} & \boldsymbol{\Sigma}_\tau & \mathbf{0} & \mathbf{0} \\ \mathbf{0} & \mathbf{0} & \boldsymbol{\Sigma}_h & \mathbf{0} \\ \mathbf{0} & \mathbf{0} & \mathbf{0} & \boldsymbol{\Sigma}_\gamma \end{bmatrix} \right), \tag{A5}$$

where:

$$\underset{(2T\times 1)}{\mathbf{y}} = \begin{bmatrix} (\pi_1^G, \cdots, \pi_T^G)' \\ (\pi_1^S, \cdots, \pi_T^S)' \end{bmatrix}, \underset{(2T\times 1)}{\boldsymbol{\tau}} = \begin{bmatrix} (\tau_1^G, \cdots, \tau_T^G)' \\ (\tau_1^S, \cdots, \tau_T^S)' \end{bmatrix}, \underset{(4T\times 1)}{\mathbf{h}} = \begin{bmatrix} (h_1^{\zeta^G}, \cdots, h_T^{\zeta^G})' \\ (h_1^{\zeta^S}, \cdots, h_T^{\zeta^S})' \\ (h_1^{\tau^G}, \cdots, h_T^{\tau^G})' \\ (h_1^{\tau^S}, \cdots, h_T^{\tau^S})' \end{bmatrix},$$

$$\underset{(2T\times 1)}{\boldsymbol{\gamma}} = \begin{bmatrix} (\gamma_1^\zeta, \cdots, \gamma_T^\zeta)' \\ (\gamma_1^\tau, \cdots, \gamma_T^\tau)' \end{bmatrix} \underset{(2T\times 1)}{\boldsymbol{\zeta}} = \begin{bmatrix} (\zeta_1^G, \cdots, \zeta_T^G)' \\ (\zeta_1^S, \cdots, \zeta_T^S)' \end{bmatrix} \underset{(2T\times 1)}{\mathbf{u}^\tau} = \begin{bmatrix} (u_1^{\tau^G}, \cdots, u_T^{\tau^G})' \\ (u_1^{\tau^S}, \cdots, u_T^{\tau^S})' \end{bmatrix},$$

$$\underset{(4T\times 1)}{\mathbf{u}^h} \begin{bmatrix} (u_1^{h^{\zeta^G}}, \cdots, u_T^{h^{\zeta^G}})' \\ (u_1^{h^{\zeta^S}}, \cdots, u_T^{h^{\zeta^S}})' \\ (u_1^{h^{\tau^G}}, \cdots, u_T^{h^{\tau^G}})' \\ (u_1^{h^{\tau^S}}, \cdots, u_T^{h^{\tau^S}})' \end{bmatrix}, \underset{(2T\times 1)}{\mathbf{u}^\gamma} = \begin{bmatrix} (u_1^{\gamma^\zeta}, \cdots, u_T^{\gamma^\zeta})' \\ (u_1^{\gamma^\tau}, \cdots, u_T^{\gamma^\tau})' \end{bmatrix}.$$

Initialization conditions are treated as additional parameters in our MCMC algorithm and collected as follows:

$$\underset{(2T\times 1)}{\boldsymbol{\tau}_0} = \begin{bmatrix} \tau_0^G \\ \tau_0^S \end{bmatrix} \otimes \begin{bmatrix} 1 \\ 0 \\ \vdots \\ 0 \end{bmatrix}, \underset{(4T\times 1)}{\mathbf{h}_0} = \begin{bmatrix} h_0^{\zeta^G} \\ h_0^{\zeta^S} \\ h_0^{\tau^G} \\ h_0^{\tau^S} \end{bmatrix} \otimes \begin{bmatrix} 1 \\ 0 \\ \vdots \\ 0 \end{bmatrix}, \underset{(2T\times 1)}{\boldsymbol{\gamma}_0} = \begin{bmatrix} \gamma_0^\zeta \\ \gamma_0^\tau \end{bmatrix} \otimes \begin{bmatrix} 1 \\ 0 \\ \vdots \\ 0 \end{bmatrix},$$

where $\otimes$ denotes the Kronecker operator. Next, the matrices pre-multiplying the vector of states are sparse structures defined as follows:

$$\underset{(2T\times 2T)}{\mathbf{L}_\tau} = \mathbf{L}_\gamma = \begin{bmatrix} \mathbf{H} & \mathbf{0} \\ \mathbf{0} & \mathbf{H} \end{bmatrix}, \quad \underset{(4T\times 4T)}{\mathbf{L}_h} = \begin{bmatrix} \mathbf{H} & \mathbf{0} & \mathbf{0} & \mathbf{0} \\ \mathbf{0} & \mathbf{H} & \mathbf{0} & \mathbf{0} \\ \mathbf{0} & \mathbf{0} & \mathbf{H} & \mathbf{0} \\ \mathbf{0} & \mathbf{0} & \mathbf{0} & \mathbf{H} \end{bmatrix}, \text{ such that}$$

$$\underset{(T\times T)}{\mathbf{H}} = \begin{bmatrix} 1 & 0 & 0 & \cdots & 0 \\ -1 & 1 & 0 & \cdots & 0 \\ 0 & -1 & 1 & & \vdots \\ \vdots & \vdots & \ddots & \ddots & \\ 0 & 0 & \cdots & -1 & 1 \end{bmatrix}.$$

Finally, each covariance matrix in the system is given by

$$\underset{(2T\times 2T)}{\mathbf{\Sigma}_\ell} = \begin{bmatrix} \exp(h_1^{\ell^G}) & \cdots & 0 & \gamma_1^\ell \exp(h_1^{\ell^G}) & \cdots & 0 \\ \vdots & \ddots & \vdots & \vdots & \ddots & \vdots \\ 0 & \cdots & \exp(h_T^{\ell^G}) & 0 & \cdots & \gamma_T^\ell \exp(h_T^{\ell^G}) \\ \gamma_1^\ell \exp(h_1^{\ell^G}) & \cdots & 0 & \gamma_1^{\ell^2} \exp(h_1^{\ell^G}) + \exp(h_1^{\ell^S}) & \cdots & 0 \\ \vdots & \ddots & \vdots & \vdots & \ddots & \vdots \\ 0 & \cdots & \gamma_T^\ell \exp(h_T^{\ell^G}) & 0 & \cdots & \gamma_T^{\ell^2} \exp(h_T^{\ell^G}) + \exp(h_T^{\ell^S}) \end{bmatrix}, \tag{A6}$$

for $\ell = \zeta$ and τ,

$$\underset{(4T\times 4T)}{\mathbf{\Sigma}_h} = \begin{bmatrix} \sigma^2_{h^{\zeta^G}} I_T & \mathbf{0} & \mathbf{0} & \mathbf{0} \\ \mathbf{0} & \sigma^2_{h^{\zeta^S}} I_T & \mathbf{0} & \mathbf{0} \\ \mathbf{0} & \mathbf{0} & \sigma^2_{h^{\tau^G}} I_T & \mathbf{0} \\ \mathbf{0} & \mathbf{0} & \mathbf{0} & \sigma^2_{h^{\tau^G}} I_T \end{bmatrix}, \tag{A7}$$

$$\underset{(2T\times 2T)}{\mathbf{\Sigma}_\gamma} = \begin{bmatrix} \sigma^2_{\gamma^\zeta} I_T & \mathbf{0} \\ \mathbf{0} & \sigma^2_{\gamma^\tau} I_T \end{bmatrix}, \tag{A8}$$

where I_T denotes a T dimensional identity matrix.

A1.1 Priors

For convenience, we reproduce below the priors adopted in our study and discussed in Section 2.1 of the paper. Recall that there are three blocks of model parameters in our baseline Two-Sector UC model, i.e.:

$$\mathrm{z}_0 = \begin{bmatrix} \tau_0^G \\ \tau_0^S \\ h_0^{\zeta G} \\ h_0^{\zeta S} \\ h_0^{\tau G} \\ h_0^{\tau S} \\ \gamma_0^{\zeta} \\ \gamma_0^{\tau} \end{bmatrix}, \; \Omega_h = \mathtt{diag}\left(\sigma^2_{h^{\zeta G}}, \; \sigma^2_{h^{\zeta G}}, \; \sigma^2_{h^{\tau G}}, \; \sigma^2_{h^{\tau G}}\right), \text{ and } \Omega_\gamma = \mathtt{diag}\left(\sigma^2_{\gamma^\zeta}, \; \sigma^2_{\gamma^\tau}\right).$$

We assume standard independent priors for each of these three blocks of parameters. More precisely:

$$\begin{aligned} &\mathrm{z}_0 \sim \mathcal{N}\left(\widehat{\mathrm{z}}_0, \mathbf{\Sigma}_{z_0}\right), \\ &\sigma^2_{\gamma^\ell} \sim \mathcal{IG}\left(\nu_{\gamma^\ell}, \; S_{\gamma^\ell}\right), \\ &\sigma^2_{h^{\ell i}} \sim \mathcal{IG}\left(\nu_{h^{\ell i}}, \; S_{h^{\ell i}}\right) \text{ for } \ell = \zeta \text{ and } \tau \text{ and } i = G \text{ and } S. \end{aligned}$$

The choice of prior densities adopted in this paper are in line with previous studies on trend inflation that also rely on UC-SV models (e.g., see Chan, Koop and Potter, 2013, 2016). We

calibrate our priors as follows:

$$\begin{cases} \widehat{\mathrm{z}_0} = \left(\pi_1^G,\ \pi_1^S,\ 0, \cdots, 0\right)', \\ \mathbf{\Sigma}_{z_0} = 100 \times I_8, \\ \nu_{\gamma^\ell} = \frac{T}{10}, \\ S_{\gamma^\ell} = 0.2^2(\nu_{\gamma^\ell} - 1), \\ \nu_{h^{\ell i}} = \frac{T}{10}, \\ S_{h^{\ell i}} = 0.2^2(\nu_{h^{\ell i}} - 1) \text{ for } \ell = \zeta \text{ and } \tau \text{ and } i = G \text{ and } S. \end{cases} \tag{A9}$$

Notably, the values assigned to $\mathbf{\Sigma}_{z_0}$ and to the shape parameters of the inverse-gamma densities – ν_{γ^ℓ} and $\nu_{h^{\ell i}}$ – reflect relatively uninformative priors.

A1.2 Posterior Sampler

Now let $\mathbf{Z} = \{\boldsymbol{\tau},\ \mathbf{h},\ \mathrm{z}_0,\ \Omega_h,\ \Omega_\gamma\}$ denote the set of states and parameters in our Two-Sector UC model, where notation $\mathbf{Z}_{-j}$ represents all elements in $\mathbf{Z}$ except for j. An MCMC algorithm for estimating such a model entails sequentially sampling from the following conditional posterior distributions:

(1) $f(\boldsymbol{\tau}|\mathbf{y}, \mathbf{Z}_{-\boldsymbol{\tau}})$,
(2) $f(\mathbf{h}|\mathbf{y}, \mathbf{Z}_{-\mathbf{h}})$,
(3) $f(\boldsymbol{\gamma}|\mathbf{y}, \mathbf{Z}_{-\boldsymbol{\gamma}})$,
(4) $f(\mathrm{z}_0|\mathbf{y}, \mathbf{Z}_{-\mathrm{z}_0})$,
(5) $f(\Omega_h|\mathbf{y}, \mathbf{Z}_{-\boldsymbol{\Omega_h}})$,
(6) $f(\Omega_\gamma|\mathbf{y}, \mathbf{Z}_{-\Omega_\gamma})$.

Steps 1 through 3 above denote the state simulation block in our MCMC – i.e. drawing the time-varying parameters. The remaining steps correspond to drawing from the full conditional posteriors for the fixed parameters. Hence, we refer to steps 4 through 6 as the parameter sampling block in our algorithm. Below, we describe these two main blocks in

greater detail.

A1.2.1 State Simulation

• *Sampling* $\boldsymbol{\tau}$

First note that Equations (A1) and (A2) denote a linear Gaussian state space representation. Therefore, standard multivariate regression results (see, e.g., Koop, Poirier and Tobias (2007)) can be used to show that the conditional posterior for $\boldsymbol{\tau}$ is also Gaussian. More precisely, we have:

$$\boldsymbol{\tau}|\mathbf{y}, \mathbf{Z}_{-\boldsymbol{\tau}} \sim \mathcal{N}\left(\overline{\mathbf{d}}_{\tau},\ \overline{\mathbf{D}}_{\tau}\right), \text{ where } \begin{cases} \overline{\mathbf{d}}_{\tau} = \overline{\mathbf{D}}_{\tau}\left(\boldsymbol{\Sigma}_{\zeta}^{-1}\mathbf{y} + \mathbf{L}_{\tau}'\boldsymbol{\Sigma}_{\tau}^{-1}\boldsymbol{\tau}_0\right), \\ \overline{\mathbf{D}}_{\tau} = \left(\boldsymbol{\Sigma}_{\zeta}^{-1} + \mathbf{L}_{\tau}'\boldsymbol{\Sigma}_{\tau}^{-1}\mathbf{L}_{\tau}\right)^{-1}. \end{cases} \tag{A10}$$

As shown in the second equation in (A10), sampling $\boldsymbol{\tau}$ entails inverting the $2T \times 2T$ matrix $\left(\boldsymbol{\Sigma}_{\zeta}^{-1} + \mathbf{L}_{\tau}'\boldsymbol{\Sigma}_{\tau}^{-1}\mathbf{L}_{\tau}\right)$ to construct the covariance matrix $\overline{\mathbf{D}}_{\tau}$. We do so by applying precision sampling techniques proposed in Chan and Jeliazkov (2009), which provides an efficient way to expedite computation.[1]

To illustrate how we employ their algorithm, we introduce the following notation: given a lower triangular $2T \times 2T$ non-singular matrix $\mathbf{C}$ and a $2T \times 1$ vector $\mathbf{b}$, let $\mathbf{C} \setminus \mathbf{b}$ denote the unique solution to the triangular system $\mathbf{Cx} = \mathbf{b}$ obtained by forward substitution, i.e., $\mathbf{x} = \mathbf{C} \setminus \mathbf{b} = \mathbf{C}^{-1}\mathbf{b}$. Sampling $\boldsymbol{\tau}$ is then conducted by following the four operations below:

$$\begin{aligned} &(1) \quad Chol(\overline{\mathbf{D}}_{\tau}^{-1}) = \mathbf{CC}', \\ &(2) \quad \mathbf{x} = \mathbf{C} \setminus \left(\boldsymbol{\Sigma}_{\zeta}^{-1}\mathbf{y} + \mathbf{L}_{\tau}'\boldsymbol{\Sigma}_{\tau}^{-1}\boldsymbol{\tau}_0\right), \\ &(3) \quad \overline{\mathbf{d}}_{\tau} = \mathbf{C}' \setminus \mathbf{x}, \\ &(4) \quad \boldsymbol{\tau} = \overline{\mathbf{d}}_{\tau} + \mathbf{C}' \setminus \mathbf{e} \qquad \mathbf{e} \sim \mathcal{N}\left(\mathbf{0},\ I_{2T}\right). \end{aligned}$$

The first step describes the Cholesky decomposition of the inverse covariance (or precision) matrix $\overline{\mathbf{D}}_{\tau}^{-1}$. Step 2 requires solving a triangular system by forward substitution, given that

[1] A detailed comparison between precision- and Kalman filter-based techniques for state simulation – pointing out the benefits of the former over the latter – can be found in McCausland, Miller and Pelletier (2011).

$\mathbf{C}$ is a lower triangular matrix. Step 3 is analogous to Step 2, except that the solution of the triangular system, $\mathbf{C}' \setminus \mathbf{x}$, is now obtained by backward substitution, since $\mathbf{C}'$ is an upper triangular matrix. It is then straightforward to see that Steps 2 and 3 combined, by construction, yield:

$$\overline{\mathbf{d}}_\tau = \mathbf{C}'^{-1}\left(\mathbf{C}^{-1}\left(\boldsymbol{\Sigma}_\zeta^{-1}\mathbf{y} + \mathbf{L}_\tau'\boldsymbol{\Sigma}_\tau^{-1}\boldsymbol{\tau}_0\right)\right) = \left(\mathbf{C}\mathbf{C}'\right)^{-1}\left(\boldsymbol{\Sigma}_\zeta^{-1}\mathbf{y} + \mathbf{L}_\tau'\boldsymbol{\Sigma}_\tau^{-1}\boldsymbol{\tau}_0\right) = \overline{\mathbf{D}}_\tau\left(\boldsymbol{\Sigma}_\zeta^{-1}\mathbf{y} + \mathbf{L}_\tau'\boldsymbol{\Sigma}_\tau^{-1}\boldsymbol{\tau}_0\right).$$

Finally, Step 4 describes an affine transformation of standard normal random vector $\mathbf{e}$ which ensures, by definition, that after sampling $\mathbf{e} \sim \mathcal{N}(\mathbf{0},\ I_{2T})$, the expression in such a step returns a $2T \times 1$ random vector $\boldsymbol{\tau}|\mathbf{y}, \mathbf{Z}_{-\boldsymbol{\tau}} \sim \mathcal{N}\left(\overline{\mathbf{d}}_\tau,\ \overline{\mathbf{D}}_\tau\right)$.

To further expedite computation, in addition to the precision sampling techniques, we resort to an analytical solution – instead of brute-force methods – to obtain the inverse matrices $\boldsymbol{\Sigma}_\zeta^{-1}$ and $\boldsymbol{\Sigma}_\tau^{-1}$ which are components of $\overline{\mathbf{D}}_\tau^{-1}$ and show up in Step 2 of the precision sampling algorithm just described above. In particular, both $\boldsymbol{\Sigma}_\zeta^{-1}$ and $\boldsymbol{\Sigma}_\tau^{-1}$ can be partitioned into four block-diagonal matrices, as follows:

$$\boldsymbol{\Sigma}_\ell = \begin{bmatrix} \boldsymbol{\Sigma}_{\ell^G} & \boldsymbol{\Sigma}_{\ell^{G,S}} \\ \boldsymbol{\Sigma}_{\ell^{G,S}} & \boldsymbol{\Sigma}_{\ell^S} \end{bmatrix}, \tag{A11}$$

where:

$$\begin{aligned}
\boldsymbol{\Sigma}_{\ell^G} &= \texttt{diag}\left(\exp(h_1^{\ell^G}), \cdots, \exp(h_T^{\ell^G})\right), \\
\boldsymbol{\Sigma}_{\ell^S} &= \texttt{diag}\left(\gamma_1^{\ell^2}\exp(h_1^{\ell^G}) + \exp(h_1^{\ell^S}), \cdots, \gamma_T^{\ell^2}\exp(h_T^{\ell^G}) + \exp(h_T^{\ell^S})\right), \\
\boldsymbol{\Sigma}_{\ell^{G,S}} &= \texttt{diag}\left(\gamma_1^{\ell}\exp(h_1^{\ell^G}), \cdots, \gamma_T^{\ell}\exp(h_T^{\ell^G})\right), \quad \text{for } \ell = \zeta \text{ and } \tau.
\end{aligned}$$

Matrix inversion results discussed in, e.g., Anderson (1984) yield:

$$\boldsymbol{\Sigma}_\ell^{-1} = \begin{bmatrix} \left(\boldsymbol{\Sigma}_{\ell^G} - \boldsymbol{\Sigma}_{\ell^{G,S}}\boldsymbol{\Sigma}_{\ell^S}^{-1}\boldsymbol{\Sigma}_{\ell^{G,S}}\right)^{-1} & -\left(\boldsymbol{\Sigma}_{\ell^G} - \boldsymbol{\Sigma}_{\ell^{G,S}}\boldsymbol{\Sigma}_{\ell^S}^{-1}\boldsymbol{\Sigma}_{\ell^{G,S}}\right)^{-1}\boldsymbol{\Sigma}_{\ell^{G,S}}\boldsymbol{\Sigma}_{\ell^S}^{-1} \\ -\boldsymbol{\Sigma}_{\ell^S}^{-1}\boldsymbol{\Sigma}_{\ell^{G,S}}\left(\boldsymbol{\Sigma}_{\ell^G} - \boldsymbol{\Sigma}_{\ell^{G,S}}\boldsymbol{\Sigma}_{\ell^S}^{-1}\boldsymbol{\Sigma}_{\ell^{G,S}}\right)^{-1} & -\boldsymbol{\Sigma}_{\ell^S}^{-1}\boldsymbol{\Sigma}_{\ell^{G,S}}\left(\boldsymbol{\Sigma}_{\ell^G} - \boldsymbol{\Sigma}_{\ell^{G,S}}\boldsymbol{\Sigma}_{\ell^S}^{-1}\boldsymbol{\Sigma}_{\ell^{G,S}}\right)^{-1}\boldsymbol{\Sigma}_{\ell^{G,S}}\boldsymbol{\Sigma}_{\ell^S}^{-1} \end{bmatrix},$$

for $\ell = \zeta$ and τ.

It is worth noting that, despite the long algebraic expressions above, constructing each

block matrix in $\mathbf{\Sigma}_\ell^{-1}$ only entails operations between diagonal matrices. As a result, an analytical solution for $\mathbf{\Sigma}_\ell^{-1}$ can be readily derived.[2] Specifically, we have

$$\text{(I)}\ \left(\mathbf{\Sigma}_{\ell^G} - \mathbf{\Sigma}_{\ell^G,S}\mathbf{\Sigma}_{\ell^S}^{-1}\mathbf{\Sigma}_{\ell^G,S}\right)^{-1} = \texttt{diag}\left(\frac{\gamma_1^{\ell^2}\exp(h_1^{\ell^G}) + \exp(h_1^{\ell^S})}{\exp(h_1^{\ell^G} + h_1^{\ell^S})}, \cdots, \frac{\gamma_T^{\ell^2}\exp(h_T^{\ell^G}) + \exp(h_T^{\ell^S})}{\exp(h_T^{\ell^G} + h_T^{\ell^S})}\right),$$

$$\text{(II)}\ -\mathbf{\Sigma}_{\ell^S}^{-1}\mathbf{\Sigma}_{\ell^G,S}\left(\mathbf{\Sigma}_{\ell^G} - \mathbf{\Sigma}_{\ell^G,S}\mathbf{\Sigma}_{\ell^S}^{-1}\mathbf{\Sigma}_{\ell^G,S}\right)^{-1}\mathbf{\Sigma}_{\ell^G,S}\mathbf{\Sigma}_{\ell^S}^{-1} =$$
$$= \texttt{diag}\left(\frac{\gamma_1^{\ell^2}\exp(2h_1^{\ell^G})}{\gamma_1^{\ell^2}\exp(2h_1^{\ell^G} + h_1^{\ell^S}) + \exp(h_1^{\ell^G} + 2h_1^{\ell^S})}, \cdots, \frac{\gamma_T^{\ell^2}\exp(2h_T^{\ell^G})}{\gamma_T^{\ell^2}\exp(2h_T^{\ell^G} + h_T^{\ell^S}) + \exp(h_T^{\ell^G} + 2h_T^{\ell^S})}\right),$$

$$\text{(III)}\ -\left(\mathbf{\Sigma}_{\ell^G} - \mathbf{\Sigma}_{\ell^G,S}\mathbf{\Sigma}_{\ell^S}^{-1}\mathbf{\Sigma}_{\ell^G,S}\right)^{-1}\mathbf{\Sigma}_{\ell^G,S}\mathbf{\Sigma}_{\ell^S}^{-1} = -\mathbf{\Sigma}_{\ell^S}^{-1}\mathbf{\Sigma}_{\ell^G,S}\left(\mathbf{\Sigma}_{\ell^G} - \mathbf{\Sigma}_{\ell^G,S}\mathbf{\Sigma}_{\ell^S}^{-1}\mathbf{\Sigma}_{\ell^G,S}\right)^{-1} =$$
$$= \texttt{diag}\left(\frac{\gamma_1^{\ell^2}\exp(h_1^{\ell^G}) + \exp(h_1^{\ell^S})}{\exp(h_1^{\ell^G} + h_1^{\ell^S})}, \cdots, \frac{\gamma_T^{\ell}\exp(h_T^{\ell^G})}{\exp(h_T^{\ell^G} + h_T^{\ell^S})}\right), \quad \text{for } \ell = \zeta \text{ and } \tau.$$

- *Sampling* $\mathbf{h}$

To sample log-volatilities $\mathbf{h}$, we combine the auxiliary mixture sampler approach of Omori et al. (2007) with the precision sampling techniques previously described. To this end, note first that we can reexpress equations (A1) and (A2) as

$$\begin{bmatrix} \mathbf{y} - \boldsymbol{\tau} \\ \mathbf{L}_\tau\boldsymbol{\tau} - \boldsymbol{\tau}_0 \end{bmatrix} = \begin{bmatrix} \mathbf{A}_\zeta & \mathbf{0} \\ \mathbf{0} & \mathbf{A}_\tau \end{bmatrix} \begin{bmatrix} \mathbf{\Lambda}_{h^\zeta} & \mathbf{0} \\ \mathbf{0} & \mathbf{\Lambda}_{h^\tau} \end{bmatrix} \boldsymbol{\varepsilon},$$
$$\begin{bmatrix} \mathbf{A}_\zeta & \mathbf{0} \\ \mathbf{0} & \mathbf{A}_\tau \end{bmatrix}^{-1} \begin{bmatrix} \mathbf{y} - \boldsymbol{\tau} \\ \mathbf{L}_\tau\boldsymbol{\tau} - \boldsymbol{\tau}_0 \end{bmatrix} = \begin{bmatrix} \mathbf{\Lambda}_{h^\zeta} & \mathbf{0} \\ \mathbf{0} & \mathbf{\Lambda}_{h^\tau} \end{bmatrix} \boldsymbol{\varepsilon}, \tag{A12}$$

[2] We also conducted estimations where $\mathbf{\Sigma}_\zeta^{-1}$ and $\mathbf{\Sigma}_\tau^{-1}$ were constructed via brute-force inversion. Results, as expected, are unchanged, albeit the MCMC sampler takes a bit longer to carry out state simulation.

where

$$\boldsymbol{\varepsilon} \sim \mathcal{N}\left(\mathbf{0},\ I_{4T}\right),$$

$$\mathbf{A}_\ell = \begin{bmatrix} I_T & \mathbf{0} \\ \texttt{diag}\left(\gamma_1^\ell, \cdots, \gamma_T^\ell\right) & I_T \end{bmatrix}, \tag{A13}$$

$$\mathbf{\Lambda}_{h^\ell} = \begin{bmatrix} \texttt{diag}\left(\exp(h_1^{\ell^G}), \cdots, \exp(h_T^{\ell^G})\right) & \mathbf{0} \\ \mathbf{0} & \texttt{diag}\left(\exp(h_1^{\ell^S}), \cdots, \exp(h_T^{\ell^S})\right) \end{bmatrix}, \tag{A14}$$

for $\ell = \zeta$ and τ.

Next, let $\widetilde{\mathbf{y}}_\tau$ and $\mathbf{v}$ denote the left- and right-hand side of Equation (A12), respectively. Squaring and subsequently taking natural logarithms of each element in the $4T \times 1$ vectors $\widetilde{\mathbf{y}}_\tau$ and $\mathbf{v}$ leads to the following linear state space representation for $\mathbf{h}$:

$$\widetilde{\mathbf{y}}_\tau^* = \mathbf{h} + \widetilde{\mathbf{v}}, \tag{A15}$$

$$\mathbf{L}_h \mathbf{h} = \mathbf{h}_0 + \mathbf{u}^h, \tag{A16}$$

where the state equation for $\mathbf{h}$ comes from (A3). The system above – albeit linear – is no longer Gaussian. More precisely, each entry in $\widetilde{\mathbf{v}}$ follows a log chi-square distribution with one degree of freedom. To bring the state space representation back to Gaussian form, Omori et al. (2007) suggest approximating the distribution of $\widetilde{\mathbf{v}}$ as a mixture of ten Normal densities.[3] Formally, let $\widetilde{\mathbf{v}}^*$ denote such mixture approximation, i.e.:

$$\widetilde{\mathbf{v}}^* \sim p_1 \mathcal{N}\left(\boldsymbol{\alpha}_1,\ \mathbf{\Sigma}_1\right) + \cdots + p_{10} \mathcal{N}\left(\boldsymbol{\alpha}_{10},\ \mathbf{\Sigma}_{10}\right),$$

where $\boldsymbol{\alpha}_s$, $\mathbf{\Sigma}_s$ and the component-density probabilities p_s for $s = 1, \cdots, 10$ are predetermined and given in Table 1 in Omori et al. (2007). Therefore, for a given particular component-density $\mathcal{N}\left(\boldsymbol{\alpha}_s,\ \mathbf{\Sigma}_s\right)$, the state space in (A15)-(A16) can be recast in (conditionally) Gaussian

[3] Their approach extends the seven-component auxiliary mixture sampling from Kim, Shephard and Chib (1998).

form as:

$$\widetilde{\mathbf{y}}_{\tau}^{*} = \mathbf{h} + \boldsymbol{\alpha}_{s} + \widetilde{\mathbf{v}}_{s}^{*}, \tag{A17}$$

$$\mathbf{L}_{h}\mathbf{h} = \mathbf{h}_{0} + \mathbf{u}^{h}, \tag{A18}$$

$$\begin{bmatrix} \widetilde{\mathbf{v}}_{s}^{*} \\ \mathbf{u}^{h} \end{bmatrix} \sim \mathcal{N}\left(\begin{bmatrix} \mathbf{0} \\ \mathbf{0} \end{bmatrix} \begin{bmatrix} \boldsymbol{\Sigma}_{s} & \mathbf{0} \\ \mathbf{0} & \boldsymbol{\Sigma}_{u^{h}} \end{bmatrix} \right). \tag{A19}$$

Given the parametrization above, our MCMC sampler needs to be augmented to sample both $\mathbf{h}$ and the vector of component-density indicators, $\mathbf{s}$. Formally, this entails sequentially sampling from the following full conditional posterior distributions:[4]

`Step` 1 $f(\mathbf{s}|\widetilde{\mathbf{y}}_{\tau}^{*}, \mathbf{Z})$,

`Step` 2 $f(\mathbf{h}|\widetilde{\mathbf{y}}_{\tau}^{*}, \mathbf{Z}_{-\mathbf{h}}, \mathbf{s})$.

•`Step` 1

The auxiliary sampler of Omori et al. (2007) allows each element of $\mathbf{s} = (s_1, \cdots, s_T)$ to be drawn independently from a multinomial distribution parameterized by the full conditional posterior probabilities $\mathbb{P}\mathrm{r}\left(s_t = i|\widetilde{y}_{\tau,t}^{*}, Z_t\right)$ given by:

$$\mathbb{P}\mathrm{r}\left(s_t = i|\widetilde{y}_{\tau,t}^{*}, z_t\right) = \frac{\psi\left(h_t + \alpha_{s=i},\ \sigma_{s=i}^{2}\right) p_{s=i}}{\sum_{j=1}^{10} \psi\left(h_t + \alpha_{s=j},\ \sigma_{s=j}^{2}\right) p_{s=j}} \quad \text{for } i = 1, \cdots, 10,$$

where $\psi\left(h_t + \alpha_s,\ \sigma_s^2\right)$ denotes a Gaussian density evaluated at mean $h_t + \alpha_s$ and variance σ_s^2. Again, α_s and σ_s^2 values are given in Table 1 in Omori et al. (2007). h_t denotes posterior draws obtained from (A20) as presented below.

Given $\mathbb{P}\mathrm{r}\left(s_t = i|\widetilde{y}_{\tau,t}^{*}, Z_t\right)$ posterior draws for s_t can then be generated via the inverse

[4]Here, Steps 1 and 2 are consistent with the discussion in Del Negro and Primiceri (2015) that applies more broadly for models with stochastic volatility.

transform method for $t = 1, \cdots, T$ as follows:[5]

(a) Generate $e_t \sim Uniform(0,\ 1)$,

(b) Find the smallest $i \in \{1, 2, \cdots, 10\}$ that satisfies $\sum_{j=1}^{i} \Pr\left(s_t = j | \widetilde{y}^*_{\tau,t}, Z_t\right) \geq e_t$,

(c) Return $\left(s_t | \widetilde{y}^*_{\tau,t}, Z_t\right) = i$.

•Step 2

$$\mathbf{h}|\widetilde{\mathbf{y}}^*, \mathbf{Z}, \mathbf{s} \sim \mathcal{N}\left(\overline{\mathbf{d}}_h,\ \overline{\mathbf{D}}_h\right), \text{ where } \begin{cases} \overline{\mathbf{d}}_h = \overline{\mathbf{D}}_h \left(\boldsymbol{\Sigma}_s^{-1} \widetilde{\mathbf{y}}^*_{\alpha} + \mathbf{L}_h' \boldsymbol{\Sigma}_{u^h}^{-1} \mathbf{h}_0\right), \\ \overline{\mathbf{D}}_h = \left(\boldsymbol{\Sigma}_s^{-1} + \mathbf{L}_h' \boldsymbol{\Sigma}_{u^h}^{-1} \mathbf{L}_h\right)^{-1}, \end{cases} \tag{A20}$$

where $\widetilde{\mathbf{y}}^*_{\alpha} = \widetilde{\mathbf{y}}^*_{\tau} - \mathbf{h} - \boldsymbol{\alpha}_s$. Draws from the density above are obtained using the precision sampler of Chan and Jeliazkov (2009).

• *Sampling* $\boldsymbol{\gamma}$

It's easy to see that the innovations in (A1) and (A2) can be factorized as follows:

$$\begin{bmatrix} \boldsymbol{\zeta} \\ \mathbf{u}^{\tau} \end{bmatrix} = \begin{bmatrix} \mathbf{A}_{\zeta} & \mathbf{0} \\ \mathbf{0} & \mathbf{A}_{\tau} \end{bmatrix} \begin{bmatrix} \boldsymbol{\zeta}_* \\ \mathbf{u}^{\tau}_* \end{bmatrix} \quad \text{s.t.} \tag{A21}$$

$$\begin{bmatrix} \boldsymbol{\zeta}_* \\ \mathbf{u}^{\tau}_* \end{bmatrix} \sim \mathcal{N}\left(\begin{bmatrix} \mathbf{0} \\ \mathbf{0} \end{bmatrix}, \begin{bmatrix} \boldsymbol{\Lambda}_{h^{\zeta}} & \mathbf{0} \\ \mathbf{0} & \boldsymbol{\Lambda}_{h^{\tau}} \end{bmatrix}\right).$$

Since $(\boldsymbol{\zeta},\ \mathbf{u}^{\tau})' = \left(\boldsymbol{\zeta}^G,\ \boldsymbol{\zeta}^S,\ \mathbf{u}^{\tau^G},\ \mathbf{u}^{\tau^S}\right)'$ and using the fact that both $\mathbf{A}_{\zeta}$ and $\mathbf{A}_{\tau}$ have a

[5] See algorithm 3.2 in Kroese, Taimre and Botev (2013) for a more detailed discussion of the inverse transform method for discrete random variables.

block-lower triangular structure – as shown in (A13) – then (A21) can be recast as:

$$\begin{bmatrix} \boldsymbol{\zeta}^G \\ \boldsymbol{\zeta}^S \\ \mathbf{u}^{\tau^G} \\ \mathbf{u}^{\tau^S} \end{bmatrix} = \begin{bmatrix} \boldsymbol{\zeta}^{\zeta^G} \\ \mathbf{X}_{\boldsymbol{\gamma}^\zeta}\boldsymbol{\zeta}^G + \boldsymbol{\zeta}^S_* \\ \mathbf{u}^{\tau^G} \\ \mathbf{X}_{\boldsymbol{\gamma}^\tau}\mathbf{u}^{\tau^G} + \mathbf{u}^{\tau^S}_* \end{bmatrix}, \tag{A22}$$

where $\mathbf{X}_{\boldsymbol{\gamma}^\ell} = \texttt{diag}\left(\gamma_1^\ell, \cdots, \gamma_T^\ell\right)$ for $\ell = \zeta$ and τ.

Given the block-lower triangular structure of $\mathbf{A}_\zeta$ and $\mathbf{A}_\tau$ and the modular nature of MCMC algorithms, one can collect the draws associated with the goods sector in $\boldsymbol{\tau}$ and $\boldsymbol{\tau}_0$ – i.e. $\boldsymbol{\tau}^G$ and $\boldsymbol{\tau}_0^G$, respectively – to back out $\boldsymbol{\zeta}^G = \mathbf{y}^G - \boldsymbol{\tau}^G$ and $\mathbf{u}^{\tau^G} = \mathbf{H}\boldsymbol{\tau}^G - \boldsymbol{\tau}_0^G$. As a result, these two vectors of innovations can be treated as predetermined controls in the second and fourth equations in (A22). Similarly, we back out $\boldsymbol{\zeta}^S$ and $\mathbf{u}^{\tau^S}$ on the left-hand side of (A22) by setting $\boldsymbol{\zeta}^S = \mathbf{y}^S - \boldsymbol{\tau}^S$ and $\mathbf{u}^{\tau^S} = \mathbf{H}\boldsymbol{\tau}^S - \boldsymbol{\tau}_0^S$ and treat these vectors of innovations as regressands in a standard linear regression setting. Consequently, by a simple change of variables, we can use the second and fourth equations in (A22) to obtain the following state space representation for $\boldsymbol{\gamma}$:[6]

$$\mathbf{e}^S = \mathbf{X}_{e^G}\boldsymbol{\gamma} + \mathbf{e}^S_*, \tag{A23}$$

$$\mathbf{L}_\gamma\boldsymbol{\gamma} = \boldsymbol{\gamma}_0 + \mathbf{u}^\gamma \tag{A24}$$

$$\begin{bmatrix} \mathbf{e}^S_* \\ \mathbf{u}^\gamma \end{bmatrix} \sim \mathcal{N}\left(\begin{bmatrix} \mathbf{0} \\ \mathbf{0} \end{bmatrix}, \begin{bmatrix} \boldsymbol{\Sigma}_{e^S_*} & \mathbf{0} \\ \mathbf{0} & \boldsymbol{\Sigma}_\gamma \end{bmatrix}\right), \tag{A25}$$

[6]To be clear, we refer to the following change of variables: $\mathbf{X}_{\boldsymbol{\gamma}^\zeta}\boldsymbol{\zeta}^G$ and $\mathbf{X}_{\boldsymbol{\gamma}^\tau}\mathbf{u}^{\tau^G}$ can be equivalently expressed as $\texttt{diag}\left(\zeta_1^G, \cdots, \zeta_T^G\right)\boldsymbol{\gamma}^\zeta$ and $\texttt{diag}\left(u_1^{\tau^G}, \cdots, u_T^{\tau^G}\right)\boldsymbol{\gamma}^\tau$, respectively.

where: $\mathbf{e}^S = \begin{bmatrix} \boldsymbol{\zeta}^S \\ \mathbf{u}^{\tau^S} \end{bmatrix}$, $\mathbf{e}^S_* = \begin{bmatrix} \boldsymbol{\zeta}^S_* \\ \mathbf{u}^{\tau^S}_* \end{bmatrix}$,

$$\boldsymbol{\Sigma}_{e^S_*} = \begin{bmatrix} \texttt{diag}\left(\exp(h_1^{\zeta^S}), \cdots, \exp(h_T^{\zeta^S})\right) & \mathbf{0} \\ \mathbf{0} & \texttt{diag}\left(\exp(h_1^{\tau^S}), \cdots, \exp(h_T^{\tau^S})\right) \end{bmatrix} \text{ and}$$

$$\mathbf{X}_{e^G} = \begin{bmatrix} \texttt{diag}\left(\zeta_1^G, \cdots, \zeta_T^G\right) & \mathbf{0} \\ \mathbf{0} & \texttt{diag}\left(u_1^{\tau^G}, \cdots, u_T^{\tau^G}\right) \end{bmatrix}.$$

Thus, standard regression results can be applied to the system in (A23)-(A25) to obtain the following expressions for the full conditional posterior for $\boldsymbol{\gamma}$:

$$\boldsymbol{\gamma}|\mathbf{y}, \mathbf{Z}_{-\boldsymbol{\gamma}} \sim \mathcal{N}\left(\overline{\mathbf{d}}_\gamma,\ \overline{\mathbf{D}}_\gamma\right), \text{ where } \begin{cases} \overline{\mathbf{d}}_\gamma = \overline{\mathbf{D}}_\gamma \left(\mathbf{X}'_{e^G} \boldsymbol{\Sigma}^{-1}_{e^S} \mathbf{e}^S + \mathbf{L}'_\gamma \boldsymbol{\Sigma}^{-1}_\gamma \boldsymbol{\gamma}_0\right), \\ \overline{\mathbf{D}}_\gamma = \left(\mathbf{X}'_{e^G} \boldsymbol{\Sigma}^{-1}_{e^S} \mathbf{X}_{e^G} + \mathbf{L}'_\gamma \boldsymbol{\Sigma}^{-1}_\gamma \mathbf{L}_\gamma\right)^{-1}. \end{cases} \tag{A26}$$

Again, to obtain draws from the density above, we apply precision sampling methods.

A1.2.2 Parameter Sampling

• *Sampling Ω_h and Ω_γ*

Recall that both Ω_h and Ω_γ are diagonal covariance matrices. Therefore, variance hyperparameters for the states $\mathbf{h}$ and $\boldsymbol{\gamma}$ can be sampled one by one from an inverse-gamma density. Formally, we have:

$$\sigma^2_{\gamma^\ell}|\mathbf{y}, \mathbf{Z}_{-\sigma^2_{\gamma^\ell}} \sim \mathcal{IG}\left(\overline{\nu}_{\gamma^\ell},\ \overline{S}_{\gamma^\ell}\right), \text{ where } \begin{cases} \overline{\nu}_{\gamma^\ell} = \frac{T}{2} + \nu_{\gamma^\ell}, \\ \overline{S}_{\gamma^\ell} = \frac{\sum_{t=1}^{T} \left(u_t^{\gamma^\ell}\right)^2}{2} + S_{\gamma^\ell} \quad \text{for } \ell = \zeta \text{ and } \tau, \end{cases} \tag{A27}$$

and

$$\sigma^2_{h^{\ell i}}|\mathbf{y},\mathbf{Z}_{-\sigma^2_{h^{\ell i}}} \sim \mathcal{IG}\left(\overline{\nu}_{h^{\ell i}},\ \overline{S}_{h^{\ell i}}\right),\ \text{where}\ \begin{cases} \overline{\nu}_{h^{\ell i}} = \frac{T}{2} + \nu_{h^{\ell i}}, \\ \overline{S}_{h^{\ell i}} = \frac{\sum_{t=1}^{T}\left(u_t^{h^{\ell i}}\right)^2}{2} + S_{h^{\ell i}} \quad \text{for } \ell = \zeta \text{ and } \tau \text{ and } i = G \text{ and } S, \end{cases} \tag{A28}$$

where $u_t^{h^{\ell i}}$ and $u_t^{\gamma^\ell}$ are the innovations in state Equations (7) and (8), respectively, in Section 2.1.

• *Sampling* z_0

Let $\mathbf{L}_0 = I_8 \otimes \iota_0$ where $\iota_0 = (1, 0, \cdots, 0)'$. The state equations (A2), (A3) and (A4) can then be expressed as

$$\mathbf{Lz} = \mathbf{L}_0 \mathrm{z}_0 + \mathbf{u}, \tag{A29}$$

where $\mathbf{z} = \begin{bmatrix} \boldsymbol{\tau} \\ \mathbf{h} \\ \boldsymbol{\gamma} \end{bmatrix}$, $\mathbf{L} = \begin{bmatrix} \mathbf{L}_\tau & \mathbf{0} & \mathbf{0} \\ \mathbf{0} & \mathbf{L}_h & \mathbf{0} \\ \mathbf{0} & \mathbf{0} & \mathbf{L}_\gamma \end{bmatrix}$ and $\mathbf{u} = \begin{bmatrix} \mathbf{u}^\tau \\ \mathbf{u}^h \\ \mathbf{u}^\gamma \end{bmatrix} \sim \mathcal{N}\left(\mathbf{0},\ \boldsymbol{\Sigma}_u\right)$, such that

$$\boldsymbol{\Sigma}_u = \begin{pmatrix} \boldsymbol{\Sigma}_\tau & \mathbf{0} & \mathbf{0} \\ \mathbf{0} & \boldsymbol{\Sigma}_h & \mathbf{0} \\ \mathbf{0} & \mathbf{0} & \boldsymbol{\Sigma}_\gamma \end{pmatrix}.$$

Combining (A29) with the Gaussian prior $\mathrm{z}_0 \sim \mathcal{N}\left(\widehat{\mathrm{z}_0}, \boldsymbol{\Sigma}_{z_0}\right)$ yields

$$\mathrm{z}_0|\mathbf{y},\mathbf{Z}_{-\mathrm{z}_0} \sim \mathcal{N}\left(\overline{\mathbf{d}}_{\mathrm{z}_0},\ \overline{\mathbf{D}}_{\mathrm{z}_0}\right),\ \text{where}\ \begin{cases} \overline{\mathbf{d}}_{\mathrm{z}_0} = \overline{\mathbf{D}}_{\mathrm{z}_0}\left(\mathbf{L}_0'\boldsymbol{\Sigma}_u^{-1}\mathbf{Lz} + \boldsymbol{\Sigma}_{z_0}\widehat{z_0}\right), \\ \overline{\mathbf{D}}_{\mathrm{z}_0} = \left(\mathbf{L}_0'\boldsymbol{\Sigma}_u^{-1}\mathbf{L}_0 + \boldsymbol{\Sigma}_{z_0}^{-1}\right)^{-1}. \end{cases} \tag{A30}$$

A2 Robustness

A2.1 Prior Sensitivity

The state variables that model changes in the conditional (log-) volatility (i.e., h^{ℓ^i} for $\ell = \zeta$ and τ and $i = G$ and S) play a key role in our exercise. It is thus important to assess if our main result is sensitive to the choice of priors adopted for the standard deviation of the innovations governing the dynamics of h^{ℓ^i}. We take two approaches to address this issue.

First, we set the scale hyperparameter of the associated inverse gamma prior to be up to five times greater than that in the baseline UC model. Formally, we redefine $S_{h^{\ell^i}}$ in (A9) as $S_{h^{\ell^i}} = \kappa 0.2^2(\nu_{h^{\ell^i}} - 1)$ such that $\kappa \in \{2,\ 3,\ 4,\ 5\}$. In other words, we allow for priors that are conducive to more flexible dynamics in the (conditional) variance of sector-specific trends.

Second, we replace the above-mentioned inverse gamma priors with uniform priors, i.e., $\sigma^2_{h^{\ell^i}} \sim U(0,\ 1)$ for $\ell = \zeta$ and τ and $i = G$ and S. The motivation for this particular check is twofold: (i) it mimics the prior choice of Stock and Watson (2016) for the same parameter; and (ii) it is in line with the critique by Gelman (2006) on the use of inverse gamma priors for variance parameters in the context of hierarchical models (such as ours). More precisely, posterior estimates may be overly influenced by the steep descent around zero that characterizes inverse gamma priors. Hence, the overall effect of such a feature depends on the behavior of the likelihood function near the origin.

Figures A1 and A2 shows the decomposition of the volatility of aggregate trend inflation (based on Equation (12) in Section 3.2 of the paper) that results from each of the prior checks discussed above. In short, our main result (i.e., the variation of trend inflation being dominated by services inflation since the 1990s) carries over to all prior-sensitivity checks considered.

Figure A1: Decomposition of Volatility of Aggregate Trend Inflation (Prior Check 1)

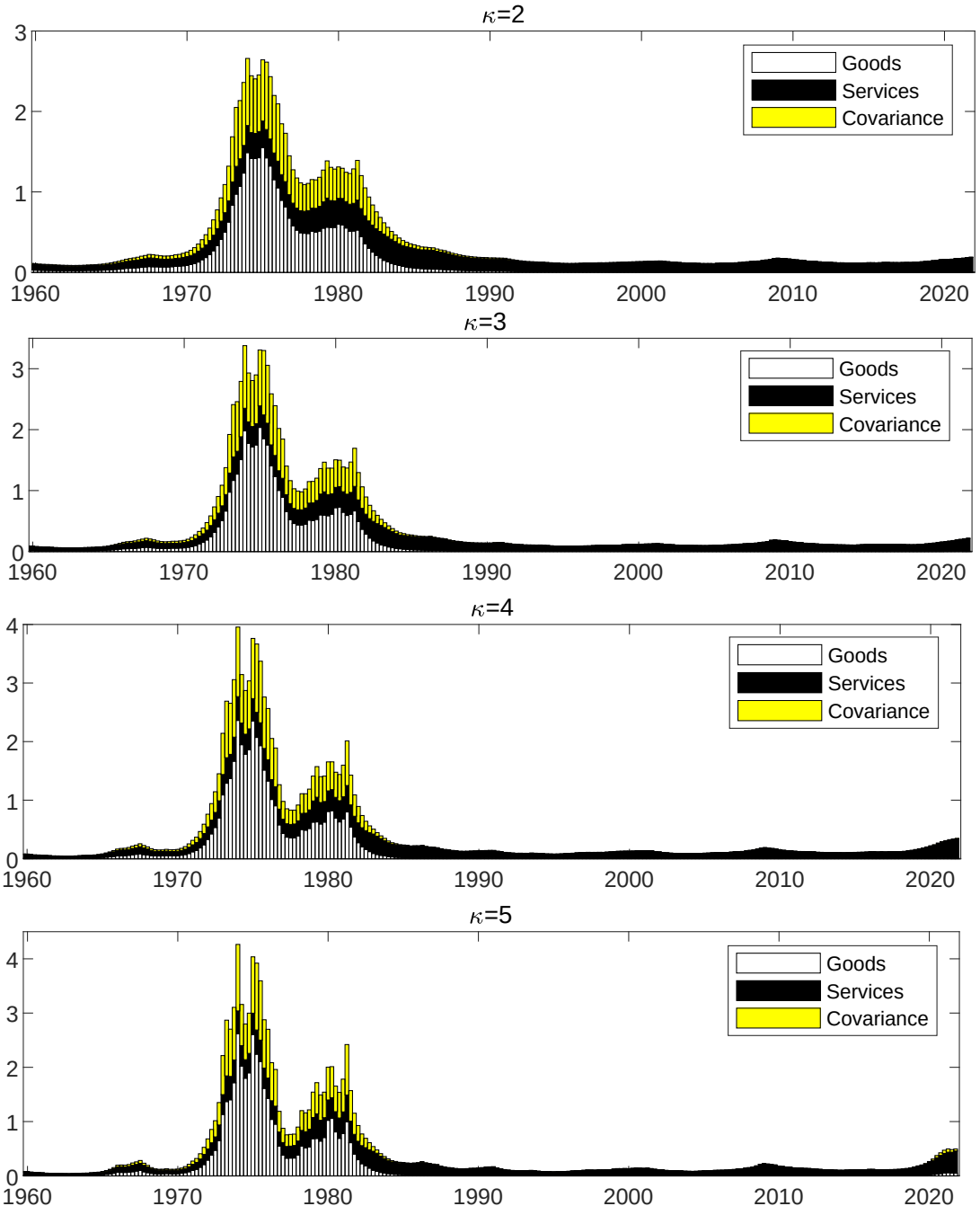

Notes: for prior check 1 we redefine the scale hyperparameter of the inverse gamma prior associated with (the variance of) the innovations driving all log-volatility states in (A9) *as* $S_{h^{\ell i}} = \kappa 0.2^2(\nu_{h^{\ell i}} - 1)$ *such that* $\kappa \in \{2,\ 3,\ 4,\ 5\}$. *The components of aggregate trend inflation are obtained using the decomposition presented in Equation (12) in the main text.*

Figure A2: Decomposition of Volatility of Aggregate Trend Inflation (Prior Check 2)

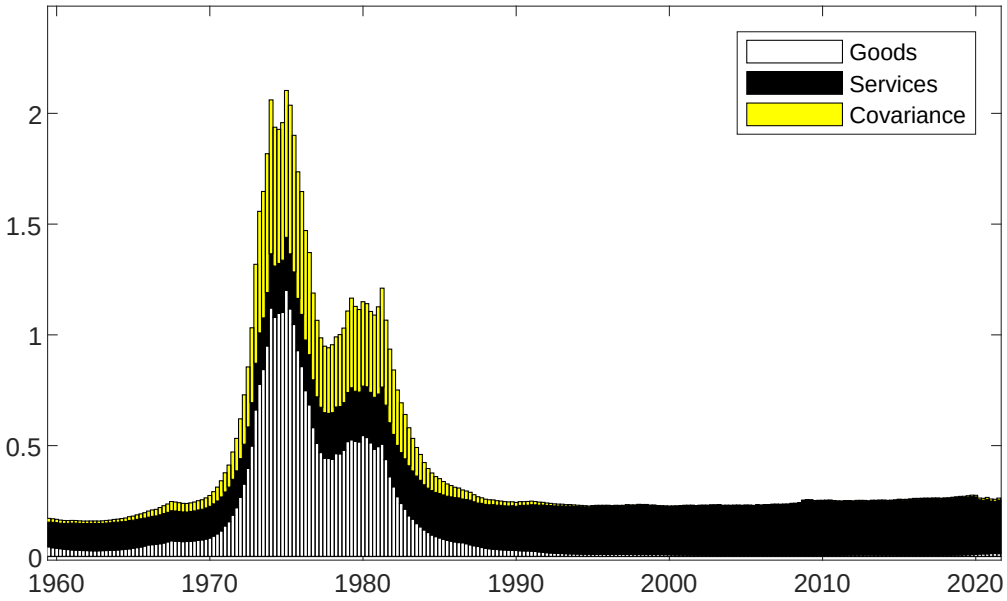

Notes: for prior check 2 we replace inverse gamma priors used in prior check 1 with uniform priors, i.e., $\sigma^2_{h^{\ell^i}} \sim U(0,\ 1)$ *for* $\ell = \zeta$ *and* τ *and* $i = G$ *and* S*. The components of aggregate trend inflation are obtained using the decomposition presented in Equation (12) in the main text.*

A2.2 Model Comparison: Allowing for Persistence in the Inflation Gap

Recall that our baseline model assumes that the transitory component of inflation in each sector follows a normally distributed serially uncorrelated process. To evaluate the ability of such a specification to fit inflation data, we conduct a model comparison exercise where we allow for persistence in the transitory component of (sector-specific) inflation. As discussed in Section 2.1 of the main text, we propose two alternatives to model sectoral inflation gap, c^i_t, for $i = G$ and S, namely – and similar to previous studies (e.g., see Chan, Koop and Potter, 2013, 2016) – gaps are modeled as an AR(1) and as a time-varying parameter (TVP) AR process, i.e.:

• **Two-Sector UC-SV-AR**

$$c_t^i = \phi^i c_{t-1} + \zeta_t^i, \quad \text{for } i = G \text{ and } S. \tag{A31}$$

• **Two-Sector UC-SV-TVP-AR**

$$c_t^i = \phi_t^i c_{t-1} + \zeta_t^i, \tag{A32}$$

$$\phi_t^i = \phi_{t-1}^i + u_t^{\phi^i}, \quad u_t^{\phi^i} \sim \mathcal{N}\left(0,\ \sigma_{\phi^i}^2\right) \text{ for } i = G \text{ and } S. \tag{A33}$$

Table (A1) reports estimates of the log marginal likelihood, which is the metric for model comparison we adopt. To compute the log marginal likelihood, we follow Geweke and Amisano (2011) and carry out a recursive one-step-ahead forecasting exercise.[7] Applying the usual recommendations for interpreting the Bayes factor – i.e. the ratio between the marginal likelihood from two competing models – as in, e.g., Raftery (1995), one can see that there is very strong evidence in favor of our assumption to model sector-specific inflation gaps a serially uncorrelated processes, thus reinforcing our choice to follow Stock and Watson (2007) and Stock and Watson (2016) on how to model the transitory component of inflation.

Table A1: Model comparison results based on predictive simulations

Identifier	Log Marginal Likelihood Estimates
Two-Sector UC-SV	**-2256.9**
Two-Sector UC-SV-AR	-2951.1
Two-Sector UC-SV-TVP-AR	-2960.2

We have also examined whether assuming alternative specifications for the transitory component of inflation would affect our main result. As shown in Figure (A3), introducing persistence in the transitory component of (sector-specific) inflation leaves our main result (i.e., since the 1990s variation in trend inflation has been driven almost entirely by the services sector) virtually unchanged.

[7] In this forecasting procedure, we start from the fifth observation in our sample for each sectoral inflation to reduce the sensitivity to priors.

Figure A3: Decomposition of Volatility of Aggregate Trend Inflation Under Different Specifications for the Inflation Gap

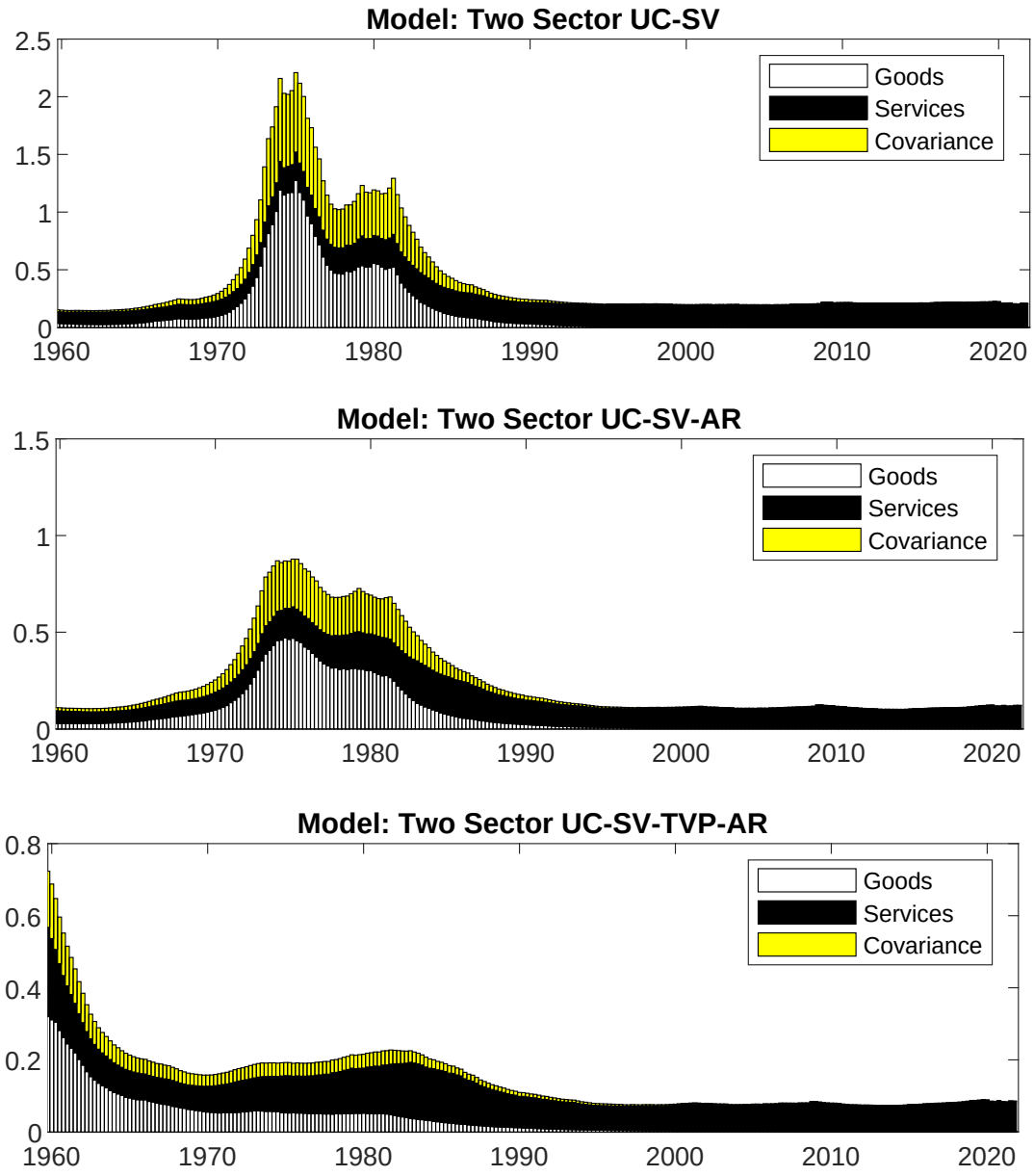

Notes: The components of aggregate trend inflation are obtained using the decomposition presented in Equation (12) in the main text.

A2.2.1 Extensions to the Baseline MCMC Algorithm

To accommodate an AR transitory component, we slightly modify the stacked representation in Equation (A1). In particular, for the Two-Sector UC-AR and Two-Sector UC-TVP-AR models we express the measurement equation as

$$\mathbf{y} = \boldsymbol{\tau} + \mathbf{c}, \tag{A34}$$

where

$$\underset{(2T\times 1)}{\mathbf{c}} = \begin{bmatrix} (c_1^G, \cdots, c_T^G)' \\ (c_1^S, \cdots, c_T^S)' \end{bmatrix}.$$

- *Two-Sector UC-SV-AR*

The only additional parameters in the case of the Two-Sector UC-AR model are the AR coefficients for the sector-specific gaps. The (stacked) representation of the state equation for $\mathbf{c}$ is given by

$$\mathbf{c} = \mathbf{X}_c\boldsymbol{\phi} + \boldsymbol{\zeta}, \tag{A35}$$

where

$$\underset{(2T\times 2)\ (2\times 1)}{\mathbf{X}_c\boldsymbol{\phi}} = \underbrace{\begin{bmatrix} 0 & 0 \\ c_1^G & 0 \\ \vdots & \vdots \\ c_{T-1}^G & 0 \\ 0 & 0 \\ 0 & c_1^S \\ \vdots & \vdots \\ 0 & c_{T-1}^S \end{bmatrix}}_{\mathbf{X}_c} \underbrace{\begin{bmatrix} \phi^G \\ \phi^S \end{bmatrix}}_{\boldsymbol{\phi}}.$$

We employ a Gaussian prior for $\boldsymbol{\phi}$. Specifically, we set $\boldsymbol{\phi} \sim \mathcal{N}(\boldsymbol{\mu}_\phi,\ \boldsymbol{\Sigma}_\phi)$ such that $\boldsymbol{\mu}_\phi = (0.5,\ 0.5)'$ and $\boldsymbol{\Sigma}_\phi = 10^{-3} \times I_2$. Combining such prior with (A35) yields the following full conditional posterior for $\boldsymbol{\phi}$:

$$\boldsymbol{\phi}|\mathbf{y}, \mathbf{Z}_{-\boldsymbol{\phi}} \sim \mathcal{N}\left(\overline{\mathbf{d}}_\phi,\ \overline{\mathbf{D}}_\phi\right), \text{ where } \begin{cases} \overline{\mathbf{d}}_\phi = \overline{\mathbf{D}}_\phi \left(\mathbf{X}_c' \boldsymbol{\Sigma}_\zeta^{-1} \mathbf{c} + \boldsymbol{\Sigma}_\phi^{-1} \boldsymbol{\mu}_\phi\right), \\ \overline{\mathbf{D}}_\tau = \left(\mathbf{X}_c' \boldsymbol{\Sigma}_\zeta^{-1} \mathbf{X}_c + \boldsymbol{\Sigma}_\phi^{-1}\right)^{-1}. \end{cases} \tag{A36}$$

• *Two-Sector UC-SV-TVP-AR*

When assigning a law of motion to the AR coefficients, the model is augmented by an additional state equation plus two sets of parameters, namely the initial conditions for the new state variables and variances for the innovations associated with such states. Formally, we have:

$$\mathbf{c} = \mathbf{X}_c \boldsymbol{\phi} + \boldsymbol{\zeta}, \tag{A37}$$

$$\mathbf{L}_\phi \boldsymbol{\phi} = \boldsymbol{\phi}_0 + \mathbf{u}^\phi, \quad \mathbf{u}^\phi \sim \mathcal{N}(\mathbf{0},\ \boldsymbol{\Sigma}_\phi), \tag{A38}$$

where

$$\underset{(2T \times 2T)}{\mathbf{X}_c} = \begin{bmatrix} \texttt{diag}\left(0, c_1^G, \cdots, c_{T-1}^G\right) & \mathbf{0} \\ \mathbf{0} & \texttt{diag}\left(0, c_1^S, \cdots, c_{T-1}^S\right) \end{bmatrix}, \quad \underset{(2T \times 1)}{\boldsymbol{\phi}} = \begin{bmatrix} \left(\phi_1^G, \cdots, \phi_T^G\right)' \\ \left(\phi_1^S, \cdots, \phi_T^S\right)' \end{bmatrix},$$

$$\underset{(2T \times 2T)}{\boldsymbol{\Sigma}_\phi} = \begin{bmatrix} \sigma_{\phi^G}^2 I_T & \mathbf{0} \\ \mathbf{0} & \sigma_{\phi^S}^2 I_T \end{bmatrix}, \ \underset{(2T \times 2T)}{\mathbf{L}_\phi} = \begin{bmatrix} \mathbf{H} & \mathbf{0} \\ \mathbf{0} & \mathbf{H} \end{bmatrix}, \text{ such that: } \underset{(T \times T)}{\mathbf{H}} = \begin{bmatrix} 1 & 0 & 0 & \cdots & 0 \\ -1 & 1 & 0 & \cdots & 0 \\ 0 & -1 & 1 & & \vdots \\ \vdots & \vdots & \ddots & \ddots & \\ 0 & 0 & \cdots & -1 & 1 \end{bmatrix}.$$

Initialization conditions for $\boldsymbol{\phi}$ are collected as

$$\underset{(2T\times 1)}{\boldsymbol{\phi}_0} = \begin{bmatrix} \phi_0^G \\ \phi_0^S \end{bmatrix} \otimes \begin{bmatrix} 1 \\ 0 \\ \vdots \\ 0 \end{bmatrix}.$$

Combining (A37) and (A38) yields the following full conditional posterior for $\boldsymbol{\phi}$:

$$\boldsymbol{\phi}|\mathbf{y}, \mathbf{Z}_{-\boldsymbol{\phi}} \sim \mathcal{N}\left(\overline{\mathbf{d}}_\phi,\ \overline{\mathbf{D}}_\phi\right), \text{ where } \begin{cases} \overline{\mathbf{d}}_\phi = \overline{\mathbf{D}}_\phi \left(\mathbf{X}_c' \boldsymbol{\Sigma}_\zeta^{-1} \mathbf{c} + \mathbf{L}_\phi' \boldsymbol{\Sigma}_\phi^{-1} \boldsymbol{\phi}_0\right), \\ \overline{\mathbf{D}}_\tau = \left(\mathbf{X}_c' \boldsymbol{\Sigma}_\zeta^{-1} \mathbf{X}_c + \mathbf{L}_\phi' \boldsymbol{\Sigma}_\phi^{-1} \mathbf{L}_\phi\right)^{-1}. \end{cases} \tag{A39}$$

Drawing from the density above is carried out using the precision sampling methods discussed in Section A1.2.1. Finally, sampling $\{\sigma^2_{\phi^G},\ \sigma^2_{\phi^S}\}$ and $\{\phi_0^G,\ \phi_0^S\}$ follows the same steps as in (A27) and (A30), respectively.

A3 Additional Analysis on Transitory Components and Core Inflation

A3.1 Time-Varying Volatility and Correlation of Transitory Components

Figure A4: Estimates of Time-Varying Volatility and Correlation of the Transitory-Noise Innovations

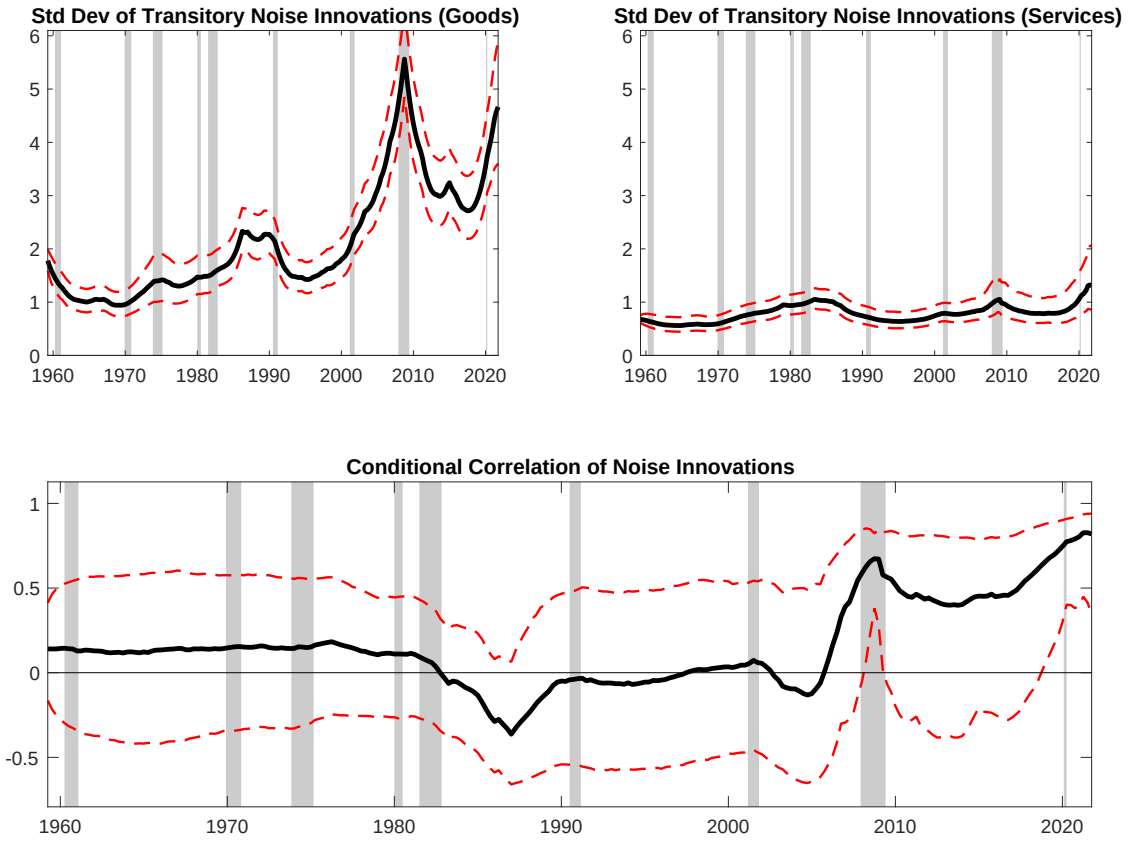

Notes: All (posterior median) estimates are plotted with their associated 67% posterior credible intervals. The shaded areas denote NBER recession dates.

Figure A4 presents the estimated time-varying standard deviation of the innovations to transitory components of goods and services inflation (i.e., $std(\zeta_t^G)$ and $std(\zeta_t^S)$), as well as their estimated correlation between the two sectors. We do not observe any discernible pattern with the volatility of the transitory component of services inflation, although we note that it rises modestly towards the end of the sample. In contrast, the volatility of the

transitory component for goods inflation has become increasingly volatile over time with two noticeable peaks near the end of the sample corresponding to the Great Recession and the COVID-19 pandemic. In conjunction with Figures 2 and 4 from the main text, Figure A4 also demonstrates that while goods inflation has always been relatively volatile, what has changed in fact is the *composition* of the overall volatility. Unlike the 1970s, where the overall volatility of goods inflation exhibited a substantial permanent component, since the 1990s variation in goods inflation has been driven almost exclusively by the transitory component.

Turning to the time-varying correlation of the innovations to the transitory components, our results suggest that comovement between transitory components in these two sectors was fairly muted until the 2008/09 financial crisis. Since then, the comovement between the transitory components has remained elevated and peaked during the COVID-19 pandemic. This indicates that, unlike the Great Inflation of the 1970s, the comovement between goods and services inflation during the last two recessions seems to be originated from the transitory components. In the next subsection, we show that much of this (transitory component-related) result can be attributed to volatile components such as food and energy prices.

A3.2 Core Inflation Measures

A3.2.1 Constructing Core Goods and Core Services Inflation Series

We consider excluding food and energy from goods and services. This would be closer to core inflation since the Federal Reserve tracks PCE inflation excludes food and energy. The idea is since energy and food are volatile components, the Federal Reserve treats these components as noise and thus strips them out. To construct the core goods and core services inflation series, we use data from the BEA Tables 2.3.4 (Price Indexes for Personal Consumption Expenditures by Major Type of Product) and 2.3.5 (Personal Consumption Expenditures by Major Type of Product). Specifically, we use the price indices and expenditure weights for the following categories: (i) Goods; (ii) Services; (iii) Gasoline and Other Energy Goods (which are energy components for goods); (iv) Food and beverages purchased for off-premises consumption; and (v) Energy Goods and Services (which are energy components for both goods and services). Notably, since a services-only energy component is not available, we

construct such a measure by removing the energy components from the Energy Goods and Services category. We then re-construct chain-weighted measures of the PCE deflator for goods and services that exclude the food and energy components. The latter is carried out by applying a Tornqvist formula – as suggested in Whelan (2002) – which is close to the ideal Fisher formula.

Figure A5 plots the constructed core goods and core services inflation series. We also plot the original goods and services inflation series for reference. Given that the food and energy component of inflation is largely in goods, and less so in services, it is not so surprising that the core goods inflation series deviates considerably from goods inflation. In particular, goods inflation does inherit much of the volatility in food and energy inflation, which forms

Figure A5: Goods and Services Excluding Energy Inflation

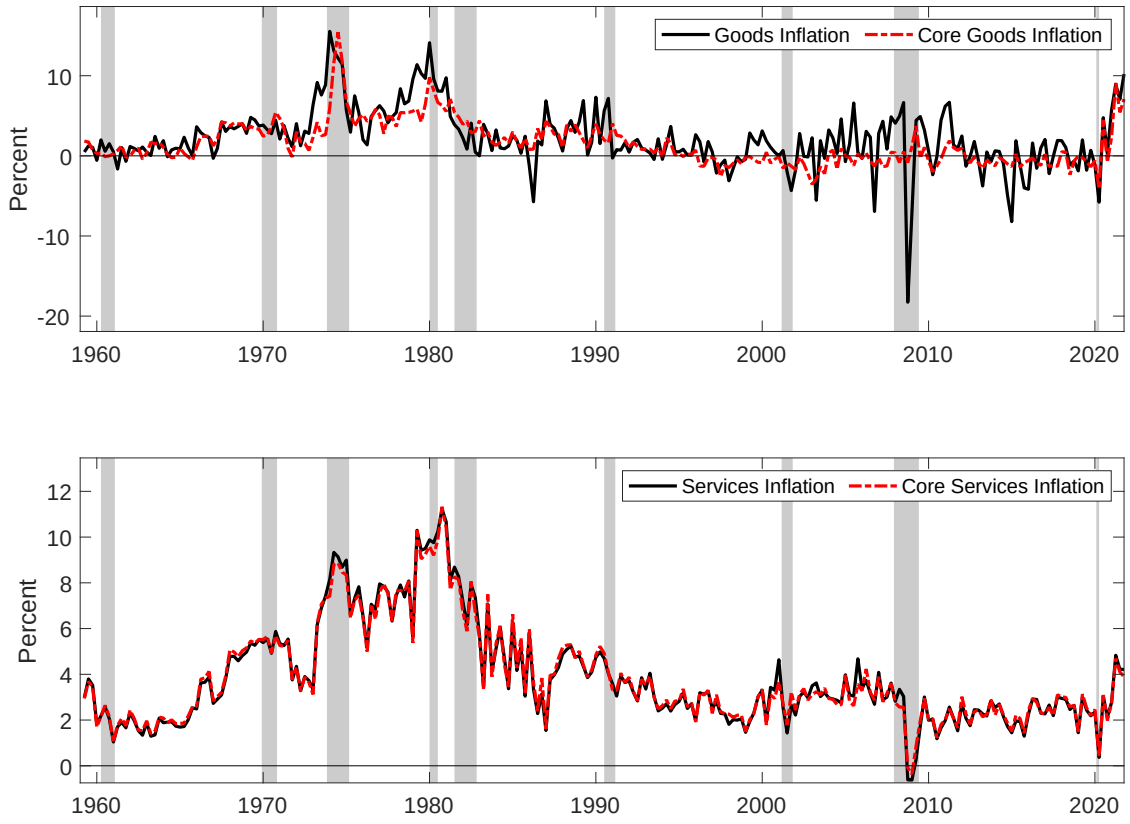

Notes: Inflation in terms of annualized quarter-on-quarter inflation.

part of our motivation for re-estimating our Two-Sector UC-SV model excluding the food and energy components. Core services inflation, on the other hand, closely matches services inflation due to the small share of energy and the absence of a food component in services inflation.

A3.2.2 Results for Core Inflation

Figure A6: Estimated Conditional Standard Deviation and Correlation of Innovations (Ex-food and energy)

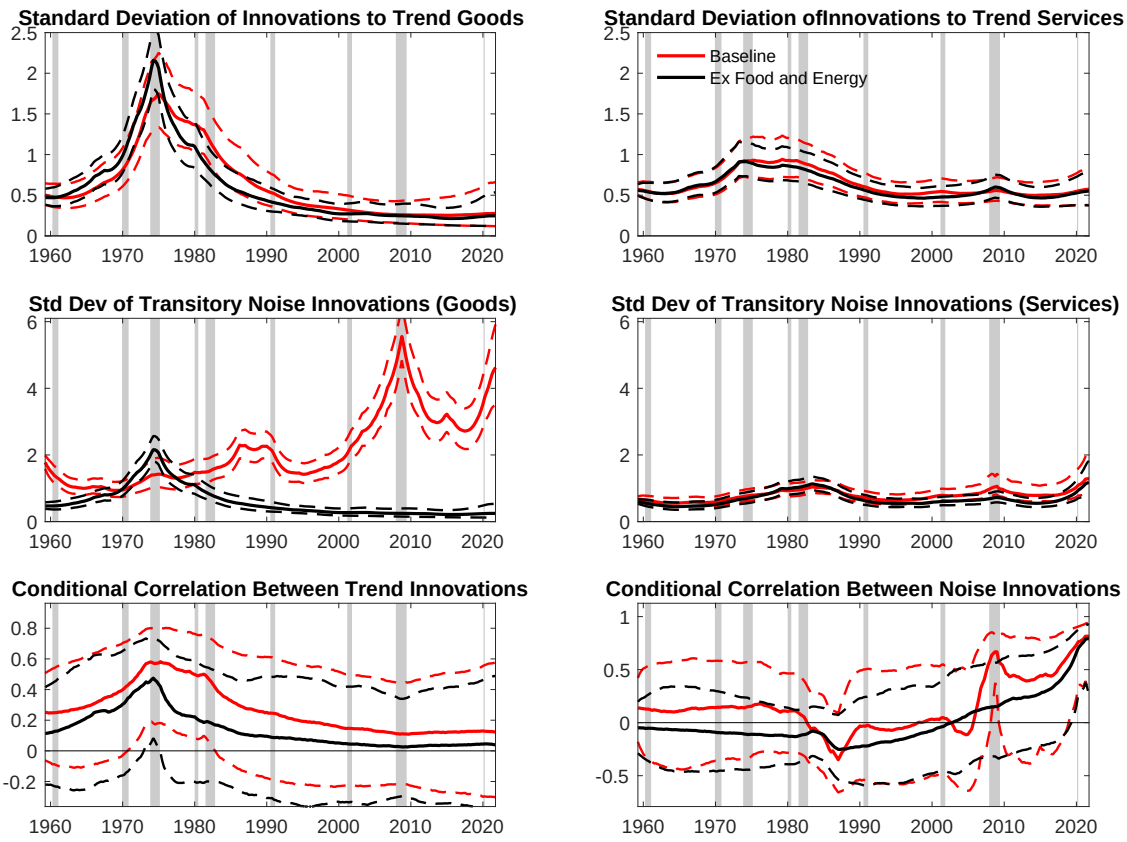

Notes: All (posterior median) estimates are plotted with their associated 67% *posterior credible intervals. The shaded areas denote NBER recession dates.*

Figure A6 presents the estimated standard deviation of the innovations from reestimating our model with goods ex-energy and food and services ex-energy and food. We also plot the estimates from our baseline model in red. The top panel of Figure A6 presents the

Figure A7: Decomposition of Volatility of Aggregate Trend Inflation (Ex-food and energy)

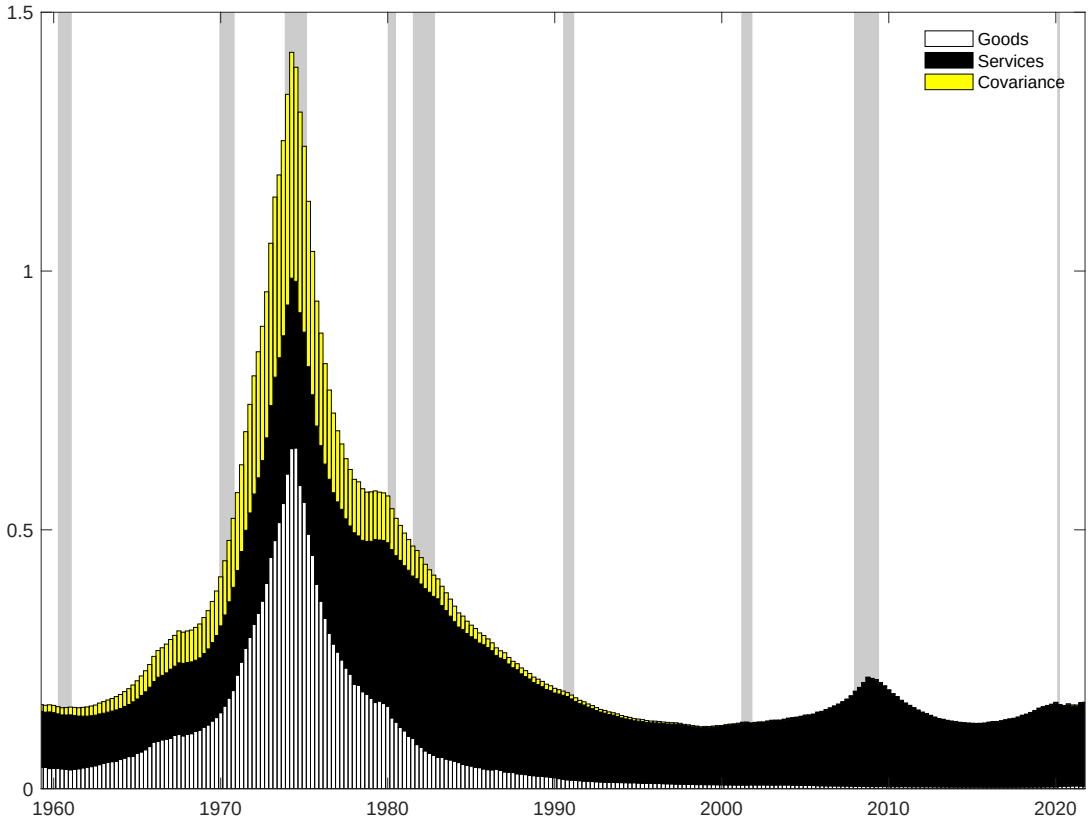

Notes: Trend inflation is in units of annualized quarter-on-quarter inflation. Goods, services, and covariance refer to the decomposition components of aggregate trend inflation, as presented in Equation (12) in the main text. The shaded areas denote NBER recession dates.

estimated standard deviation of the trend goods and services innovations, the middle panels the transitory noise components and the bottom panels the estimated conditional correlation of the trend and transitory noise innovations. In short, all the results are almost identical to what we find in the main text except for the estimated standard deviation of the transitory noise component of goods inflation. It is clear that most of what the transitory noise component in goods was capturing in our benchmark model is energy and food prices. Figure A7 is analogous to Figure 3 in the main text. Basically, the main result that almost all the variation in aggregate trend inflation is dominated by the services sector is unchanged even

if we exclude food and energy. While excluding food and energy has a meaningful impact on the estimates of the noise component of goods inflation, our main results on trend inflation in the main text are not affected by the inclusion or exclusion of food and energy prices.

A4 Further Comparisons with Other Approaches

Following on from Section 4 of the main text, we present further comparisons of our Two-Sector UC-SV relative to alternative approaches. These alternative approaches are the univariate UC-SV by Stock and Watson (2007) (labelled SW07) and also the multi-sector factor UC-SV by Stock and Watson (2016) (labelled SW16). In the main text, we compared relative to the 17-sector version of the Stock and Watson (2016) model, but noted that one is also able to model 2 sectors with their approach. We therefore also compare relative to applying the multi-sector factor UC-SV approach to 2 sectors, the goods and services sector, as per our baseline Two-Sector UC-SV. We remind the reader that the key goal of comparing relative to the SW07 and 17-sector version of the SW16 model is to provide some external validation to our approach, to the extent that one can still reconcile the aggregate implications from both papers. We undertake two more exercises to externally validate our Two-Sector UC-SV, comparison respective to measured inflation expectations and out-of-sample forecasting.

A4.1 Comparison Relative to Measures of Inflation Expectations

Given the documented divergence of the trend inflation estimates at the end of the sample presented in the paper, we compared our estimates of aggregate trend inflation relative to survey inflation expectations. Figure A8 plots the posterior median estimates of trend inflation of the various trend models against 1-year and 10-year ahead inflation survey inflation expectations which we obtain from the Survey of Professional Forecasters (SPF). Note that while we estimate trend inflation using PCE data, we compare our estimates to CPI inflation expectations, which have a considerably longer history. We note that throughout the COVID-19 pandemic and its aftermath, survey inflation expectations, while rising, are slightly above 2% in 2021Q4, which is very close to the estimated trend inflation from the Two-sector UC-SV model. On the other hand, trend inflation estimates from the SW07 and SW16 models deviate quite substantially from SPF forecasts at the end of the sample. We do caution that this does not conclusively validate one trend inflation estimate as being more credible than the other. We point out that trend inflation estimates have historically

Figure A8: Comparison of Two-Sector UC-SV and univariate UC-SV against Survey Inflation Expectations

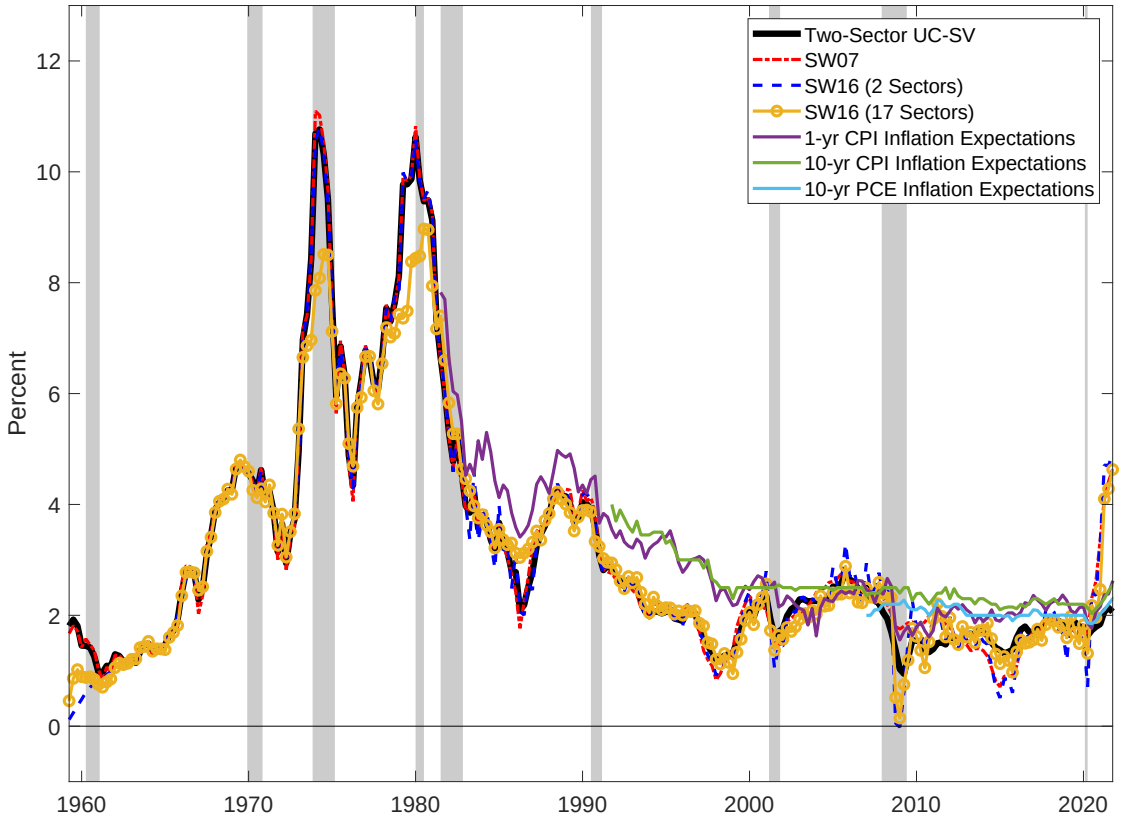

Notes: Shaded bars are NBER dated recessions. All units are in terms of annualized quarter-on-quarter inflation. The posterior median estimates of trend inflation is obtained from the various models and presented with with survey inflation expectations by the Survey of Professional Forecasters.

deviated from survey inflation expectations, albeit by a smaller margin than during the COVID-19 pandemic, so one should be cautious about putting too much weight on the two-sector UC-SV trend inflation estimates being much closer to survey expectations.

Nonetheless, our exercise of comparing relative to survey inflation expectations does suggest that the trend inflation estimates obtained by the two-sector UC-SV are not entirely out of line with what one would expect from measured inflation expectations series during the COVID-19 pandemic. Finally, we should remind the reader that given the divergence happens at the end of the sample, the greater than usual degree of estimation uncertainty

suggests the trend inflation estimates at the end of the sample may well end up being, possibly heavily, revised in the future, which naturally suggests an avenue for future work to resolve the Two-sector UC-SV and other models with the availability of more data in the future.

A4.2 Forecasting Exercise

We also conducted an out-of-sample forecasting exercise for h-quarter ahead PCE inflation.[8] More precisely, our out-of-sample uses only one vintage of the data (the vintage that we used to do the estimation), and does not consider data revisions (which would require using multiple sets of real-time datasets instead of the final vintage data). We use an expanding window of one observation at a time of the same vintage of data to estimate trend inflation, then use these estimates to forecast out-of-sample. We conduct the exercise for h = 4, 8, and 12, similar to Stock and Watson (2016), given trend inflation estimates are partly designed to be good predictors of inflation in the medium to long term. These horizons coincide with predicting the average inflation over a 1-year, 2-year, and 3-year ahead horizon.

Since the transitory component does not feature dynamics in all the models, the h-step ahead forecast of inflation is always the current estimate of trend inflation. For multiple sector models such as our Two-Sector UC-SV or SW16 model, we construct trend inflation by using the time t consumption weights to aggregate all the sector-specific trend inflation measures (i.e. see Equation (11) in the main text for the two-sector model). We then use the median of the posterior distribution of aggregate trend inflation as our point estimate of aggregate trend inflation and construct the point forecast for aggregate inflation.

Table A2 presents the results of the out-of-sample forecasting exercise. We report the out-of-sample relative root mean squared error (RRMSE) relative to our Two-Sector UC-SV. We compare two samples, 1980Q1-2021Q4 and a shorter evaluation period of 2000Q1-2021Q4. Note that since these RRMSEs are relative to our Two-Sector UC-SV, numbers greater than

[8]To be precise, let p_t be the natural log of the PCE index. We define annualized quarter-on-quarter inflation, $\pi_t = 400 \times [p_t - p_{t-1}]$. When we compute an h-step-ahead forecast, we are forecasting $\frac{1}{h}\sum_{j=1}^{h} \pi_{t+j}$ with the model estimated up to time t. This is equivalent to forecasting $\frac{1}{h}400 \times [p_{t+h} - p_t]$, which is the change in the price level from t to $t+h$, with a scaling factor to account for the annualization and the horizon.

Table A2: Forecasting Results

		1980Q1-2021Q4	
h	**SW07**	**SW16 (2 Sectors)**	**SW16 (17 Sectors)**
4	1.00	1.09	0.99
8	1.01	1.09	0.97
12	1.01	1.08	0.95*
		2000Q1-2021Q4	
h	**SW07**	**SW16 (2 Sectors)**	**SW16 (17 Sectors)**
4	1.03	1.17*	1.00
8	1.05	1.27	0.98
12	1.07***	1.36	0.97

Notes: Results from out-of-sample forecasting exercise of inflation for two sample periods: 1980Q1-2019Q2 and 2000Q1-2021Q4. h refers to the forecast horizon. The results are reported in terms of the relative root mean squared error of the inflation forecast relative to the two-sector UC-SV model. Values greater than 1 indicate superior forecasting performance of the two-sector UC-SV model. SW07 is the univariate UC-SV model by Stock and Watson (2007). SW16 is the multi-sector UC-SV model by Stock and Watson (2016). 17 and 2 refer to the number of sectors used in the multi-sector factor UC-SV model. ∗, ∗∗, and ∗ ∗ ∗ refers to forecast being statistically different at a 10, 5, and 1% level of significance using a Diebold and Mariano (1995) test.

1 indicate that our Two-Sector UC-SV produces more accurate forecasts.

In general, the forecasting performance across our Two-Sector UC-SV, the SW07 model, and the 17-sector version of SW16 model are comparable. Nonetheless, we highlight four findings from the forecasting exercise. First, the 2-sector version of the SW16 model forecasts extremely poorly, with RRMSE up from 8 to 30% worse than our Two-Sector UC-SV. This suggests that for a model that only considers the goods and services sector, our approach is probably more appropriate than the SW16 approach. Second, we forecast very similarly to both the SW07 and 17-sector version of the SW16 model though these forecasts are not often statistically significant from the perspective of the Diebold and Mariano (1995) test. That said, even if often not statistically significant, the Two-Sector UC-SV does in general produce better point forecasts relative to the SW07 model and the 17-sector version of the SW16 model does forecast better than the Two-Sector UC-SV. Third, moving from the 1980Q1-2021Q4 evaluation sample to the 2000Q1-2021Q4 evaluation sample, the forecast performance of the Two-Sector UC-SV improves relative to both SW07 and the 17-sector

version of the SW16 model. Relative to SW07, the Two-Sector UC-SV starts to outperform the univariate SW07 model with a sample starting in 2000Q1. Relative to the 17-sector version of the SW16 model, the forecasting performance narrows to the point that they are indistinguishable. Fourth, it is known that aggregation of disaggregated forecasts can lead to better forecasts of the aggregates as long as the misspecification is not large (for further discussion, see Lutkepohl, 2006; Hendry and Hubrich, 2011). Indeed, our forecasting results do suggest that our approach does better than the univariate SW07 model, especially over the 2000Q1-2021Q4 period, and further disaggregation of using the 17-sector version of the SW16 model does slightly better than us, suggesting that any misspecification with the disaggregation from the SW07 to the Two-Sector UC-SV, and the Two-Sector UC-SV to the 17-sector version of the SW16 is probably small. Nonetheless, an analogous conclusion that one may also draw is that given disaggregation leads to a large deterioration of the forecast from the 2-sector version of the SW16 model, the 2-sector version of the SW16 model is perhaps badly misspecified when compared to the Two-Sector UC-SV if one seeks to only model the goods and service sector.

A4.3 Summary

Overall, further to what we document in the paper, we find further evidence that the implications for aggregate trend inflation which we obtain from our two-sector UC-SV model are comparable to those one obtains from another approach, apart from the end of the sample during the COVID-19 pandemic. At the end of the sample, while we do urge caution in interpreting the level of the estimates of aggregate trend inflation given the large degree of estimation uncertainty, trend inflation estimates from our two-sector UC-SV model suggest a more muted increase in trend inflation, and these trend inflation estimates are more in line with what one observes from surveys of inflation expectations. On forecasting, we obtain very similar forecasts to the SW07 and 17-sector version of the SW16 model.

A5 Comparison and Reconciling with the Stock and Watson (2016) Model

In this section we provide a discussion on how our UC-based approach relates to the (factor-based) inferential framework adopted in Stock and Watson (2016). We first discuss matters in a two-sector (i.e., goods and services) context and subsequently generalize the analysis to a multisector environment.

The key ideas we want to convey in this section are: (i) in the context of a two-sector split, by not overparameterizing the covariance matrix for sectoral-trend innovations, our UC approach provides an inferential framework that is more robust to prior choice; and (ii) both Stock and Watson (2016) and our UC-based approach provide inferential frameworks that are more closely related than their state-space representations may lead one to believe. In particular, we show that the difference between these two approaches can be established in terms of the number of state variables in the covariance matrix for sectoral-trend innovations. Such difference reflects contrasting strategies to model sectoral comovement. While we adopt a time-varying correlation approach, as discussed in Section 2 of the main text, Stock and Watson (2016) model comovement by introducing a common-trend that embeds stochastic volatility and time-varying loadings.

A5.1 The Parametrization of Sectoral Trend Inflation in Stock and Watson (2016)

For convenience, below we reproduce the representation of each sectoral trend inflation as in Stock and Watson (2016) when applied to a goods and services split:

$$\tau_t^G = \alpha_t^G \tau_t^c + \tau_t^{G,*}, \tag{A40}$$

$$\tau_t^S = \alpha_t^G \tau_t^c + \tau_t^{S,*}. \tag{A41}$$

The representation above defines the trend for each sector as the composition of three latent variables: a common trend (or factor), τ_t^c, that captures common (low-frequency) dynamics

between goods and services inflation; the time-varying loadings, α_t^i for $i = G$ and S, that weight the importance of common dynamics in the determination sectoral trends; and a sector-specific idiosyncratic trend component given by $\tau_t^{i,*}$, for $i = G$ and S. All these state variables are specified as random walk process, i.e.:

$$\tau_t^c = \tau_{t-1}^c + u_t^c \quad s.t.\ u_t^c \sim (0,\ \exp(h_t^c)), \tag{A42}$$

$$\tau_t^{G,*} = \tau_{t-1}^G + u_t^{G,*}\ s.t.\ u_t^{G,*} \sim \left(0,\ \exp\left(h_t^G\right)\right), \tag{A43}$$

$$\tau_t^{S,*} = \tau_{t-1}^S + u_t^{S,*}\ s.t.\ u_t^{S,*} \sim \left(0,\ \exp\left(h_t^S\right)\right), \tag{A44}$$

$$\alpha_t^G = \alpha_{t-1}^G + u_t^{\alpha^G}\ s.t.\ u_t^{\alpha^i} \overset{i.i.d.}{\sim} \left(0,\ \sigma_{\alpha^G}^2\right), \tag{A45}$$

$$\alpha_t^S = \alpha_{t-1}^S + u_t^{\alpha^S}\ s.t.\ u_t^{\alpha^S} \overset{i.i.d.}{\sim} \left(0,\ \sigma_{\alpha^S}^2\right). \tag{A46}$$

Next, note that the conditional variance of the innovations driving τ_t^c, $\tau_t^{G,*}$ and τ_t^{S*} is also time-varying, which introduces three additional stochastic-volatility states h_t^c, h_t^G and h_t^S, i.e.:

$$h_t^c = h_{t-1}^c + \eta_t^{h^c}\ s.t.\ \eta_t^{h^c} \overset{i.i.d.}{\sim} \left(0,\ \sigma_{h^c}^2\right), \tag{A47}$$

$$h_t^G = h_{t-1}^G + \eta_t^G\ s.t.\ \eta_t^G \overset{i.i.d.}{\sim} \left(0,\ \sigma_G^2\right), \tag{A48}$$

$$h_t^S = h_{t-1}^S + \eta_t^S\ s.t.\ \eta_t^S \overset{i.i.d.}{\sim} \left(0,\ \sigma_S^2\right). \tag{A49}$$

A5.1.1 The Decomposition of Aggregate Trend Inflation Volatility

Given the representation of sectoral trends discussed above, we now discuss how this can be used to compute the decomposition of aggregate trend inflation volatility for which results are reported in Table 3 of the main text. Since the parameterization of aggregate and sector-specific trends by Stock and Watson (2016) is different than the one in our two-sector setting, the volatility decomposition from their factor-based framework will have a different algebraic expression than ours in Equation (12) of the main text. Nevertheless, just like in our approach, one can decompose the overall variation of trend inflation into three components, namely a covariance, a goods-specific volatility and a services-specific volatility term. To

this end, note first that we can approximate trend inflation (τ_t) as follows:[9]

$$\tau_t \approx \sum_{i \in \{G,\ S\}} w_t^i \tau_t^i = \sum_{i \in \{G,\ S\}} w_t^i \left(\alpha_t^i \tau_t^c + \tau_t^{i*}\right), \tag{A50}$$

where w_t^i denotes the sector-specific expenditure share. Next, let $\mathtt{V}(\bullet)$ denote the *conditional* variance operator. Assuming w_t^i are given, applying $\mathtt{V}(\bullet)$ to the expression for τ_t in Equation (A50) yields:[10]

$$\begin{aligned}
\mathtt{V}\left(\tau_t\right) &\approx \sum_{i \in \{G,\ S\}} \left(w_t^i\right)^2 \mathtt{V}\left(\alpha_t^i \tau_t^c\right) + \sum_{i \in \{G,\ S\}} \left(w_t^i\right)^2 \mathtt{V}\left(\tau_t^{i*}\right), \\
&= \sum_{i \in \{G,\ S\}} \left(w_t^i\right)^2 \left[\mathtt{V}\left(\alpha_t^i\right) \mathtt{V}\left(\tau_t^c\right) + \mathtt{V}\left(\alpha_t^i\right) \mathtt{E}^2\left(\tau_t^c\right) + \mathtt{V}\left(\tau_t^c\right) \mathtt{E}^2\left(\alpha_t^i\right)\right] + \sum_{i \in \{G,\ S\}} \left(w_t^i\right)^2 \mathtt{V}\left(\tau_t^{i*}\right), \\
&= \overbrace{\sum_{i \in \{G,\ S\}} \left(w_t^i\right)^2 \left[\sigma_{\alpha^i}^2 \exp\left(h_t^c\right) + \sigma_{\alpha^i}^2 \left(\tau_{t-1}^c\right)^2 + \exp\left(h_t^c\right) \left(\alpha_{t-1}^i\right)^2\right]}^{\texttt{Covariance}} + \overbrace{\left(w_t^G\right)^2 \exp\left(h_t^G\right)}^{\texttt{Goods}} + \overbrace{\left(w_t^S\right)^2 \exp\left(h_t^S\right)}^{\texttt{Services}}.
\end{aligned} \tag{A51}$$

To be clear, we refer to the term inside the summation of the last expression above as '`Covariance`' since it consists exclusively of the states associated with the common trend across sectors. From (A43) and (A44), it is easy to see that the remaining two terms capture the contribution from sector-specific volatilities.

We now turn to demonstrate why the additional flexibility in the representation given by (A40)-(A49) is less desirable in the context of a two-sector state space model relative to our Two-Sector UC-SV approach.

[9] Again, the term 'approximation' here follows from the fact that there are no weights for the components of the PCE price index. Therefore, as in Stock and Watson (2016), aggregation relies on approximating sectoral weights using nominal expenditure shares for the goods and services components out of total (nominal) PCE.

[10] As in our model, Stock and Watson (2016) also specify the state variables as random walks, hence the use of conditional moments to construct second-moment based decompositions.

A5.2 On the Appropriateness of the UC Approach in a 2-Sector Setting

To fix ideas, note that by substituting Equations (A42) and (A43) into (A40) and, similarly, (A42) and (A44) into (A41) allows us to reexpress τ_t^G and τ_t^S as follows:[11]

$$\tau_t^G = \alpha_t^G \tau_{t-1}^c + \tau_{t-1}^{G*} + \overbrace{\alpha_t^G u_t^c + u_t^{G,*}}^{u_t^{\tau^{G,SW}}}, \tag{A52}$$

$$\tau_t^S = \alpha_t^S \tau_{t-1}^c + \tau_{t-1}^{S*} + \overbrace{\alpha_t^S u_t^c + u_t^{S,*}}^{u_t^{\tau^{S,SW}}}. \tag{A53}$$

Next, since both τ_t^G and τ_t^S share a common innovation, u_t^c, the composite error terms $u_t^{\tau^{G,SW}}$ and $u_t^{\tau^{S,SW}}$ are correlated and, consequently, akin to our UC approach, exhibit a full covariance matrix. In other words, their joint distribution can be expressed as:

$$\begin{bmatrix} u_t^{\tau^{G,SW}} \\ u_t^{\tau^{G,SW}} \end{bmatrix} \sim \mathcal{N}\left(\begin{bmatrix} 0 \\ 0 \end{bmatrix}, \overbrace{\begin{bmatrix} \sigma^2_{\tau^G,t} & \sigma_{\tau,t} \\ \sigma_{\tau,t} & \sigma^2_{\tau^S,t} \end{bmatrix}}^{\Omega_{\tau,t}^{SW}} \right), \tag{A54}$$

where:

$$\Omega_{\tau,t}^{SW} = \begin{bmatrix} \left(\alpha_t^G\right)^2 \exp\left(h_t^c\right) + \exp\left(h_t^G\right) & \alpha_t^G \alpha_t^S \exp\left(h_t^c\right) \\ \alpha_t^G \alpha_t^S \exp\left(h_t^c\right) & \left(\alpha_t^S\right)^2 \exp\left(h_t^c\right) + \exp\left(h_t^S\right) \end{bmatrix}. \tag{A55}$$

From (A54), it is clear that $\Omega_{\tau,t}^{SW}$ has the same number of (unrestricted) second moments as in our UC setting. Also, as shown in (A55), the factor-based approach by Stock and Watson (2016) elicits *five* states (i.e. α_t^G, α_t^S, h_t^c, h_t^G and h_t^S) to capture the *three* time-varying moments in $\Omega_{\tau,t}^{SW}$, hence overparameterizing the latter. In contrast, our UC-based approach provides a more parsimonious parameterization of such a covariance matrix, as we elicit three states to model the *same* three time-varying second moments. To illustrate this point more

[11] Through the remainder of this section we will at times use the superscripts SW and EUW to refer to Stock and Watson (2016) and our framework, respectively.

clearly, for convenience, below we reproduce the UC representation of the sectoral trends discussed in Section 2 of the main text:

$$\tau_t^G = \tau_{t-1}^G + u_t^{\tau^{G,EUW}}, \tag{A56}$$

$$\tau_t^S = \tau_{t-1}^S + u_t^{\tau^{S,EUW}}. \tag{A57}$$

$$\begin{bmatrix} u_t^{\tau^{G,EUW}} \\ u_t^{\tau^{G,EUW}} \end{bmatrix} \sim \mathcal{N}\left(\begin{bmatrix} 0 \\ 0 \end{bmatrix}, \overbrace{\begin{bmatrix} \sigma^2_{\tau^G,t} & \sigma_{\tau,t} \\ \sigma_{\tau,t} & \sigma^2_{\tau^S,t} \end{bmatrix}}^{\Omega^{EUW}_{\tau,t}} \right), \tag{A58}$$

where:

$$\Omega^{EUW}_{\tau,t} = \begin{bmatrix} 1 & 0 \\ \gamma_t^\tau & 1 \end{bmatrix} \begin{bmatrix} \exp\left(h_t^{\tau^G}\right) & 0 \\ 0 & \exp\left(h_t^{\tau^S}\right) \end{bmatrix} \begin{bmatrix} 1 & \gamma_t^\tau \\ 0 & 1 \end{bmatrix}. \tag{A59}$$

From (A58) and (A59), one can see that the three (conditional) second-moment moments $\sigma^2_{\tau^G,t}$, $\sigma^2_{\tau^S,t}$ and $\sigma_{\tau,t}$ are governed by three state variables $h_t^{\tau^G}$, $h_t^{\tau^S}$ and γ_t^τ.

Notably, the overparametrization of $\Omega^{SW}_{\tau,t}$ in (A55) is a consequential issue. First, as shown in Table A2, applying the factor-based framework by Stock and Watson (2016) to a *two-sector* setting weakens the forecasting performance relative to our UC-based strategy, with our approach leading to gains in 12-quarter-ahead forecasting of up to 36%. Second (and related to the previous point), 'redundant' states may be weakly identified, a issue that can be examined in terms of prior sensitivity (or lack thereof) for some results of interest. We thus investigate the extent to which estimation of sectoral trends may be sensitive to prior calibration in both our Two-Sector UC-SV setting and in the factor-based framework of Stock and Watson (2016), the latter also applied to a two-sector setting.

In keeping with our prior-sensitivity exercise in Section A2.1, we address prior sensitivity in terms of different calibrations for the inverse gamma prior. However, unlike exercise in Section A2.1, we now focus on the shape hyperparameter of the inverse gamma prior as it

controls the (shape of the) tail of such a distribution, hence allowing to change the degree of prior informativeness more directly.[12] Also, as discussed in Stock and Watson (2016), in the context of their model, the inverse gamma prior is associated with the (standard deviation of the) innovations driving the time-varying loadings (α_t^G and α_t^S) in Equations (A45) and (A46). Importantly, as shown in (A55), these two states parameterize changes in $\Omega_{\tau,t}^{SW}$.

The bottom panel of Table A3 reports prior sensitivity-related results. In particular, we report the mean squared error (MSE) associated with the estimation of the sectoral trends obtained from both the UC and factor-based approaches. To be clear, the MSEs in Table A3 are obtained as follows: trends for goods and services inflation are first estimated using the baseline calibration to the shape parameters for the relevant inverse gamma priors, i.e., $T/10$ as shown in (A9). We then re-estimate both models under a much tighter parametrization of the inverse gamma prior, where shape parameters are set to 10^6. This produces a new set of trend estimates (again, posterior medians) for each sector, which are then compared against our baseline estimates to compute the MSEs for each sectoral trend reported in Table A3.

To be clear, the measure of 'error' used to computed the MSEs refers to the difference between the same sectoral trend estimated under the two prior calibrations described above. The ideas is a simple one, the less sensitive to prior calibration a model is, the closer to zero trend-related MSEs should be. In this regard, the MSEs corresponding to the model by Stock and Watson (2016) are much greater than the ones obtained from our UC setting. For goods inflation, in particular, the MSE from their model is approximately 10^3 greater than its counterpart from our model, indicating that (at least within the context of a two-sector analysis) our inferential framework is more robust to prior choice.

[12] Specifically, higher (lower) values of the shape hyperparameter imply thinner (fatter) tails, i.e., more informative (diffuse) priors.

Table A3: Parametrization of the covariance matrix for sectoral-trend innovations ($\Omega^i_{\tau,t}$ for $i = EUW$ and SW) and prior sensitivity-related results based on our framework (EUW) and the factor approach in Stock and Watson (2016) (SW) in a 2-sector setting.

Parametrization of $\Omega^i_{\tau,t}$		
Identifier	# of second-moments in $\Omega^i_{\tau,t}$	# of states used to parameterize $\Omega^i_{\tau,t}$
EUW	3	3
SW	3	5
MSE for trend estimates under two prior calibrations		
Identifier	Goods	Services
EUW	0.0008	0.0002
SW	0.8428	0.0119

Notes: MSE stands for mean squared error.

A5.3 Reconciling UC- and Factor-Based Approaches More Broadly

We now extend the comparison between Stock and Watson (2016) and our UC-based approach to the case where *both* frameworks are applied to a general *multisector* state-space setting. Therefore, in what follows we replace the superscripts 'G' and 'S' in the system (A40)-(A49) by the superscript 'i' to denote any sector $i = 1, ..., N$. The superscript 'c' is preserved to denote the common trend (or factor) within an N-sector setting.

Next, using the fact that Stock and Watson (2016) sets $\tau^c_0 = 0$, note that we can recast equations (A40) through (A49) more compactly (and adjusted to an N-sector framework) according to the following stacked representation:

$$\boldsymbol{\tau}^{SW} = \boldsymbol{\Lambda}\boldsymbol{\tau}^c + \boldsymbol{\tau}^*, \tag{A60}$$

$$\mathbf{L}\boldsymbol{\tau}^* = \boldsymbol{\tau}_0 + \mathbf{u}^*, \tag{A61}$$

$$\mathbf{H}\boldsymbol{\tau}^c = \mathbf{u}^c, \tag{A62}$$

$$\mathbf{u}^* \sim \mathcal{N}\left(\mathbf{0}, \boldsymbol{\Sigma}^{SW}_*\right), \tag{A63}$$

$$\mathbf{u}^c \sim \mathcal{N}\left(\mathbf{0}, \boldsymbol{\Sigma}^{SW}_c\right), \tag{A64}$$

where:

$$\underset{(NT\times 1)}{\boldsymbol{\tau}^{SW}} = \begin{bmatrix} \left(\tau_1^{1,SW},\cdots,\tau_T^{1,SW}\right)' \\ \vdots \\ \left(\tau_1^{N,SW},\cdots,\tau_T^{N,SW}\right)' \end{bmatrix}, \quad \underset{(NT\times 1)}{\boldsymbol{\tau}^{*}} = \begin{bmatrix} \left(\tau_1^{1,*},\cdots,\tau_T^{1,*}\right)' \\ \vdots \\ \left(\tau_1^{N,*},\cdots,\tau_T^{N,*}\right)' \end{bmatrix}, \quad \underset{(NT\times 1)}{\mathbf{u}^{*}} = \begin{bmatrix} \left(u_1^{1,*},\cdots,u_T^{1,*}\right)' \\ \vdots \\ \left(u_1^{N,*},\cdots,u_T^{N,*}\right)' \end{bmatrix},$$

$$\underset{(NT\times T)}{\boldsymbol{\Lambda}} = \begin{bmatrix} \mathtt{diag}\left(\alpha_1^1,\cdots,\alpha_T^1\right) \\ \vdots \\ \mathtt{diag}\left(\alpha_1^N,\cdots,\alpha_T^N\right) \end{bmatrix}, \quad \underset{(T\times T)}{\mathbf{H}} = \begin{bmatrix} 1 & 0 & 0 & \cdots & 0 \\ -1 & 1 & 0 & \cdots & 0 \\ 0 & -1 & 1 & & \vdots \\ \vdots & \vdots & \ddots & \ddots & \\ 0 & 0 & \cdots & -1 & 1 \end{bmatrix}, \quad \underset{(NT\times NT)}{\mathbf{L}} = \begin{bmatrix} \mathbf{H} & \mathbf{0} & \cdots & \mathbf{0} \\ \mathbf{0} & \mathbf{H} & & \mathbf{0} \\ \vdots & & \ddots & \vdots \\ \mathbf{0} & \mathbf{0} & \cdots & \mathbf{H} \end{bmatrix},$$

$$\underset{(T\times 1)}{\boldsymbol{\tau}^{c}} = \left(\tau_1^c,\cdots,\tau_T^c\right)', \quad \underset{(NT\times 1)}{\boldsymbol{\tau}_0} = \left(\tau_0^{*,1},\cdots \tau_0^{*,N},0,\cdots,0\right), \quad \underset{(T\times 1)}{\mathbf{u}^{c}} = \left(u_1^c,\cdots,u_T^c\right)',$$

$$\underset{(NT\times NT)}{\boldsymbol{\Sigma}_*^{SW}} = \begin{bmatrix} \mathtt{diag}\left(\exp\left(h_1^1\right),\cdots,\exp\left(h_T^1\right)\right) & \mathbf{0} & \cdots & \mathbf{0} \\ \mathbf{0} & \ddots & & \mathbf{0} \\ \vdots & & \ddots & \vdots \\ \mathbf{0} & \mathbf{0} & \cdots & \mathtt{diag}\left(\exp\left(h_t^N\right),...,\exp\left(h_T^N\right)\right) \end{bmatrix} \text{ and}$$

$$\underset{(T\times T)}{\boldsymbol{\Sigma}_c^{SW}} = \mathtt{diag}\left(\exp\left(h_1^c\right),\cdots,\exp\left(h_T^c\right)\right).$$

From (A61) and (A62) we, respectively, have: $\boldsymbol{\tau}^* = \mathbf{L}^{-1}\boldsymbol{\tau}_0 + \mathbf{L}^{-1}\mathbf{u}^*$ and $\boldsymbol{\tau}^c = \mathbf{H}^{-1}\mathbf{u}^c$. It is then easy to verify that by plugging the right-hand side of the last two expressions into (A60) and by a simple change of variable, $\widetilde{\boldsymbol{\tau}}_0 = \mathbf{L}^{-\mathbf{1}}\boldsymbol{\tau}_0$, we obtain the following stacked (and more compact) representation for the system in (A60)-(A64), summarized in the box below:

Stacked representation of sectoral trends in Stock and Watson (2016)

$$\boldsymbol{\tau}^{SW} = \widetilde{\boldsymbol{\tau}}_0 + \mathbf{u}^{\tau,SW}, \tag{A65}$$

$$\mathbf{u}^{\tau,SW} \sim \mathcal{N}(\mathbf{0},\ \overbrace{\widetilde{\boldsymbol{\Lambda}}\boldsymbol{\Sigma}_c^{SW}\widetilde{\boldsymbol{\Lambda}}' + \mathbf{L}^{-1}\boldsymbol{\Sigma}_*^{SW}\mathbf{L}^{-1'}}^{\boldsymbol{\Sigma}_\tau^{SW}}), \tag{A66}$$

where $\mathbf{u}^{\tau,SW} = \widetilde{\boldsymbol{\Lambda}}\mathbf{u}^c + \mathbf{L}^{-1}\mathbf{u}^*$ and $\widetilde{\boldsymbol{\Lambda}} = \boldsymbol{\Lambda}\mathbf{H}^{-1}$. We discuss the composite parametrization of $\boldsymbol{\Sigma}_\tau^{SW}$ in (A66) in greater detail below. But before doing this, it is useful to establish that our UC-based framework also delivers a similar stacked representation for the sectoral trends as in the box above. To this end, note that, as shown in Section A1, our framework also allows to cast sectoral trends more compactly as follows:

$$\mathbf{L}\boldsymbol{\tau}^{EUW} = \boldsymbol{\tau}_0 + \mathbf{u}^{\tau}, \tag{A67}$$

$$\mathbf{u}^{\tau} \sim \mathcal{N}\left(\mathbf{0},\ \boldsymbol{\Sigma}_\tau\right), \tag{A68}$$

where $\boldsymbol{\tau}^{EUW}$ collects terms exactly like $\boldsymbol{\tau}^{SW}$. Similarly, $\mathbf{L}$ and $\boldsymbol{\tau}_0$ are defined as in (A61).

Now recall that, instead of introducing a common trend across N sectors (as in Stock and Watson (2016)), our UC framework absorbs common sectoral dynamics in the form of mutually correlated innovations, which is directly applied to the vector of innovations $\mathbf{u}^{\tau}$. As a result, given the stacked representation for $\mathbf{u}^{\tau}$, the covariance matrix $\boldsymbol{\Sigma}_\tau$ in (A68) for a N-sector UC model is given by:

$$\boldsymbol{\Sigma}_\tau = \begin{bmatrix} \boldsymbol{\Sigma}_{1,1} & \boldsymbol{\Sigma}_{1,2} & \cdots & \boldsymbol{\Sigma}_{1,N} \\ \boldsymbol{\Sigma}_{2,1} & \boldsymbol{\Sigma}_{2,2} & \ddots & \vdots \\ \vdots & \ddots & \ddots & \boldsymbol{\Sigma}_{N-1,N} \\ \boldsymbol{\Sigma}_{N,1} & \cdots & \boldsymbol{\Sigma}_{N,N-1} & \boldsymbol{\Sigma}_{N,N} \end{bmatrix} = \overbrace{\begin{bmatrix} \mathbf{0} & \boldsymbol{\Sigma}_{1,2} & \cdots & \boldsymbol{\Sigma}_{1,N} \\ \boldsymbol{\Sigma}_{2,1} & \mathbf{0} & \ddots & \vdots \\ \vdots & \ddots & \ddots & \boldsymbol{\Sigma}_{N-1,N} \\ \boldsymbol{\Sigma}_{N,1} & \cdots & \boldsymbol{\Sigma}_{N,N-1} & \mathbf{0} \end{bmatrix}}^{\boldsymbol{\Sigma}_c^{EUW}} + \overbrace{\begin{bmatrix} \boldsymbol{\Sigma}_{1,1} & \mathbf{0} & \cdots & \mathbf{0} \\ \mathbf{0} & \boldsymbol{\Sigma}_{2,2} & \ddots & \vdots \\ \vdots & \ddots & \ddots & \mathbf{0} \\ \mathbf{0} & \cdots & \mathbf{0} & \boldsymbol{\Sigma}_{N,N} \end{bmatrix}}^{\boldsymbol{\Sigma}_*^{EUW}}, \tag{A69}$$

where $\boldsymbol{\Sigma}_{i,i} = \texttt{diag}\left(\sigma^2_{\tau^i,1}, \cdots, \sigma^2_{\tau^i,T}\right)$ and $\boldsymbol{\Sigma}_{i,j} = \texttt{diag}\left(\sigma_{\tau^{i,j},1}, \cdots, \sigma_{\tau^{i,j},T}\right)$ for i and $j = 1, ..., N$ such that $i \neq j$. As a result, we can recast the system in (A67)-(A68) as in the box below:

Stacked representation of sectoral trends in our framework

$$\boldsymbol{\tau}^{EUW} = \widetilde{\boldsymbol{\tau}}_0 + \mathbf{u}^{\tau,EUW}, \tag{A70}$$

$$\mathbf{u}^{\tau,EUW} \sim \mathcal{N}(\mathbf{0}, \overbrace{\mathbf{L}^{-1}\boldsymbol{\Sigma}_c^{EUW}\mathbf{L}^{-1'} + \mathbf{L}^{-1}\boldsymbol{\Sigma}_*^{EUW}\mathbf{L}^{-1'}}^{\boldsymbol{\Sigma}_{\boldsymbol{\tau}}^{EUW}}), \tag{A71}$$

where $\mathbf{u}^{\tau,EUW} = \mathbf{L}^{-1}\mathbf{u}^{\tau}$ and $\widetilde{\boldsymbol{\tau}}_0 = \mathbf{L}^{-1}\boldsymbol{\tau}_0$.

A few comments are in order. First, by comparing Equations (A65) and (A70) it is easy to see that both vectors $\boldsymbol{\tau}^{EUW}$ and $\boldsymbol{\tau}^{SW}$ are similarly parameterized in terms of a vector collecting initial conditions ($\widetilde{\boldsymbol{\tau}}_0$) and a multivariate normally distributed error term. It is then perhaps not too surprising that both our approach and Stock and Watson (2016) deliver somewhat similar results in Section 4.1 of the main text.

Second, by comparing (A66) and (A71), it can be seen that $\boldsymbol{\Sigma}_{\boldsymbol{\tau}}^{SW}$ and $\boldsymbol{\Sigma}_{\boldsymbol{\tau}}^{EUW}$ are decomposed in a very similar fashion, i.e., they both denote the sum of two quadratic forms, where the first quadratic form captures commonalities (or covariances) across sectors and the second captures sector-specific variances. The latter quadratic form, in particular, shares the exact same structure in both our UC framework and Stock and Watson (2016). Consequently, the key distinction between the two approaches ultimately boils down to the choice of modeling the first quadratic form in (A66) and (A71) or, more specifically, the number of states one wants to introduce into the model to parameterize comovement. To illustrate, in an N-sector setting, our UC model requires $N(N-1)/2$ additional states to model $\mathbf{L}^{-1}\boldsymbol{\Sigma}_c^{EUW}\mathbf{L}^{-1'}$ in (A71), whereas the approach in Stock and Watson (2016) requires $N+1$ additional states to model $\widetilde{\boldsymbol{\Lambda}}\boldsymbol{\Sigma}_c^{SW}\widetilde{\boldsymbol{\Lambda}'}$ in (A66). It is easy then easy to verify that when $N = 2$, as in the setting for goods and services, the UC approach is a more parsimonious option, as it introduces only a single additional state to model common dynamics between trend inflation in the goods and services sectors, whereas the framework in Stock and Watson (2016) entails three states to capture the same moment. However, when N is larger, say, seventeen, the number of states required to model comovement in our UC-based framework proliferates. Specifically, it would require 136 additional states to parameterize $\mathbf{L}^{-1}\boldsymbol{\Sigma}_c^{EUW}\mathbf{L}^{-1'}$. Therefore, modeling comovement via time-varying correlations, as in our setting, makes estimation virtually prohibitive from a computational stance. In contrast, the factor approach by Stock and

Watson (2016) only requires 18 states to model comovement in $\widetilde{\mathbf{\Lambda}}\mathbf{\Sigma}_c^{SW}\widetilde{\mathbf{\Lambda}'}$ when $N = 17$ thus providing a more parsimonious and computationally tractable strategy.

A6 International Evidence

We apply our model to international data to explore whether our results are generalizable. To this end, we estimated our model using data on Australia and Canada.[13] For Australia, our sample covers 1976Q1-2021Q4, and for Canada, 1961Q2-2021Q4.[14] We stress that we did not set out to explore Australia and Canada specifically. The choice of sample was driven purely by limitations of the data coverage for other comparable economies. Nevertheless, Australia and Canada do possess some interesting features, which at least mark them out as useful points of comparison relative to our benchmark results for the U.S. First, both countries had similar inflation experiences to those of the U.S., in the sense that the Great Inflation saw very high inflation rates, which then fell and became very stable in the 1990s. In particular, the Reserve Bank of Australia and Bank of Canada adopted explicit inflation targets in 1997 and 1992, respectively. In the U.S., the inflation target was implicit until it was made explicit in 2012. Therefore, a comparison with the U.S. can provide some perspective on whether our key results are U.S.-specific, or perhaps can be extended to different inflation-targeting regimes. Second, as small open economies that do not have much pricing power in the international goods market, goods and services reflecting the traded versus nontraded dichotomy is perhaps much sharper for Australia and Canada. This feature at least allows us to form a firmer view on the globalization of inflation hypothesis through the lens of our framework.

Figure A9 presents the decomposition of the variance from the innovations to trend inflation for both Australia and Canada using Equation (12) in the main text. Similarly to the U.S., we find that while all three components contributed to the variation in aggregate trend inflation during the 1980s, and even part of the 1990s for Australia, the variation in aggregate trend inflation in both countries since around the 1990s has been dominated by

[13] A major challenge when seeking international evidence is that few economies retain long time series of goods and services inflation that are either constructed using a consistent methodology or have been rendered consistent by their respective statistical agencies to the level of the U.S. data. For example, for the UK, we are unable to go back beyond 1981, and for New Zealand, 1987. It is important to have long time series because the thrust of our key results is to make comparisons relative to the period of the Great Inflation in the 1970s. At a minimum, we require the sample coverage of the international data to at least include the rise and then fall of inflation in order to compare them with our key results for the U.S.

[14] Details on how we construct the goods and services deflator for both economies are provided in Section A6.1 of this appendix.

Figure A9: Decomposition of Volatility of Aggregate Trend Inflation for Australia and Canada

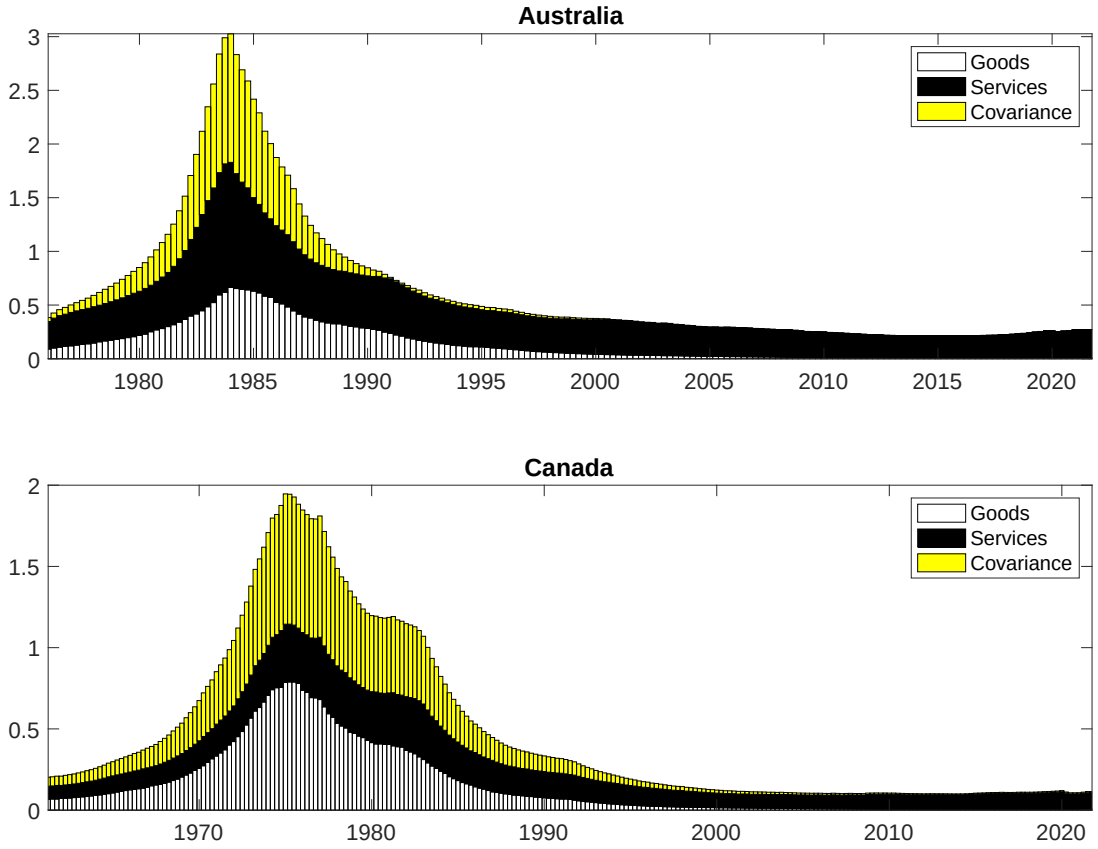

Notes: Trend inflation is in units of annualized quarter-on-quarter inflation. Goods, services and covariance refer to the decomposition components of aggregate trend inflation, as presented in Equation (12) in the main text.

that in trend services inflation. In particular, this result is once again driven by the goods and covariance component no longer contributing to the overall variation in aggregate trend inflation.

Therefore, given similar patterns observed in both Australia and Canada, we conclude that our findings are not a U.S.-specific phenomenon. As we mentioned at the outset of this section, both Australia and Canada are small open economies. Thus, more so than the U.S., they are price takers in the international goods market, and their services sectors likely reflect their domestic economic environments.

A6.1 Construction of Goods and Services Deflators for Australia and Canada

Australia does not provide a goods and services breakdown. We construct the goods and services deflators by once again using the Household Final Consumption Expenditure in the quarterly national accounts, provided by the Australian Bureau of Statistics (ABS).[15] The breakdown of consumption expenditure for goods and services in Australia is not reported. Instead, categories for consumption expenditure is reported. We classified the following as services: Rent and other dwelling services, Electricity, gas and other fuel, Furnishings and household equipment, Health Operation of vehicles, Transport services, Communications, Recreation and culture, Education services, Hotels, cafes and restaurants, and Insurance and other financial services. We then obtain the value of goods by subtracting the sum of these services categories. For both goods and services, we create nominal and real price series by taking the appropriate categories from the ABS tables: the seasonally current prices (nominal) and seasonally adjusted chain-weighted volume measure (real). We then create the deflators by dividing the nominal measure by the real measure, then multiplying by 100. Sector-specific inflation rates are then obtained by once again taking the annualized difference of the natural logarithms.

Statistics Canada reports, as part of its quarterly national accounts, a breakdown of goods and services in its household final consumption expenditure.[16] This breakdown means that the structure of the Canadian data exactly mimics the U.S. data. We create sector-specific deflators by dividing the measure of the current price by the measure of the real price. The sector-specific inflation rates are then constructed using the annualized difference of the natural logarithm of the deflator, which once again corresponds approximately to annualized quarter-on-quarter percentage point change in the sector-specific deflator.

[15] See https://www.abs.gov.au/AUSSTATS/abs@.nsf/DetailsPage/5206.0Mar%202020?OpenDocument for an example of a March 2020 release of the national accounts.

[16] See http://www150.statcan.gc.ca/t1/tbl1/en/tv.action?pid=3610012401

A6.2 Other Australia and Canada Results

To present results analogous our main results, Figures A10 and A11 present estimates of the standard deviation of the trend components of inflation for both Australia and Canada, as well as the estimated conditional correlation. In general, we observe the hump-shaped pattern in volatility as we see in the U.S. We also see the conditional correlation peak during the 1970s and 1980s for Canada and Australia, respectively, before this correlation disappeared in the 1990s. One difference is that the correlation is not very precisely estimated for Australia, with the 67% posterior credible set always containing zero. For completeness, we also present the estimated aggregate trend inflation estimates as well as the estimated sectoral trend inflation estimates in Figures A12 and A13.

The implication of all these results is that, like the U.S., both Australia and Canada have seen the composition of variation in aggregate trend inflation change from being shared between goods and services to, since the 1990s, being almost fully dominated by variation in trend services inflation.

Figure A10: Estimated Conditional Standard Deviation and Correlation of Innovations - Canada

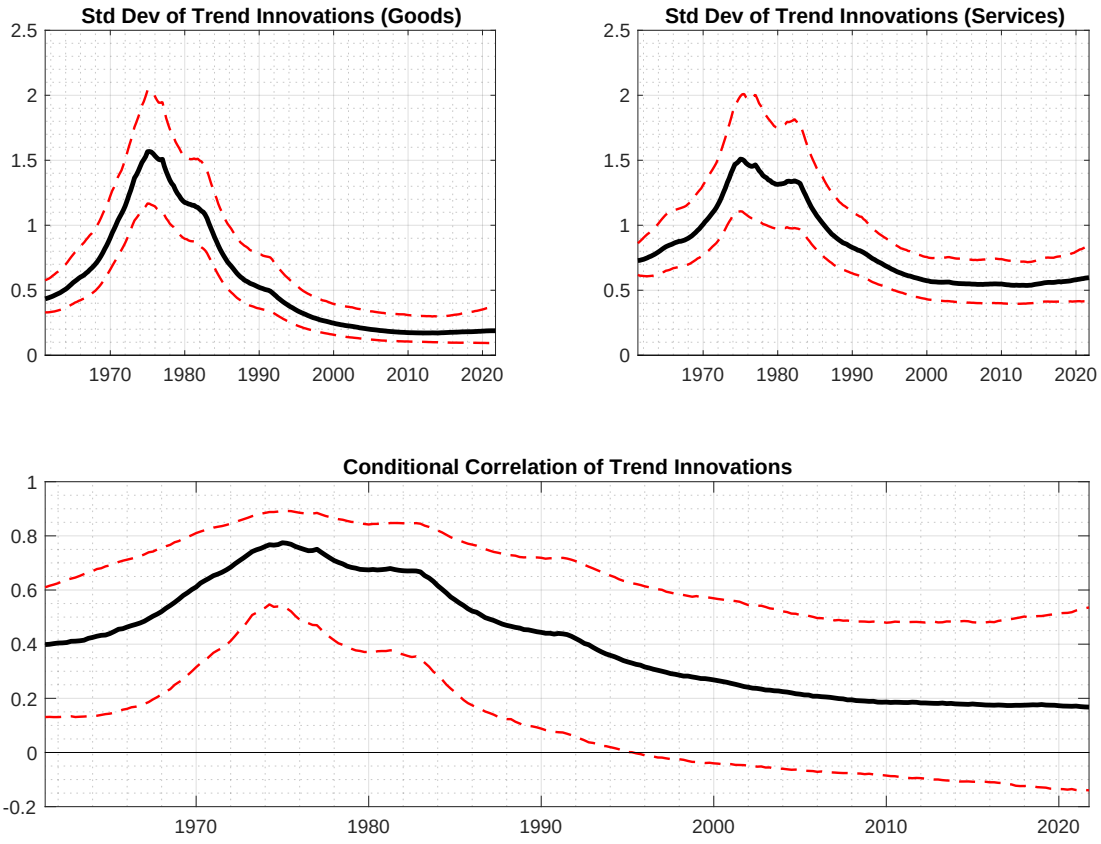

Notes: Posterior median estimate with associated 67% *posterior credible interval.*

Figure A11: Estimated Conditional Standard Deviation and Correlation of Innovations - Australia

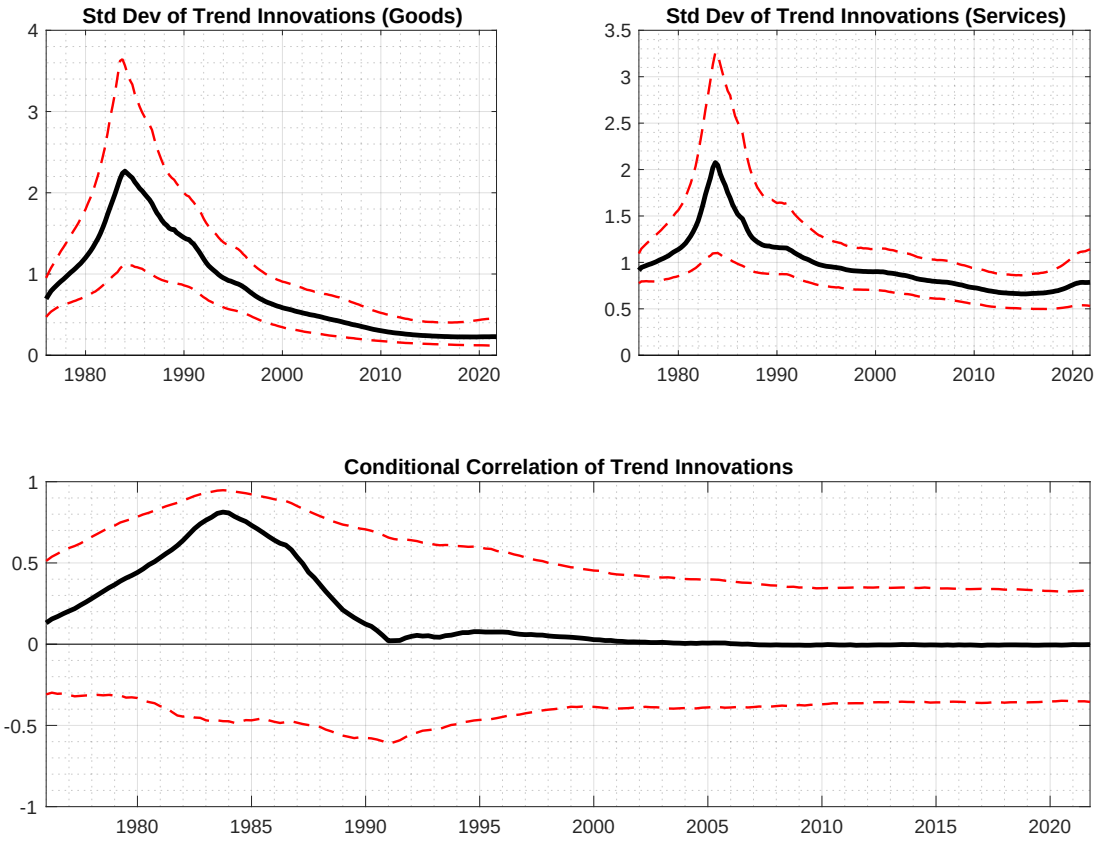

Notes: Posterior median estimate with associated 67% *posterior credible interval.*

Figure A12: Estimated Trend Inflation - Australia

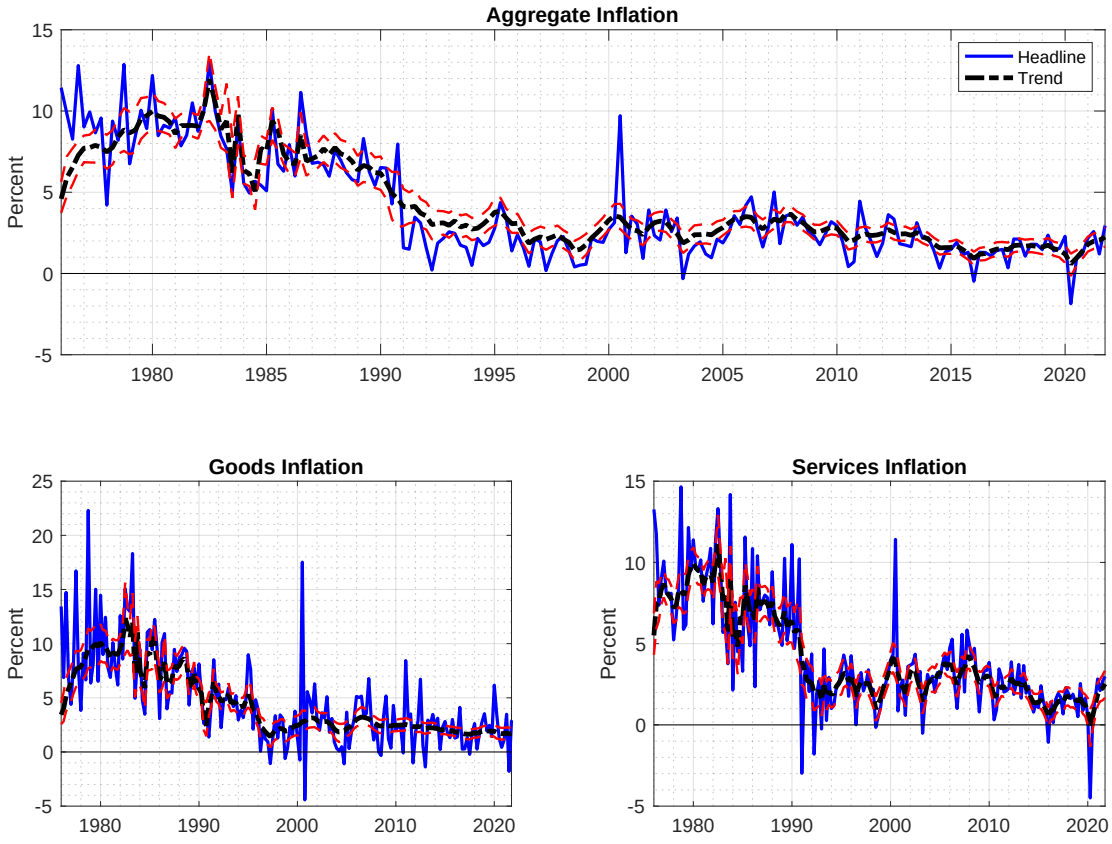

Notes: All units are in terms of annualized quarter-on-quarter inflation. Trend inflation estimates in terms of the posterior median estimate.

Figure A13: Estimated Trend Inflation - Canada

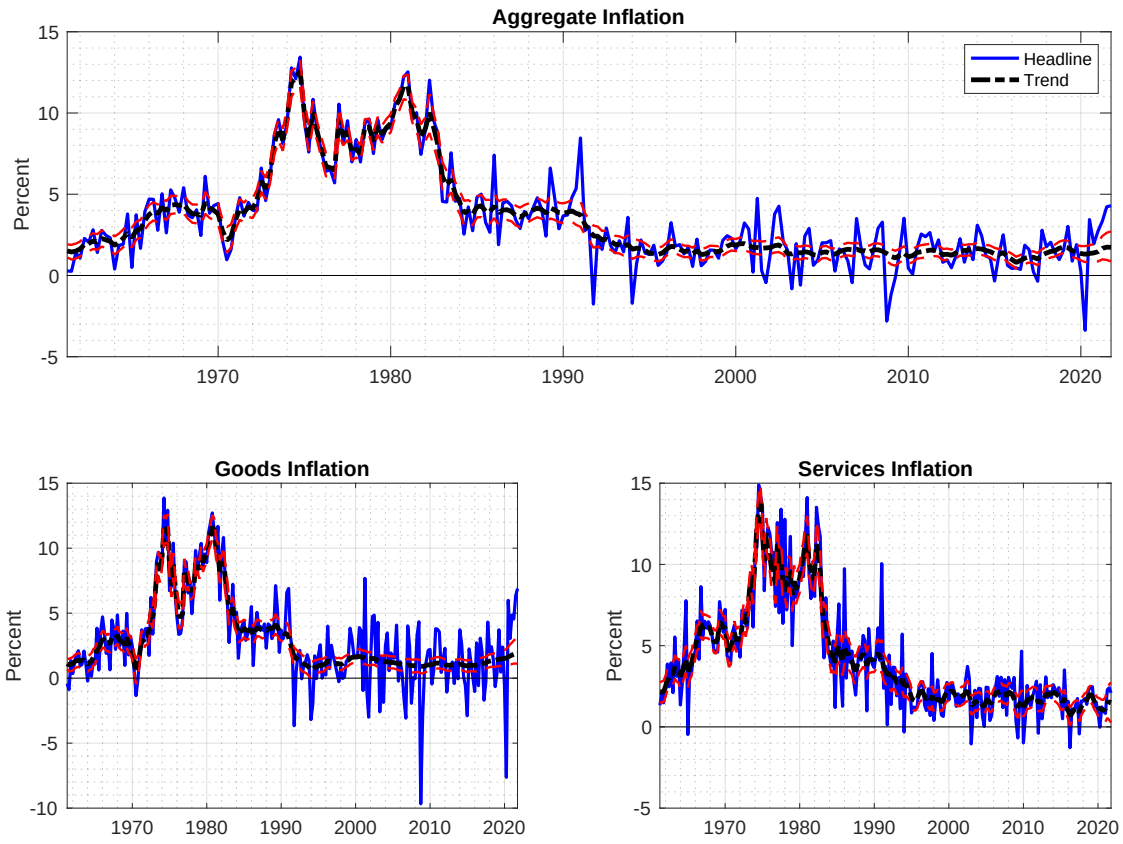

Notes: All units are in terms of annualized quarter-on-quarter inflation. Trend inflation estimates in terms of the posterior median estimate.

References

Anderson, Theodore W. 1984. *An Introduction to Multivariate Statistical Analysis.* Wiley.

Chan, Joshua C. C., Gary Koop, and Simon M. Potter. 2013. "A New Model of Trend Inflation." *Journal of Business & Economic Statistics*, 31(1): 94–106.

Chan, Joshua C. C., Gary Koop, and Simon M. Potter. 2016. "A Bounded Model of Time Variation in Trend Inflation, Nairu and the Phillips Curve." *Journal of Applied Econometrics*, 31(3): 551–565.

Chan, Joshua CC, and Ivan Jeliazkov. 2009. "Efficient Simulation and Integrated Likelihood Estimation in State Space Models." *International Journal of Mathematical Modelling and Numerical Optimisation*, 1(1-2): 101–120.

Del Negro, Marco, and Giorgio E Primiceri. 2015. "Time Varying Structural Vector Autoregressions and Monetary Policy: A Corrigendum." *The review of economic studies*, 82(4): 1342–1345.

Diebold, Francis X, and Robert S Mariano. 1995. "Comparing predictive accuracy." *Journal of Business & Economic Statistics*, 13(3): 253–263.

Gelman, Andrew. 2006. "Prior Distributions for Variance Parameters in Hierarchical Models." *Bayesian Analysis*, 1(3): 515–534.

Geweke, John, and Gianni Amisano. 2011. "Hierarchical Markov normal mixture models with applications to financial asset returns." *Journal of Applied Econometrics*, 26(1): 1–29.

Hendry, David F., and Kirstin Hubrich. 2011. "Combining Disaggregate Forecasts or Combining Disaggregate Information to Forecast an Aggregate." *Journal of Business & Economic Statistics*, 29(2): 216–227.

Kim, Sangjoon, Neil Shephard, and Siddhartha Chib. 1998. "Stochastic Volatility: Likelihood Inference and Comparison with ARCH Models." *The Review of Economic Studies*, 65(3): 361–393.

Koop, Gary, Dale J Poirier, and Justin L Tobias. 2007. *Bayesian Econometric Methods.* Vol. 7, Cambridge University Press.

Kroese, Dirk P, Thomas Taimre, and Zdravko I Botev. 2013. *Handbook of Monte Carlo Methods.* Vol. 706, John Wiley & Sons.

Lutkepohl, Helmut. 2006. "Forecasting with VARMA Models." In *Handbook of Economic Forecasting*. Vol. 1 of *Handbook of Economic Forecasting*, , ed. G. Elliott, C. Granger and A. Timmermann, Chapter 6, 287–325. Elsevier.

McCausland, William J, Shirley Miller, and Denis Pelletier. 2011. "Simulation Smoothing For State-Space Models: A Computational Efficiency Analysis." *Computational Statistics & Data Analysis*, 55(1): 199–212.

Omori, Yasuhiro, Siddhartha Chib, Neil Shephard, and Jouchi Nakajima. 2007. "Stochastic Volatility with Leverage: Fast and Efficient Likelihood Inference." *Journal of Econometrics*, 140(2): 425–449.

Raftery, Adrian E. 1995. "Bayesian Model Selection in Social Research." *Sociological methodology*, 111–163.

Stock, James H., and Mark W. Watson. 2007. "Why Has U.S. Inflation Become Harder to Forecast?" *Journal of Money, Credit and Banking*, 39(s1): 3–33.

Stock, James H., and Mark W. Watson. 2016. "Core Inflation and Trend Inflation." *The Review of Economics and Statistics*, 98(4): 770–784.

Whelan, Karl. 2002. "A guide to US chain aggregated NIPA data." *Review of income and wealth*, 48(2): 217–233.